

ISTANBUL TECHNICAL UNIVERSITY ★ INSTITUTE OF SCIENCE AND TECHNOLOGY

**LOCATING HARMONIC SOURCES IN
ELECTRICAL POWER SYSTEMS**

**Ph.D. Thesis by
Oben DAĞ**

Department : Electrical Engineering

Programme : Electrical Engineering

JANUARY 2010

**LOCATING HARMONIC SOURCES IN
ELECTRICAL POWER SYSTEMS**

**Ph.D. Thesis by
Oben DAĞ
(504022002)**

Date of submission : 04 September 2009

Date of defence examination : 08 January 2010

Supervisor (Chairman) : Prof. Dr. Ömer USTA (ITU)
Second Supervisor : Assoc. Prof. Dr. Canbolat UÇAK (YU)
Members of the Examining Committee : Prof. Dr. Serhat ŞEKER (ITU)
Prof. Dr. Celal KOCATEPE (YTU)
Assoc. Prof. Dr. Belgin TÜRKAY (ITU)
Assis. Prof. Dr. Deniz YILDIRIM (ITU)
Assis. Prof. Dr. Yılmaz ASLAN (DPU)

JANUARY 2010

**ELEKTRİK GÜÇ SİSTEMLERİNDE
HARMONİK KAYNAKLARININ
YERİNİN SAPTANMASI**

**DOKTORA TEZİ
Oben DAĞ
(504022002)**

**Tezin Enstitüye Verildiği Tarih : 04 Eylül 2009
Tezin Savunulduğu Tarih : 08 Ocak 2010**

**Tez Danışmanı : Prof. Dr. Ömer USTA (İTÜ)
Tez Eş Danışmanı : Doç. Dr. Canbolat UÇAK (YÜ)
Diğer Jüri Üyeleri : Prof. Dr. Serhat ŞEKER (İTÜ)
Prof. Dr. Celal KOCATEPE (YTÜ)
Doç. Dr. Belgin TÜRKEY (İTÜ)
Y. Doç. Dr. Deniz YILDIRIM (İTÜ)
Y. Doç. Dr. Yılmaz ASLAN (DPÜ)**

OCAK 2010

FOREWORD

I would like to express my deep appreciation and thanks to my advisor Prof. Dr. Ömer Usta for his precious time and valuable support during my studies.

I would also like to express my sincere gratitude to my co-advisor Assoc. Prof. Dr. Canbolat Uçak, for his time, guidance and support. This dissertation has benefited tremendously from his great enthusiastic attitude.

This work is supported by ITU Institute of Science and Technology.

I am grateful to my family whose love and support make my career in Electrical Engineering possible.

September 2009

Oben Dağ
Electrical Engineer, MSc.

TABLE OF CONTENTS

	<u>Page</u>
FOREWORD	v
TABLE OF CONTENTS	xi
ABBREVIATIONS	ix
LIST OF TABLES	xi
LIST OF FIGURES	xiii
SUMMARY	xv
ÖZET	xvii
1. INTRODUCTION	1
1.1 Purpose of the Thesis.....	3
1.2 Literature Review.....	4
1.3 Hypothesis.....	8
2. HARMONIC ANALYSIS IN POWER SYSTEMS	11
2.1 Introduction.....	11
2.2 Measures of Harmonic Distortion.....	11
2.3 Harmonic Sources.....	14
2.4 Effects of Harmonic Distortion.....	15
2.5 Modelling of System Components.....	16
2.6 Modelling of Harmonic Sources.....	20
2.7 Periodic Steady State Analysis.....	22
2.7.1 Current injection method.....	22
2.7.2 Harmonic power flow.....	23
2.8 Harmonic State Estimation.....	23
3. LOCATION OF SINGLE HARMONIC SOURCE USING DISTANCE MEASURE APPROACH	27
3.1 Introduction.....	27
3.2 The Distance Measure Index.....	28
3.2.1 Analysis on a 3-branch n -node electric circuit model.....	32
3.3 The Nodal Analysis Approach.....	33
3.4 Results.....	35
4. LOCATION OF SINGLE HARMONIC SOURCE USING IMPEDANCE NETWORK APPROACH	37
4.1 Introduction.....	37
4.2 Harmonic Source Location Procedure.....	42
4.2.1 Unique sets.....	42
4.2.2 Non-unique sets.....	43
4.3 Selection of Measurement Pairs.....	44
4.4 Optimal Meter Placement Algorithm (<i>OMPA</i>).....	45
4.4.1 Step 1.....	46
4.4.2 Step 2.....	47
4.5 Application of the Method to Model Systems.....	53
4.5.1 <i>IEEE</i> 30-bus test system analysis.....	58

4.6 Results	62
5. MONTE CARLO VALIDATION OF THE OPTIMAL METER PLACEMENT ALGORITHM.....	65
5.1 Introduction	65
5.2 Purpose	66
5.3 Procedure	69
5.4 Results of the Analysis	72
5.4.1 Summary of the analyses.....	82
5.5 Results	84
6. CONCLUSION AND RECOMMENDATIONS	85
6.1 Future Work.....	90
REFERENCES	91
APPENDICES	97
CURRICULUM VITA	101

ABBREVIATIONS

ac	: alternative current
dc	: direct current
ANN	: Artificial Neural Network
ANSI	: American National Standards Institute
CIGRE	: International Council on Large Electric Systems
HVDC	: High voltage direct Current
HSE	: Harmonic State Estimation
IEEE	: Institute of Electrical and Electronics Engineers
PWM	: Pulse-width Modulation
OA	: Observability Analysis
THD	: Total Harmonic Distortion
VAR	: Volt-ampere reactive
WLS	: Weighted Least-Squares
RMS	: Root-mean-square
ICA	: Independent component analysis
GPS	: Global positioning system
MCS	: Monte Carlo Simulation
OMPA	: Optimal meter placement algorithm
NOMP	: Non-optimal meter placement
OM	: Optimal meter pairs
NOM	: Non-optimal meter pairs

LIST OF TABLES

	<u>Page</u>
Table 2.1: Voltage distortion limits.	21
Table 4.1: Meter placement in <i>IEEE</i> 30-bus test system.	60
Table A.1.1: Bus load and injection data of <i>IEEE</i> 30-bus system.....	98
Table A.1.2: Reactive power limit of <i>IEEE</i> 30-bus system.	98
Table A.1.3: Line parameter of <i>IEEE</i> 30-bus system.	99

LIST OF FIGURES

	<u>Page</u>
Figure 2.1 : Linear passive load models: (a) model 1; (b) model 2; (c) model 3; (d) model 4; (e) model 5	19
Figure 2.2 : Equivalent π model of a transmission line.....	20
Figure 3.1 : Superposition of networks to form a harmonic network.....	28
Figure 3.2 : Harmonic source location in a single-phase network.....	30
Figure 3.3 : A n -node electrical circuit model.....	31
Figure 3.4 : A 7-node 3-branch electrical circuit model.....	33
Figure 3.5 : A $(n+m+p)$ -node 3-branch electrical circuit model.....	34
Figure 4.1 : Part <i>a</i> of the flow chart for the location algorithm.....	48
Figure 4.2 : Part <i>b</i> of the flow chart for the location algorithm.....	49
Figure 4.3 : Part <i>c</i> of the flow chart for the location algorithm.....	51
Figure 4.4 : An 8-node network topology.....	54
Figure 4.5 : A 22-node network topology.....	54
Figure 4.6 : An 18-node radial network topology.....	55
Figure 4.7 : An 18-node radial & ring network topology.....	57
Figure 4.8 : An 18-node ring network topology.....	57
Figure 4.9 : <i>IEEE</i> 30-bus test system.....	59
Figure 5.1 : The flow chart of the algorithm that compares the performance of location approach using <i>OMPA</i> and <i>NOMP</i>	71
Figure 5.1 : (contd.) The flow chart of the algorithm that compares the performance of location approach using <i>OMPA</i> and <i>NOMP</i>	72
Figure 5.2 : The performance plot for the location algorithm with <i>OMPA</i> (thick line) and <i>NOMP</i> (dashed line) for the deviation 0	74
Figure 5.3 : The performance plot for the location algorithm with <i>OMPA</i> (thick line) and <i>NOMP</i> (dashed line) for the deviation 10^{-10}	75
Figure 5.4 : The performance plot for the location algorithm with <i>OMPA</i> (thick line) and <i>NOMP</i> (dashed line) for the deviation 10^{-9}	76
Figure 5.5 : The performance plot for the location algorithm with <i>OMPA</i> (thick line) and <i>NOMP</i> (dashed line) for the deviation 10^{-8}	76
Figure 5.6 : The performance plot for the location algorithm with <i>OMPA</i> (thick line) and <i>NOMP</i> (dashed line) for the deviation 10^{-7}	77
Figure 5.7 : The performance plot for the location algorithm with <i>OMPA</i> (thick line) and <i>NOMP</i> (dashed line) for the deviation 10^{-6}	77
Figure 5.8 : The performance plot for the location algorithm with <i>OMPA</i> (thick line) and <i>NOMP</i> (dashed line) for the deviation 10^{-5}	78
Figure 5.9 : The performance plot for the location algorithm with <i>OMPA</i> (thick line) and <i>NOMP</i> (dashed line) for the deviation 10^{-4}	78
Figure 5.10 : The performance plot for the location algorithm with <i>OMPA</i> (thick line) and <i>NOMP</i> (dashed line) for the deviation 10^{-3}	79
Figure 5.11 : The performance plot for the location algorithm with <i>OMPA</i> (thick	

	line) and <i>NOMP</i> (dashed line) for the deviation 10^{-2}	79
Figure 5.12 :	The performance plot for the location algorithm with <i>OMPA</i> (thick line) and <i>NOMP</i> (dashed line) for the deviation 10^{-1}	80
Figure 5.13 :	The performance plot for the location algorithm with <i>OMPA</i> (thick line) and <i>NOMP</i> (dashed line) for 300 iterations	81
Figure 5.14 :	Percentage performance difference between <i>OMPA</i> and <i>NOMP</i>	82
Figure 5.15 :	Comparative performances of <i>OMPA</i> and <i>NOMP</i>	83

LOCATING HARMONIC SOURCES IN ELECTRICAL POWER SYSTEMS

SUMMARY

Harmonic distortion in power systems has been a common area of study for a long time. Its importance become significant for many customers and for the overall system since (i) the increase in the use of non-linear devices and loads cause increased harmonic distortion problems in power systems; (ii) and the increase in the use of shunt capacitors for power factor correction produces resonance problem due to the harmonics.

Harmonic current injection from customer loads into the utility supply system can cause harmonic voltage distortion on the utility systems' supply voltage. The main effects of voltage and current harmonics within the power system are (i) reduction in the efficiency of the generation, transmission and utilization of electric energy by overheating of rotating equipment, transformers, current-carrying conductors and by failure of operation of protective devices; (ii) loss of life of the insulation of electrical plant components with consequent shortening of their useful life; (iii) malfunctioning of system or plant components; (iv) amplification of harmonic levels due to series and parallel resonances which can result in overheating of utility transformers, power-carrying conductors, and other power equipments.

IEEE Std 519-1992 outlines typical harmonic current limits for customers and harmonic voltage limits for utility supply voltage. Customers and utilities in general should obey these limits to minimize the effects of harmonic distortion on the supply and end-user systems. In order to improve the process of controlling harmonic limits and mitigating harmonic problem in a power system, the knowledge of the locations of the harmonic sources may be helpful. The knowledge about harmonic sources' locations can also be used in order to solve disputes between utilities and customers. It is obvious that, all end users that experience harmonic distortion may not have significant sources of harmonics or even may not have nonlinear loads. Nevertheless, due to harmonic distortion that originate because of some other end user's nonlinear load, unexpected voltage distortion at the users that do not contribute to the harmonic generation can occur. By locating the harmonic sources, responsible parties may be penalized for causing distortion in the supplied power that result in the loss of efficiency in power systems.

In this thesis two methods are proposed to determine the harmonic source location in power systems.

It is assumed in the thesis that, (i) the network harmonic impedances were obtained prior to analyses; (ii) the power system consists of linear devices; (iii) the distorting device is represented by linear models which inject harmonic currents; (iv) the network is balanced three-phase system and (v) the injected harmonic current levels are independent of the voltage distortion at the device terminals. Last assumption implies that the equivalent circuits of the system at various harmonic frequencies are independent from each other. According to the superposition theory, power system harmonic circuit can be represented as a combination of the circuit with fundamental frequency and the circuits for the other harmonic orders. By solving the system at each frequency, each source and its effect can be considered independently. For an harmonic source with multiple harmonic orders, the harmonic network can be analyzed at each harmonic order circuit to locate the source. For this reason harmonic networks at each harmonic order are analyzed according to the superposition theory.

In the thesis, first a harmonic source location approach in analogy to two-end impedance-based fault location method is developed. In this approach, the distance from the harmonic source to one of the metering points is used as a measure to locate the harmonic source in the network. It is shown that when this measure is used; there is no need to obtain harmonic source impedance and harmonic source current values for calculating the distance. It is also demonstrated that for a n -node m -branch system, m -measurements (one measurement at each branch end node) are sufficient to correctly locate the harmonic source. However, it is reported that as the number of branches in a network increase, correctly defining the distance measure index correctly become so difficult that the method can only be used for networks up to 3-branches.

In addition to the developed approach based on distance measure, a harmonic source location method and an original optimal meter placement algorithm based on impedance network approach are developed in this thesis. It is shown that a harmonic source can be located with an accuracy of 100%, when harmonic impedance values are not subject to deviations. In addition, the Monte Carlo simulations performed for the *IEEE* 30-bus test system also verifies the performance and accuracy of the new approach when harmonic impedance values are subject to deviations. It is shown and reported that the developed method is both simple in theory and easy to perform in practical applications.

ELEKTRİK GÜÇ SİSTEMLERİNDE HARMONİK KAYNAKLARININ YERİNİN SAPTANMASI

ÖZET

Elektrik güç sistemlerinde harmonik bozulmaların incelenmesi uzun bir süredir gündemde olan bir konudur. Bu konunun elektrik tüketicileri ve diğer elektrik güç sistemi bileşenleri için önem sahibi olmasının başlıca nedenleri, (i) güç sisteminde kullanımı sürekli artan doğrusal olmayan cihaz ve yüklerin oluşturduğu harmonik bozulma ve (ii) güç faktörü düzeltmek amacıyla kullanılan kapasitörlerin artan kullanımı sebebiyle harmonik frekanslarda oluşan rezonans problemi olarak sıralanabilir.

Tüketici yüklerinden elektrik güç sistemine enjekte edilen akım harmonikleri elektrik şebekesi geriliminde harmonik bozulmalara sebep olmaktadır. Bununla birlikte, akım ve gerilim harmoniklerinin elektrik güç sistemlerindeki başlıca etkileri: (i) dönen cihazların, transformatörlerin, akım taşıyan iletkenlerin aşırı ısınması ve koruma elemanlarının çalışma aksaklıkları nedeniyle elektrik enerjisinin üretim, iletim ve kullanım etkinliğinin azalması; (ii) elektrik şebekesindeki yalıtkanların kullanım ömürlerinin azalması; (iii) elektrik şebeke bileşenlerinin işlevlerini kaybetmesi; (iv) seri ve paralel rezonans olayları nedeniyle harmonik seviyelerinin artması ve bu sebeple transformatörlerin, iletkenlerin ve diğer cihazların aşırı ısınması olarak sıralanabilir.

IEEE Std 519-1992 standardı elektrik güç tüketicileri için karakteristik harmonik akım sınırlarını ve elektrik şebeke gerilimleri için karakteristik gerilim sınırlarını ana hatlarıyla özetlemektedir. Elektrik tüketicileri ve elektrik güç sağlayıcıları; besleme ve son kullanıcı sistemleri üzerindeki harmonik bozulma etkilerini en aza indirmek amacıyla bu sınırlara uymalıdır. Harmonik sınırlarının kontrol edilmesi ve harmonik problemlerinin ortadan kaldırılması işlemlerinin iyileştirilmesi amacıyla harmonik kaynak yerleri hakkında bilgi faydalı olabilir. Diğer taraftan, harmonik kaynaklarının yerinin bilinmesi elektrik güç sağlayıcıları ve elektrik tüketicileri arasında, kullanılan elektrik enerjisinin kalitesi konusunda, oluşan anlaşmazlıkların çözümü için de faydalı olabilir. Harmonik bozulmaya maruz kalan tüm tüketiciler kayda değer bir harmonik bozucu kaynağı bulundurmaz veya doğrusal olmayan yüklerle sahip olmayabilir. Bununla birlikte, başka son kullanıcıların doğrusal olmayan yüklerinden kaynaklanan harmonik bozulma sonucu, harmonik üretimine katkıda bulunmayan kullanıcılar da beklenmeyen harmonik gerilim bozulması ile karşılaşabilir. Harmonik kaynaklarının yeri saptanarak, besleme geriliminin bozulması nedeniyle elektrik güç sisteminin verimliliğini azaltan sorumlu taraflar cezalandırılabilir.

Bu tezde, elektrik güç sistemlerinde harmonik kaynak yeri saptanması için iki metod geliştirilmiştir.

Tezde yapılan analizler için, (i) harmonik devre empedanslarının önceden elde edilmiş olduğu; (ii) elektrik güç sisteminin doğrusal elemanlarla modellendiği; (iii) harmonik bozucu elemanının harmonik akım enjekte eden doğrusal modeller ile ifade edildiği; (iv) ilgilenilen devrenin dengeli üç fazlı olduğu; (v) enjekte edilen harmonik akımlarının akım enjekte edilen noktadaki harmonik gerilim bozulmasından bağımsız olduğu varsayımları yapılmıştır. Son varsayım elektrik sisteminde her harmonik derecesindeki eşdeğer devrelerin birbirinden bağımsız olması sonucunu doğurur. Süperpozisyon ilkesine göre elektrik güç sistemi harmonik eşdeğer devresi; temel frekans eşdeğer devre ve harmonik frekanslardaki eşdeğer devrelerin birleşik etkisi ile modellenmektedir. Elektrik şebekesi her harmonik için ayrı ayrı çözümlenerek; her harmonik derecesindeki kaynağın etkisi, bu kaynakların birbirlerinden bağımsız olarak analiz edilebilir. Birden fazla harmonik derecesi içeren bir harmonik kaynağı için harmonik devresi her bir harmonik frekansında ayrı ayrı çözümlenerek kaynak yeri saptanabilir. Bu sebeple, her bir harmonik derecesine karşılık gelen harmonik eşdeğer devreleri süperpozisyon ilkesine göre analiz edilmiştir.

Bu tezde, ilk olarak harmonik kaynak yeri tespiti için, iki-uçlu empedans-tabanlı arıza yeri tespit etme metoduna örnekseme yapılarak bir harmonik kaynak yeri tespit etme yaklaşımı geliştirilmiştir. Bu yaklaşımda, harmonik kaynağı ile ölçüm alınan noktalardan biri arasındaki mesafe bir ölçüt olarak kullanılarak harmonik kaynağının yeri tespit edilmektedir. Geliştirilen ölçüt için harmonik kaynağın empedansı ve harmonik kaynağın akım değerinin bilinmesine gerek olmadığı saptanmıştır. Ayrıca n -düğümlü m -dallı bir şebekede, m -ölçüm yapılarak (her dal ucunda bir ölçüm olmak üzere) harmonik kaynağının yerinin saptanabileceği gösterilmiştir. Bununla beraber, elektrik şebekesindeki dal sayısının artması halinde mesafe ölçütünün doğru bir şekilde tanımlanma zorluğunun artması sebebiyle bu yaklaşımın en çok 3-dallı elektrik şebekelere kadar kullanılabilirdiği belirtilmiştir.

Önerilen mesafe yaklaşımına ek olarak empedans devreleri yaklaşımına dayanan, harmonik kaynağı yeri saptama ve özgün bir *ölçü aleti en iyi yerleştirme algoritması* geliştirilmiştir. Geliştirilen yöntem 30-baralı *IEEE* test sisteminde uygulanarak, harmonik kaynağının yerinin harmonik impedans değerlerinde sapma olmaması durumunda % 100 başarı ile saptandığını görülmüştür. Bununla birlikte yapılan Monte Carlo benzetimleri, geliştirilen yeni yaklaşımın harmonik empedans değerleri değişimlere maruz kaldığı durumlarda da başarılı olduğunu göstermiştir. Geliştirilen metodun teorik olarak basit ve uygulama olarak da pratik bir yaklaşım olduğu ifade edilmiştir.

1. INTRODUCTION

Power system harmonics are defined as sinusoidal voltage and current waveforms that are integer multiples of the (fundamental) frequency at which the supply system is designed to operate. Harmonics combine with the fundamental voltage or current and produce waveform distortion. Harmonic distortion exists due to the nonlinear characteristics of devices and loads connected to the power network.

Any periodic distorted waveform is composed of sinusoids (sinusoidal waveforms) at different frequencies: These sinusoids are a waveform at fundamental frequency and waveforms with harmonic components that have integer multiples of the fundamental frequency. The sum of sinusoids is referred to as a Fourier series. According to Fourier series concept, the system can be analyzed separately at each harmonic and the system response of a sinusoid (of each harmonic) can be found individually rather than analyzing the entire distorted waveforms response [1].

Harmonic distortion in power systems is not a new phenomena and it has been a common area of study for a long time. However, its importance become significant for many customers and for the overall system since;

- (i) the increase in the use of non-linear devices and loads cause increased harmonic distortion problems in power systems;
- (ii) and the increase in the use of shunt capacitors for power factor correction makes contribution to the problem through resonance.

As source of harmonic, non-linear devices can be classified as traditional types: transformers, rotating machines, arc furnaces; and modern types: fluorescent lamps, switched-mode power supplies widely used in industry and modern office electronic equipment, thyristor-controlled devices. The thyristor-controlled devices include rectifiers, inverters, static volt-ampere reactive (*VAR*) compensators, cycloconverters, high voltage direct Current (*HVDC*) transmission.

The presence of capacitors, such as those used for power factor correction are normally not a source of harmonics, however they can result in local system

resonances which lead in turn to excessive currents and possible subsequent damage to the capacitors. Even with system resonances close to the harmonic frequencies, the voltage distortion levels may be acceptable. This is so, because on distribution systems most resonances are significantly damped by the resistances on the system, which reduces magnification of the harmonic currents. For this reason system response to capacitors is important since it indicates whether or not the harmonic mitigation measures are necessary.

Harmonic current injection from customer loads into the utility supply system can cause harmonic voltage distortion to appear on the utility systems' supply voltage. The main effects of voltage and current harmonics on the power system are as follows:

- A reduction in the efficiency of the generation, transmission and utilization of electric energy by overheating of rotating equipment, transformers, current-carrying conductors and by failure of operation of protective devices.
- Loss of life of the insulation of electrical plant components with consequent shortening of their useful life.
- Malfunctioning of system or plant components.
- The amplification of harmonic levels due to series and parallel resonances which can result in overheating of utility transformers, power-carrying conductors, and other power equipments [2].

IEEE Std 519-1992 [3] outlines typical harmonic current limits for customers and harmonic voltage limits for utility supply voltage, that customers and utilities in general should attempt to operate within in order to minimize the effects of harmonic distortion on the supply and end-user systems. In order to improve the process of controlling harmonic limits at a power system and mitigating harmonic problem, the knowledge of the locations of the harmonic sources may be helpful which is the main motivation of this thesis.

Locating harmonic source may also be useful in order to solve disputes between utilities and customers. For instance, when harmonic currents are injected into a power distribution system, they may cause unexpected voltage distortion among users which do not produce harmonics. That is, all end users who experience

harmonic distortion may not have significant sources of harmonics themselves, but the harmonic distortion may originate due to some end-user's load or combination of loads. By locating the harmonic source, responsible parties may be penalized for causing distortion in the supplied power that result in the loss of efficiency in power systems.

1.1 Purpose of the Thesis

The level of harmonic distortion of modern power systems is a concern as more non-linear devices are become used in energy conversion. Harmonic mitigation techniques would be more effective when the location of the harmonic distortion source is known. Once the harmonic source is located; a preventive and corrective action such as harmonic filtering can be taken to reduce distortion at the point of harmonic source.

On the other hand, for example, harmonic sources can be located both upstream and downstream of a metering point, so that both utility and customer may be responsible for harmonic distortion (some harmonics may be produced by the customer, others by the utility, and others by both customer and utility). If the relative distortion contributions can not be allocated to distinct sources, distortion costs among the responsible parties can not be assigned. Hence, by locating the source of distortion, the responsible parties can be penalized or obligated to comply with the distortion levels defined in standards.

At present, there are no standards that define the indexes and related measurement methods for the localization of harmonic sources. International standards set limits for harmonic distortion only for some voltage and current levels, for both networks and loads [4]. These limits are set for both single harmonic and total harmonic distortion by means of indexes such as the total harmonic distortion factor (*THD*). Standards also define the measurement methods used to evaluate the harmonic distortion level [4]. The standards do not define or suggest any measurement methods for the location of harmonic sources [4].

The purpose of this thesis is to develop a method to locate the harmonic sources in a power system. For this reason harmonic networks at each harmonic order, according to the superposition theory, are analyzed. It is shown that a harmonic source can be

located with an acceptable degree of accuracy when harmonic impedance errors exist. The simulations based on Monte Carlo method, performed for the *IEEE* 30-bus test system, verifies the performance and accuracy of the developed source location and meter placement approach under a variety of harmonic impedance errors. The developed method is based on system bus harmonic impedance matrix and system topology. A meter placement approach is developed for finding the optimal meter locations within the network. It is shown that this method is both simple in theory and easy to perform in practical applications.

1.2 Literature Review

Harmonic studies in literature can be categorized as forward harmonics analyses and reverse harmonic analyses.

In forward harmonics analysis, harmonic sources in a power system are assumed to be known and harmonic load-flow is carried out to determine the propagation of harmonics in the network. The aim of this analysis is to quantify the distortion in the voltage and current waveforms at various points in a power system. These studies also aim to determine whether severe resonant conditions exist in the power system. On the other hand, the goal of the reverse harmonic analysis is to identify and localize the harmonic sources in a power system from a set of available measurements in the corresponding network.

In the literature, different approaches for harmonic source localization have been presented. They can be classified mainly according to methodology into three groups: (i) index-based approaches, (ii) harmonic state estimation approaches, and (iii) artificial intelligence based approaches. All of the approaches have their advantages and drawbacks.

The index-based approaches make use of power system indices in order to locate harmonic sources. For example, it is shown by Cristaldi and Ferrero [5] that the magnitude of the load non-linearity index and the load unbalance index is proportional to the degree of load unbalance or load non-linearity. Another index named as harmonic global index is defined in [6] that attempts to localize sources of harmonic disturbance in a power system. For various values of this index; the absence of harmonic distortion at the metering location, the existence of harmonic

distortion in the load, or the existence of the harmonic source in the supply side is determined. These approaches were based on the direction of individual harmonic active power flow.

Harmonic active power flow analysis (performed by means of the decomposition of voltages and currents into Fourier series) requires the evaluation of the amplitudes and phase angles of each voltage and current harmonic. In addition to the methods like [7-9] based on the measurement of harmonic active power flow for harmonic source detection; there are also other approaches based on the definition of different harmonic indexes and nonactive powers [6] and [10-18].

The second type of approach for harmonic source localization in the literature is the harmonic state estimation (*HSE*) based techniques. *HSE* is a reverse process of harmonic simulation that analyzes the response of a power system to the given injection current sources at harmonic frequencies. The *HSE* uses the measurements from the power system to identify the harmonic sources [19].

Harmonic state estimation techniques have been developed to generate the best estimate of the harmonic levels from limited measured harmonic data and to identify the harmonic sources in electric power systems [19-22]. A large number of measurements including redundant ones are required to identify the harmonic source locations from *HSE*.

One of the difficulties with the location of the estimation is that linear loads can act like a harmonic source because of the distorted voltage waveform at the point of common coupling drawing harmonic currents. There are studies on estimation and distinguishing the actual source of the distortion [23-26].

For solving the reverse harmonic problem, Heydt et al. first proposed the idea of using least square based state-estimation technique to identify the location of sources for static harmonic state estimation [27] and a Kalman filtering methodology for dynamic state estimation [28]. However, in these methods the total number of harmonic measurements required is large. In [27], a total of 23 measurements have been used for the sample 13-bus system and 63 measurements have been considered for the *IEEE* 38-bus system. Similarly in [28], a total of 54 measurements have been used in the *IEEE* 14-bus system. Thus in both of these methods [27,28] the total cost of measurements is quite high.

Farach et al. solved the dual problem of optimal meter location and estimation of location of harmonic sources [29]. They developed a technique for optimal sensor placement for underdetermined (number of measurements is less than the number of unknown quantities) case of harmonic state estimation. The technique determines a best estimate of currents at unknown or unmeasured busses to provide an indication of the load type at those busses. Their technique is based on the minimum-variance approach where the expected value of the sum of squares of the difference between the estimated and the true variables is minimised. The technique performs best when using a priori information regarding the possible nature of the loads. For example, if a bus has no load, then it cannot be considered a harmonic source. On the other hand a bus consisting mostly of industrial customers should be assigned a higher probability of being a harmonic source than a bus that supplies mostly residential users.

Grady and Farach claimed that, if sufficient harmonic measurements are available, operators can estimate the most likely locations of harmonic sources [29]. Actually, the number of harmonic meters is limited, in other words, the problem is an *under-determined harmonic state estimation*. The “under-determined harmonic state estimator” is designed for only a few measurement usages to estimate the locations of multiple harmonics. This method is based on heuristically assigned a priori probabilities of the existence of harmonic sources. However, the method does not guarantee that the most outstanding estimated injected current implies a harmonic source at that busbar.

It is seen from literature that conventional harmonic state estimation requires a redundant number of expensive harmonic measurements. *HSE* techniques require detailed and accurate knowledge of network parameters and topology. The approximation of the system model and poor knowledge of network parameters may lead to large errors in the results. In [30], a statistical signal processing technique, known as independent component analysis (*ICA*) for harmonic source identification and estimation is developed. *ICA* is based on the statistical properties of loads. According to [30], if the harmonic currents are statistically independent, *ICA* is able to estimate the currents using a limited number of harmonic voltage measurements and without knowledge of the system admittances or topology. However, the proposed approach is developed for no measurement error case and the performance

incase of impedance errors is not answered. It is reported in [31,32] that measurement noise increases the estimation errors at lower load levels. Moreover, the impact of measurement numbers and location on the accuracy of the estimation are the questions also not answered in the study. In the study, the number of measurements are selected according to the number of harmonic sources, however knowing the number of these sources is not practical. The approach requires time series of measurements which increases the measurement costs. On the other hand, although the algorithm does not require prior knowledge of network parameters, it needs prior information regarding the characteristics of harmonic sources in the system. Moreover, the FastICA algorithm used in the study requires the number of harmonic sources in the system (which is not practical).

Artificial intelligence based techniques are also utilized in the harmonic source localization problem. It is known from literature that artificial neural networks (*ANN*) and fuzzy clustering, has been applied to solve many practical engineering problems. An *ANN* is able to map complex and highly non-linear input-output pairs and has numerous applications in the area of power engineering.

To reduce the measurement cost it is necessary to limit the number of meters required for harmonic state estimation. The quality of estimation depends on the location of these harmonic meters. Hartana et al [33] suggested the use of *ANN* for harmonic state estimation. In their approach an *ANN* has been used to supply pseudo-measurements to the harmonic state estimator and thus the number of actual measurements (meters) required can be reduced significantly. A similar method is proposed in [34] such that an *ANN* is used to determine the meter places and then state estimation is used to locate the dominant harmonic sources.

Fuzzy theory is also applied to the harmonic source locating process. A methodology proposed in [35] makes use of fuzzy theory implemented in an *ANN* to localize multiple harmonic distortion sources. A fuzzy clustering approach is used to partition the power system into clusters. The number of clusters is equal to the number of meters to be placed in the power system. The *ANN* is then trained with the back-propagation algorithm to identify all individual harmonic sources in the power system. It is claimed that such approach requires a smaller number of meters when compared to the methods reported in [19,27].

Similar approaches were also seen in the literature [36,37]. These approaches show that the application of artificial neural networks is widely used in power system harmonic studies. However, the training of an *ANN* is a time consuming process and minimization is not guaranteed. In addition, determining the proper architecture of *ANN* can be a cumbersome process. Moreover, estimation with neural network algorithms requires prior information about sources for training the neural network.

According to the literature survey it is seen that none of the methods are without their limitations such that some of them require prior knowledge of exact network parameters and some of them require prior information regarding the characteristics of harmonic sources.

1.3 Hypothesis

This study has provided a unique opportunity to look at harmonic source location problem. Two approaches are developed. The first one is based on distance measure approach and the other one is based on impedance network approach using a new optimal meter placement algorithm.

The contributions of this dissertation are summarized in the list below.

- A harmonic source location method in analogy to two-terminal impedance-based fault location approach is developed to locate the harmonic source in networks. In this approach harmonic source impedance and harmonic source current values are not needed. The required data is the system impedance values and voltage measurements at each end nodes of a m -branch and n -node network. When the number of branches increases, the complexity of obtaining the measure index limits the approach. Thus, it is not practically applicable to networks with 3-branches or more.
- For networks with 3-branch or more, the nodal analysis can be used to locate harmonic sources in the network. However, voltage measurements at all of the nodes are required, which is not practical. For this reason, a new optimal meter placement algorithm is proposed to obtain limited number of meter positions for harmonic source location process.
- A different method based on impedance network approach is used in the thesis. The approach uses impedance ratios of harmonic impedance matrix

corresponding to measurement pairs obtained by a new optimal meter placement algorithm. The impedance ratios are matched with voltage ratios at corresponding meter locations to locate the harmonic source. The meter placement approach selects measurement pairs with impedance ratios that have maximum distance between their closest members to overcome harmonic impedance errors. Simulations on *IEEE* 30-bus test system verify the accuracy of the proposed approach.

- Obtaining the exact values of network harmonic impedances may be difficult in practice; hence harmonic source location approach may need to tolerate deviations in network impedance values. For this reason, the accuracy of the harmonic source location is analyzed by applying a variety of deviations into the harmonic impedance matrix. Monte Carlo simulation is used to investigate the affect of errors and random variations of harmonic impedance matrix on the performance of the harmonic location algorithm. It is seen that the location approach with optimal meter placement algorithm can accurately locate the harmonic source when there is no deviation in harmonic impedance matrix. On the other hand, when deviations are included into the impedance matrix, its performance is always better than location with arbitrarily selected meter positions. This shows that the proposed optimal meter placement algorithm is capable of dealing with the affects of deviations in network impedance values, which is a practical situation in real life.

2. HARMONIC ANALYSIS IN POWER SYSTEMS

2.1 Introduction

A harmonic waveform is composed of sinusoidal waves of different frequencies; a waveform at the fundamental frequency and a number of sinusoids or harmonic components with frequencies that are integer multiples of the fundamental. Distorted periodic voltage or current waveforms can be expressed in terms of a Fourier series which represents an effective way to study and analyze harmonic distortion. Fourier series theory allows inspecting the various components of a distorted waveform through decomposition.

Linear networks in balanced power systems have their responses to different harmonics independent of others. This property makes it possible to study each harmonic separately, by constructing the equivalent circuit for each harmonic and solving for current and voltage variables. The total response is obtained by adding the response of each harmonic component.

2.2 Measures of Harmonic Distortion

A distorted periodic current or a voltage waveform expanded into a Fourier series are:

$$i(t) = \sum_{h=1}^{\infty} I_h \cdot \cos(h\omega_o t + \phi_h), \quad (2.1)$$

$$v(t) = \sum_{h=1}^{\infty} V_h \cdot \cos(h\omega_o t + \theta_h), \quad (2.2)$$

where

h is the harmonic order,

I_h is the h^{th} harmonic peak current,

V_h is the h^{th} harmonic peak voltage,

ϕ_h is the h^{th} harmonic current phase,

θ_h is the h^{th} harmonic voltage phase,

ω_o is the fundamental angular frequency, $\omega_o = 2\pi f_o$,

f_o is the fundamental frequency, $f_o = 50\text{ Hz}$.

The expressions for the root-mean-square (*RMS*) voltage and current can be given as

$$V_{rms} = \sqrt{\sum_{h=1}^{\infty} V_{h,rms}^2}, \quad (2.3)$$

and

$$I_{rms} = \sqrt{\sum_{h=1}^{\infty} I_{h,rms}^2}. \quad (2.4)$$

Voltage distortion factor, also known as voltage total harmonic distortion is defined as

$$THD_V = \frac{1}{V_1} \sqrt{\sum_{h=2}^{\infty} V_h^2} = \sqrt{\left(\frac{V_{rms}}{V_{1,rms}}\right)^2 - 1}, \quad (2.5)$$

where V_1 represent the fundamental peak voltage. Current distortion factor also known as current total harmonic distortion is defined as

$$THD_I = \frac{1}{I_1} \sqrt{\sum_{h=2}^{\infty} I_h^2} = \sqrt{\left(\frac{I_{rms}}{I_{1,rms}}\right)^2 - 1}, \quad (2.6)$$

where I_1 represent the fundamental peak current. *RMS* voltage and current can be also expressed in terms of *THD* as

$$V_{rms} = V_{1,rms} \sqrt{1 + THD_V^2} \quad (2.7)$$

and

$$I_{rms} = I_{1,rms} \sqrt{1 + THD_i^2} . \quad (2.8)$$

IEEE standard 519 [3] limits the individual harmonic voltage distortion to 3 percent of the fundamental and total voltage distortion to 5 percent.

The following relationships for active (real) and reactive power apply. Instantaneous power is $p(t) = v(t) \cdot i(t)$, which has the average (active power)

$$\begin{aligned} P &= \frac{1}{T} \int_0^T p(t) dt \\ &= \frac{1}{2} \sum_{h=1}^{\infty} V_h I_h \cos(\theta_h - \phi_h) , \\ &= \sum_{h=1}^{\infty} V_{h,rms} I_{h,rms} \cos(\theta_h - \phi_h) \end{aligned} \quad (2.9)$$

Reactive power according to Budeanu [12] is defined as

$$\begin{aligned} Q &= \frac{1}{2} \sum_{h=1}^{\infty} V_h I_h \sin(\theta_h - \phi_h) \\ &= \sum_{h=1}^{\infty} V_{h,rms} I_{h,rms} \sin(\theta_h - \phi_h) \end{aligned} , \quad (2.10)$$

Based on the definitions of *RMS* voltage and current, the apparent power is

$$\begin{aligned} S &= V_{rms} \cdot I_{rms} \\ &= \sqrt{\sum_{h=1}^{\infty} V_{h,rms}^2 \cdot I_{h,rms}^2} , \\ &= V_{1,rms} I_{1,rms} \sqrt{1 + THD_v^2} \sqrt{1 + THD_i^2} \\ &= S_1 \sqrt{1 + THD_v^2} \sqrt{1 + THD_i^2} \end{aligned} \quad (2.11)$$

where S_1 is the apparent power at the fundamental frequency.

When harmonics are present, apparent power S is not only comprised of active power P and reactive power Q . In addition, distortion power D according to Budeanu [12] is defined to account for the difference, where

$$D = \sqrt{S^2 - (P^2 + Q^2)} . \quad (2.12)$$

In this equation, Q consists of the sum of the reactive power values at each frequency. D represents all cross products of voltage and current at different frequencies, which yield no average power.

The power factor is the ratio of the real (active) power to the apparent power defined as,

$$pf = \frac{P}{S} = \frac{P}{S_1} \cdot \frac{1}{\sqrt{1+THD_v^2} \sqrt{1+THD_i^2}} = pf_{disp} \cdot pf_{dist}, \quad (2.13)$$

$$pf_{disp} = \frac{P}{S_1}, \quad (2.14)$$

$$pf_{dist} = \frac{1}{\sqrt{1+THD_v^2} \sqrt{1+THD_i^2}} = \frac{V_{1rms}}{V_{rms}} \cdot \frac{I_{1rms}}{I_{rms}} = \frac{S_1}{S}, \quad (2.15)$$

where

pf_{disp} is the displacement power factor,

pf_{dist} is the distortion power factor [38].

Apart from the definitions of the power quantities given above there are also other definitions of electric power quantities under sinusoidal, nonsinusoidal, balanced or unbalanced conditions. They were discussed in several papers in the literature [13], [39-46].

2.3 Harmonic Sources

The nonlinear loads inject harmonic currents into the power system, causing harmonic distortion in the voltage waveform. Harmonic sources can be classified as sources from commercial loads and sources from industrial loads. Harmonic sources from commercial loads include single-phase power supplies, fluorescent lighting, adjustable-speed drives. Harmonic sources from industrial loads consists of three-phase power converters, arching devices, and saturable devices [4].

Commercial loads are characterized by a large number of small harmonic-producing loads. Although the power rating of these equipment is small, so that the harmonic distortion is low, the number of these harmonic producing equipment can be large to cause high harmonic distortion in the system. Power electronic switching used in these converters result in non-sinusoidal current and voltage waveforms. For example, switch-mode power supplies are common single-phase power supplies used in commercial loads. They have very high third-harmonic content in the current. Since third-harmonic current components are additive in the neutral of a three-phase system, the increased application of switch-mode power supplies cause overloading of neutral conductors. Three-phase power converters differ from single-phase converters mainly because they do not generate third-harmonic currents. They can however still be significant sources of harmonics at their characteristic frequencies.

Industrial loads such as electric arc furnaces also contribute to the distortion by having a nonlinear voltage-current characteristics. The arc current contains harmonic frequencies of both integer and non-integer orders. However, integer-order harmonic frequencies (particularly low-order starting with the second and ending with the seventh) predominate over the non-integer orders [3].

Transformers and the rotating machines in a power system are traditional harmonic producing devices. Harmonics are generated due to the nonlinear magnetizing characteristics of the steel in these devices. The relationship between transformer exciting current and magnetic flux is nonlinear. Electrically unbalanced windings of rotating machines will also result in a non-sinusoidal magnetic flux distribution around the air-gap producing electromagnetic forces.

2.4 Effects of Harmonic Distortion

Harmonic distortion has several effects on electric power equipments. For example, capacitor banks are overloaded by harmonic currents, since the capacitor reactances decrease with frequency. Harmonics also increase the dielectric losses in capacitors. Additional heating and loss of life also occurs. On the other hand, capacitors combine with source inductance to form a parallel resonant circuit. In the presence of resonance, harmonics are amplified. The resulting voltages exceed the voltage rating and result in capacitor damage.

Transformers operating in a harmonic environment suffer increased load losses which comprise copper losses and stray (winding eddy-current) losses. In addition, increased hysteresis and eddy-current losses occur. The possibility of resonance between the transformer inductance and power factor correction capacitor may result in harmonic amplification. Moreover, increased insulation stress due to the increased peak voltage may occur. These losses result in transformer heating and loss of life [38]. In presence of harmonics, transformers should be de-rated. Guidelines for transformer de-rating are defined in *ANSI/IEEE* standard C57.110.2008 [47].

Moreover, copper and iron losses are increased resulting in heating on rotating machines. Pulsating torques are also produced due to the interaction of the harmonics generated magnetic fields and the fundamental frequency generated magnetic field. These result in a higher audible noise [38].

Harmonics also affect protection and control equipment, metering devices, communication circuits and electronic loads. The interruption capability of circuit breakers is reduced. Relays whose operation is governed by the voltage/current peak or zero voltage are affected by harmonics. Electromechanical relays' time delay characteristics are altered in the presence of harmonics. Metering and instrumentation devices exhibit a different response to nonsinusoidal signals.

Harmonics result in interference with telephone circuits through inductive coupling. Through the shifting of zero crossing, harmonics impair the operation of electronic equipment and control circuits. Harmonics interfere with customer loads. Harmonics shorten incandescent lamp lifetime and result in failure of fluorescent lights [3].

2.5 Modelling of System Components

An inductive element with resistance R and reactance $X_L = 2\pi f L$ has an impedance of $Z = R + jX_L$ at the fundamental frequency. In the presence of harmonics this impedance becomes,

$$Z(h) = R + jhX_L. \quad (2.16)$$

where h is the harmonic order. The reactance of a capacitive element at fundamental frequency is $X_C = 1/(2\pi f C)$. In the presence of harmonics, the reactance becomes

$$X_c(h) = \frac{X_c}{h}. \quad (2.17)$$

As the frequency increases, conductor current concentrates towards the surface, resulting in the increased ac resistance and decreased internal inductance. Transformer and generator impedance in the presence of harmonics with skin effect included is [38]

$$Z(h) = \begin{cases} h^2 \cdot R + jhX, & \text{for a transformer,} \\ \sqrt{h} \cdot R + jhX, & \text{for a generator.} \end{cases} \quad (2.18)$$

Impedance for transmission lines at high frequencies is [38]

$$Z(h) = \sqrt{h} \cdot (R + jX). \quad (2.19)$$

In the presence of harmonics, the zero, positive and negative sequence impedances of a generator, neglecting skin effect, will be [38]

$$\begin{aligned} Z_0(h) &= R_a + jhX_0, & h = 3n = 3,6,9,12,15,\dots, \\ Z_1(h) &= R_a + jhX_d'', & h = 3n + 1 = 1,4,7,10,13,\dots, \\ Z_2(h) &= R_a + jhX_2, & h = 3n - 1 = 2,5,8,11,14,\dots, \end{aligned} \quad (2.20)$$

respectively, where

R_a is the armature resistance, Ω/phase ,

X_d'' is the subtransient reactance, Ω/phase ,

X_2 is the negative-sequence reactance, Ω/phase ,

X_0 is the zero-sequence reactance, Ω/phase ,

h is the harmonic order.

Taking skin effect into consideration, the armature resistance becomes,

$$R_a(h) = \sqrt{h}R_a. \quad (2.21)$$

Induction machines can be modeled by their locked rotor inductance and resistance representing the motor losses. The motor losses such as the eddy current losses and the

skin effect is included in the model by a frequency dependent resistance which is in series with the locked rotor inductance [1]. The motor impedance can be expressed as:

$$Z_{m_h} = R_m h^\alpha + jX_{m_h} . \quad (2.22)$$

In (2.22), R_m is the motor equivalent resistance and X_m is the locked motor reactance at harmonic order h , where $X_{m_h} = hX_m$. In addition, α in (2.22) is a parameter in the range [0.5-1.5] which represents the dependency of resistance to increasing frequency.

The transformer model is determined by leakage impedance and magnetizing impedance components. For three-phase transformers, the winding connections are important in determining the effect of the transformer on zero-sequence harmonic components: For example, delta connections isolate these currents. If the transformer is not a significant source of harmonics, the magnetizing impedance can be neglected. On the other hand, if the harmonic production of the transformer is significant, the magnetizing branch can be modeled as a current source of harmonics. For single phase analysis, transformers can be modeled by its short circuit impedance [3].

Linear passive loads are modeled in aggregate form of individual loads which have an effect on the damping and resonance conditions of the network at higher frequencies. The equivalent impedance for passive loads at harmonic frequencies can be determined at the point of supply by measurement of a sufficient number of frequencies however this method is time consuming and for this reason it is not applicable. An alternative method is based on the fundamental frequency load flow solution where the equivalent impedance can be obtained from the fundamental frequency active power, reactive power, and voltages. The linear passive load models and their parameters for harmonic analysis in literature [1,48,49] are given as follows:

Model 1. Series:

$$R = P \cdot \frac{V^2}{P^2 + Q^2}, \quad X = Q \cdot \frac{V^2}{P^2 + Q^2}, \quad (2.23)$$

Model 2. Parallel:

$$R = \frac{V^2}{P}, \quad X = \frac{V^2}{Q}, \quad (2.24)$$

Model 3 (Skin effect):

$$R_h = \frac{V^2}{(0.1 \cdot h + 0.9) \cdot P}, \quad X_h = \frac{V^2}{(0.1 \cdot h + 0.9) \cdot Q}, \quad (2.25)$$

Model 4. CIGRE model

$$R_2 = \frac{V^2}{P}, \quad X_2 = 0.073 \cdot R, \quad X_1 = R_2 / (6.7(Q/P) - 0.74), \quad (2.26)$$

Model 5:

$$R_h = R\sqrt{h}, \quad X_h = hX, \quad (2.27)$$

V , P and Q in (2.23) to (2.27) are the fundamental frequency nominal voltage, active power, and reactive power of the load respectively. The linear passive load models are illustrated in Figure 2.1.

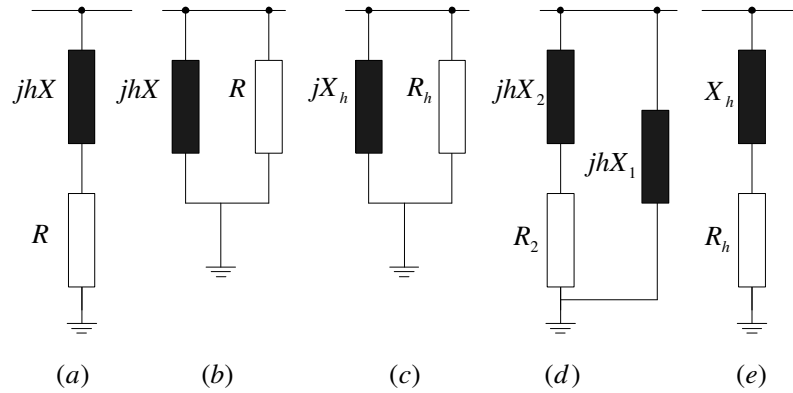


Figure 2.1 : Linear passive load models: (a) model 1; (b) model 2; (c) model 3; (d) model 4; (e) model 5.

The transmission lines can be modeled by the lumped parameter π circuit for short lines or the distributed parameter π circuit for long lines [1].

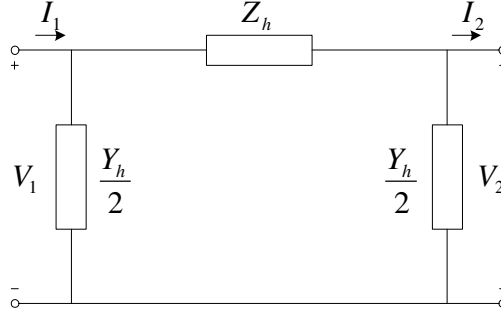


Figure 2.2 : Equivalent π model of a transmission line.

In Figure 2.2, Z_h is the multiphase coupled impedance and Y_h is the admittance at harmonic frequencies including all phase and ground conductors. The multiphase model can be simplified into a single phase π circuit using the positive sequence impedance data of the line for balanced harmonic analysis. Skin effects can be included into the line model by a frequency dependent resistance model [1],

$$R_h = R \left(1 + \frac{0.646h^2}{192 + 0.518h^2} \right), \quad (2.28)$$

where R is the resistance of the line at fundamental frequency and h is the harmonic order.

Shunt capacitors and reactors are modeled by their equivalent reactance at harmonic frequencies which is found using the rated power and voltage of the device at fundamental frequency [1]:

$$X_c = \frac{V^2}{hQ_C}, \quad X_L = h \frac{V^2}{Q_L}. \quad (2.29)$$

2.6 Modelling of Harmonic Sources

One important step in harmonic studies is to characterize and to model harmonic generating sources. Among the modern nonlinear loads, three-phase power electronic devices have a significant contribution in generating harmonics during their switching process. Though the widely spread single-phase power electronic devices such as *PCs*, *TVs*, and battery chargers also generates currents rich in odd harmonics; the harmonic magnitudes are usually small. Harmonic modeling for their group effects generally requires statistical or probabilistic approaches [50].

Many harmonic models have been proposed for representing three-phase power electronic devices [51]. The most common model is in the form of a harmonic current source, which is specified by its magnitude and phase spectrum. More detailed models become necessary if voltage distortion is significant or if voltages are unbalanced.

Harmonic flow analysis on power systems is generally performed using steady-state, linear circuit solution techniques. Harmonic sources (which are nonlinear elements) are generally considered to be injection sources into the linear network models. They can be represented as current injection sources or voltage sources.

As it is mentioned, for most harmonic flow studies, harmonic current sources are used: The current distortion for many nonlinear devices is relatively constant and independent of distortion in the supply system since the voltage distortion at the utility service bus is generally low (less than 5 percent according to the *IEEE Std 519* [3]).

Table 2.1: Voltage distortion limits.

Bus Voltage at PCC	Individual Voltage Distortion (%)	Total Voltage Distortion (%)
69 kV and below	3.0	5.0
69 kV through 160 kV	1.5	2.5
160 kV and above	1.0	1.5

Injected current values should be determined by measurements. In the absence of measurement and published data, it is common to assume that the harmonic content is inversely proportional to the harmonic number. However, this assumption is not valid for newer technology pulse-width modulation (*PWM*) drives and switch-mode power suppliers which have a higher harmonic content [4].

When the system is near resonance, a simple current source model will give a high prediction of voltage distortion. Moreover, the harmonic current will not remain constant at a high voltage distortion. As a result, the model will give an accurate response only when the resonance is eliminated.

For the cases where a more realistic response is required during resonant conditions, a Thevenin or Norton equivalent source model should be used. The additional impedance in the model characterizes the response of the parallel resonant circuit. In order to determine equivalent impedance, a simulation of the internals of the

harmonic producing load should be done by iterating on the solution or through detailed time-domain analysis [4].

2.7 Periodic Steady State Analysis

Periodic steady state analysis methods are based on the assumption that the system voltages and currents are periodic but non-sinusoidal. Fourier transform can be used for the periodic steady state analysis. When the electrical power systems consist of linear components, the superposition principle is applicable. Therefore, the electric current can be computed by summing the current contributions from each sinusoidal source for each harmonic frequency. The sinusoidal steady-state solutions can be then obtained using Fourier transform.

The periodic steady state analysis methods can be classified into two categories: (a) current injection methods and (b) harmonic power flow methods.

2.7.1 Current injection method

The current injection method is based on the assumptions that:

- (i) The power system consists of linear devices.
- (ii) The distorting devices are represented by linear models which inject harmonic currents.
- (iii) The injected harmonic current levels are independent of the voltage distortion at the device terminals.

The last assumption implies that the equivalent circuits of the system at the various harmonic frequencies are independent from each other. Therefore, at each harmonic frequency, an equivalent circuit can be developed and solved independently. By combining the results by superposition, the overall solution can be obtained.

The current injection method can be computed in an electrical power system as follows: At each frequency, the system admittance matrix will be constructed by all of the constant impedance contributions of the system loads, sources and transmission lines. Next, harmonic current sources at the corresponding harmonic frequency are combined into a current vector, according to source connectivity. Then the vector consisting of the harmonic voltage phasors at each system node is computed as:

$$\mathbf{V}_h = \mathbf{Y}_h^{-1} \mathbf{I}_h, \quad (2.30)$$

where

\mathbf{Y}_h is the system linear part admittance matrix computed at each harmonic frequency,

\mathbf{I}_h is the harmonic current vector,

\mathbf{V}_h is the harmonic voltage vector.

2.7.2 Harmonic power flow

The current injection method assumes that distorting devices generate a fixed amount of harmonics that are injected to the system. However, this assumption is an approximation and not realistic in many instances. In reality, the operation of distorting devices is affected by the voltage distortion at the interface with the network resulting in complex interactions between the distorting device and the network. The objective of the harmonic power flow method is to capture this interaction for the purpose of correctly predicting the level of harmonics at any point of the network.

The harmonic power flow method employs a nodal analysis to provide the harmonic voltages at each node of the system. For each node, the equations obtained from nodal analysis are formed for harmonics considered in the model. The resulting equations are a set of nonlinear equations. The most effective method to solve this set of equations is the use of Newton's method. The method is performed by linearizing the equations and by solving the resulting linear equations. Subsequently, the solution is updated and the process is repeated. When the equations are satisfied within a pre-specified tolerance limit, the process is declared converged. The latest iterate at this point gives the solution [1].

2.8 Harmonic State Estimation

The solution of the harmonic power flow can be determined by measurements which are voltage and current waveforms at various points of the system. Then the harmonic power flow solution can be extracted from these measurements. In general,

there may be more measurements than state variables. Then the problem becomes estimating a set of state variables from a number of measurements where the number of measurements is greater than the number of states to be estimated.

The state estimation problem is to estimate the system states (bus voltage magnitudes and phase angles) from the over-determined system equation. Generally the problem is formulated as a weighted least squares problem where the estimates of states minimize the weighted sum of the squares of the measurement error. The general structure of the state estimation is based on the single phase and single frequency model. Assuming that the system is balanced and symmetrical; voltage and current waveforms are pure sinusoidal with a constant frequency. The measurements used are the active power, reactive power, and voltage measurements in the power system. For the non-linear power flow model, the solutions are obtained iteratively.

The state estimation technique estimates the complex bus voltages which are generally used as state variables at the fundamental frequency and needs to be extended to estimate the harmonic distortion levels in the electric power systems.

The harmonic state estimation (*HSE*) technique, on the other hand, is developed to determine harmonic generation and propagation throughout the power system [19-22]. The task of the *HSE* is to generate the best estimate of the harmonic levels from limited measured harmonic data, corrupted with measurement noise. The three issues involved are the choice of state variables, some performance criteria and the selection of measurement points and quantities to be measured. State variables are those variables that, if known, completely specify the system. The voltage phasors at all of the busbars are usually chosen; as they allow the branch currents, shunt currents and currents injected into the busbar to be determined. Various performance criteria are possible, the most widely used is the weighted least-squares (*WLS*). In addition, observability analysis (*OA*) [1] is required in *HSE* to identify its solvability. The number and the location of harmonic measurements for *HSE* are determined from *OA*. A power system is said to be observable if the set of available measurements is sufficient to calculate all of the state variables of the system uniquely. A system is also observable if a unique solution can be obtained for the given measurements. A unique solution exists only if the measurement matrix has full rank [1].

Observability is dependent on the number, location and type of available measurements; and the network topology as well as the system admittance matrix. An *OA* should be performed again in each case, for a different network topology or for the same network topology but different measurement placements.

The formulation of *HSE* is presented with the following model [52]:

$$\mathbf{z} = \mathbf{h}(x) + \boldsymbol{\eta}, \quad (2.31)$$

where \mathbf{z} is a vector of harmonic measurements; \mathbf{x} is a vector of harmonic state; $\boldsymbol{\eta}$ is a vector of error; \mathbf{h} is a vector function depending on the system modeling. The harmonic state estimator is formulated by first selecting the harmonic state then by selecting the harmonic measurements and finally by selecting the harmonic system model.

The measurements (\mathbf{z}), are related to the state variables with (2.32) and (2.33) respectively;

$$\mathbf{z}_{current} = \mathbf{Y} \cdot \mathbf{x} + \mathbf{e}, \quad (2.32)$$

$$\mathbf{z}_{voltage} = \mathbf{T} \cdot \mathbf{x} + \mathbf{e}, \quad (2.33)$$

where all the values are of complex value, \mathbf{Y} is the admittance matrix of proper dimensions. \mathbf{T} is a matrix whose entries are either 1 or 0. Equations (2.32) and (2.33) can be lumped into one equation such as:

$$\mathbf{z} = \mathbf{H} \cdot \mathbf{x} + \mathbf{r}. \quad (2.34)$$

The least square estimation is formed as an optimization problem:

$$\begin{aligned} \text{minimize} & \rightarrow \mathbf{r}^H \mathbf{W} \mathbf{r}, \\ \text{subject to} & \rightarrow \mathbf{r} = \mathbf{z} - \mathbf{H}\mathbf{x}. \end{aligned} \quad (2.35)$$

where superscript H means Hermitian transpose and \mathbf{W} is the weighting matrix. The elements of the weighting matrix represent the measurement accuracy and reliability of corresponding measurement. For the sake of simplicity, the harmonic order h is dropped in (2.35), however the estimation is carried out for each harmonic order of interest. The solution of (2.35) for the state vector \mathbf{x} is

$$\mathbf{x} = (\mathbf{H}^T \mathbf{W} \mathbf{H})^{-1} \mathbf{H}^T \mathbf{W} \mathbf{z}, \quad (2.36)$$

where the measured values' states and the measurement matrix are complex values. In literature, instead of *WLS* there are also other performance criteria exist such as weighted least absolute value, least median of squares or non-quadratic estimators [52].

3. LOCATION OF SINGLE HARMONIC SOURCE USING DISTANCE MEASURE APPROACH

3.1 Introduction

When a harmonic current source is injected into a bus of an electric power system; it leads to a dynamic transition from the normal system condition to a disturbed system condition. The current and voltage waveforms measured will not only change as a function of the fundamental frequency system condition, but also change according to the parameters of the harmonic load, harmonic order and harmonic source location.

Figure 3.1 shows a representation of an electric power system disturbed with a harmonic source. It is assumed that;

- (i) the power system consists of linear devices,
- (ii) the distorting device is represented by linear models, which inject harmonic currents,
- (iii) the injected harmonic current levels are independent of the voltage distortion at the device terminals.

Last assumption implies that the equivalent circuits of the system at various harmonic frequencies are independent from each other. According to the superposition theory, power system harmonic circuit is represented as a combination of the circuit with fundamental frequency contribution and the circuits due to the harmonic sources at each harmonic frequency. The currents and voltages measured at a certain location of the power system will be the sum of the values produced independently by each of the sources in the system: Fundamental frequency components are produced by generators and harmonic components are produced by harmonic producing sources. Hence, by solving the system at each frequency, each source and its effect can be considered independently. Then the results are summed to determine a particular unknown quantity.

For the studies in this thesis, it is assumed that generators produce only the fundamental frequency components.

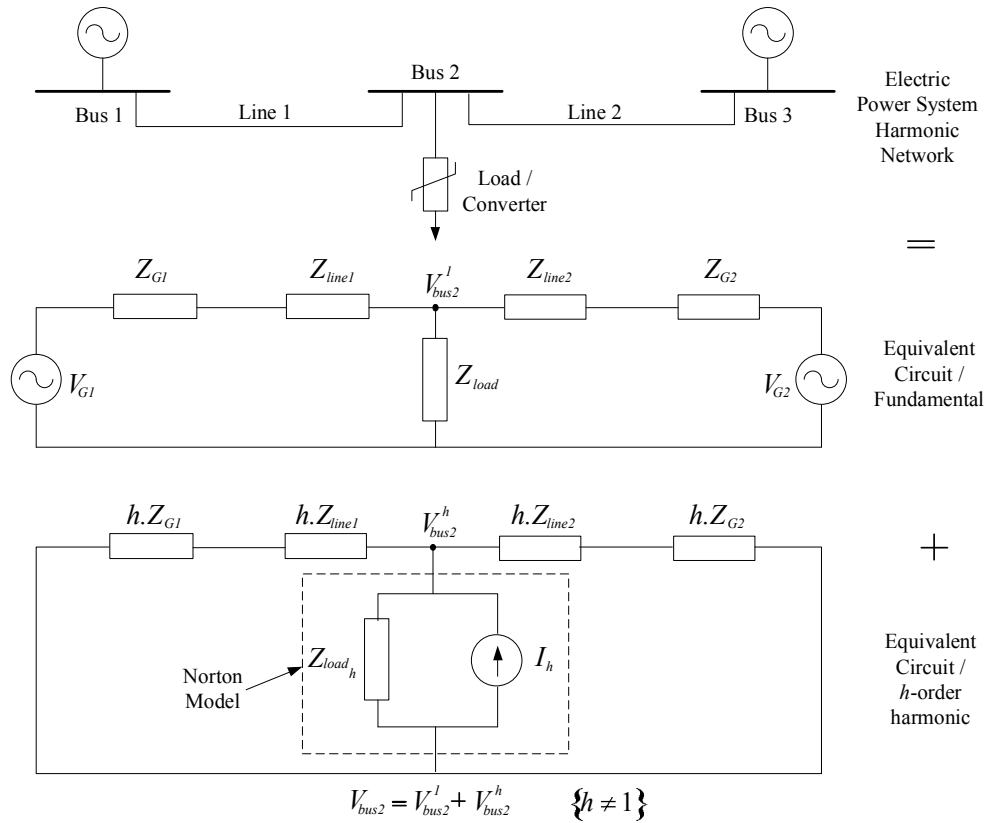


Figure 3.1 : Superposition of networks to form a harmonic network.

3.2 The Distance Measure Index

Determining the location of a fault on ac transmission and distribution lines is one of the main study areas in power engineering. One-terminal (one-end) and two-terminal (two-end) impedance-based methods are the primary approaches to determine fault location [53]. For example, one-terminal impedance-based fault locators calculate the fault location from the apparent impedance when looking into the line from one end [54]. For this approach, the line impedance should be accurately estimated to locate all fault types: Synchronous phasor measurements obtained from direct measurement from a digital relay or a fault recorder can be used to calculate impedance parameters with a high degree of accuracy. By knowing the line impedance, the distance to the fault can be determined.

The accuracy of the fault location task can be increased by using two-terminal impedance method. In this method the type of fault does not need to be calculated and therefore positive-sequence components are used only. The main drawback of this method is that data from both ends must be gathered at one location to be analyzed, whereas the one-terminal location can be done at the line terminal by the relay or other device which collect the data. On the other hand, in two-terminal method, the effect of fault resistance, loading, and charging current can be eliminated which increases the accuracy of the estimation. More information about one-terminal and two-terminal impedance methods can be found in the literature [55-57].

The aspect of two-terminal impedance-based fault location approach is used to develop a harmonic source location approach. Figure 3.2 represents an electric power system with a single harmonic source and the equivalent h order harmonic source representation for the relevant harmonic frequency. Z_h indicates the line impedance between $bus-S$ and $bus-R$. The unknown l is the distance from $bus-S$ to $bus-H$ (the bus where the harmonic source is located). All the quantities, except l , are complex values. The value of l is a real number such that it obeys $l \in [0,1]$. It is assumed that the supply sides' ($bus-S$ and $bus-R$) voltage and current measurements are available. Therefore the complex values V_{S_h} , I_{S_h} , V_{R_h} , I_{R_h} and Z_h can be obtained from measurements.

By applying Kirchoff's Voltage Law for the loops given in Figure 3.2, the voltage V_{H_h} at the harmonic source location can be determined by using the following algebraic complex equation:

$$V_{H_h} = V_{S_h} + l \cdot Z_h \cdot I_{S_h}, \quad (3.1)$$

where l is the unknown parameter (distance to the harmonic source position).

$$V_{H_h} = V_{R_h} + (1-l) \cdot Z_h \cdot I_{R_h}, \quad (3.2)$$

By subtracting (3.1) from (3.2) and re-arranging, it follows:

$$V_{S_h} - V_{R_h} + l \cdot Z_h \cdot I_{S_h} - (1-l) \cdot Z_h \cdot I_{R_h} = 0, \quad (3.3)$$

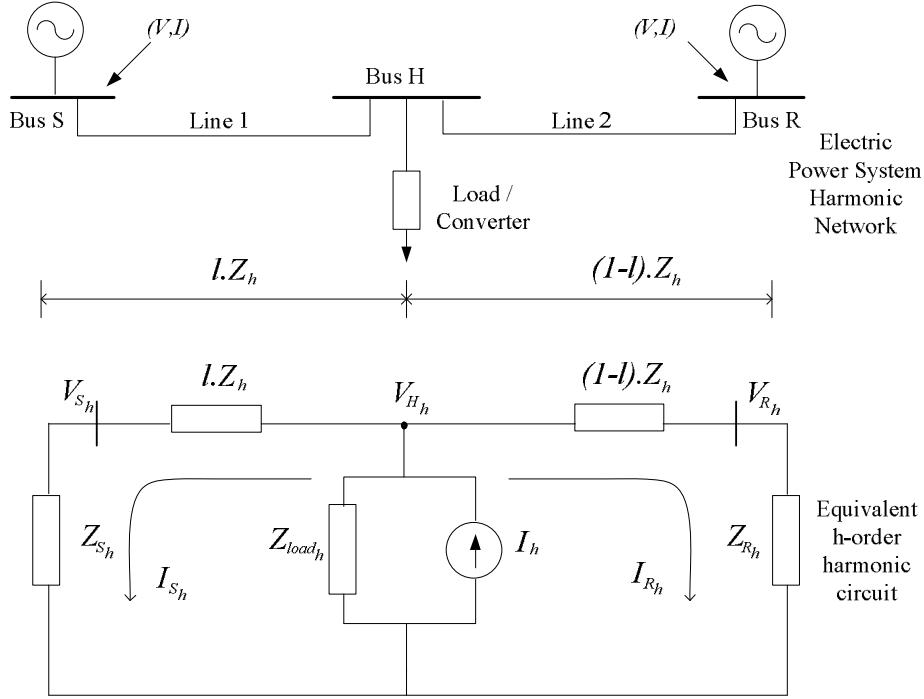


Figure 3.2 : Harmonic source location in a single-phase network.

$$l = \frac{-V_{S_h} + V_{R_h} + Z_h \cdot I_{R_h}}{Z_h \cdot (I_{S_h} + I_{R_h})}. \quad (3.4)$$

The value of the unknown variable l can be calculated from (3.4). Since the machines and loads are represented as constant impedances at harmonic frequencies, the problem becomes linear. The linear equation can be directly solved and no iteration is required. As it is seen from (3.4), there is no need to obtain harmonic source impedance and harmonic source current value to calculate the distance. The distance l can be solved for each harmonic order circuit in the given simplified single phase network.

The equation given by (3.4) can be solved for different locations between bus- S and bus- R to investigate its validity in different situations. The set of distance values when the source is at bus- S , $1/4$ away from bus- S , $2/4$ away from bus- S , $3/4$ away from bus- S and finally at bus- R are obtained respectively. According to the results of the analysis, the set of values for distance l can be given as follows:

$$l = \left\{ 0, \frac{1}{4}, \frac{2}{4}, \frac{3}{4}, 1 \right\}, \quad (3.5)$$

These results show that the equations given by (3.4) and (3.1) is valid for such a network given by Figure 3.1. For the analyses, the calculated distance should yield the same value for each harmonic order of the harmonic source. Moreover the calculated distance should obey the set given by (3.5), however if any difference show up, this would be due to measurement, modeling and some other errors. To obtain the range of error, it can be further analyzed statistically.

The distance measure set for an n -node electrical circuit can be obtained by a straightforward procedure. The circuit model for such a system is given in Figure 3.3. The harmonic order is omitted for the sake of simplicity, but it should be known that the procedure can be applied for each harmonic order of interest.

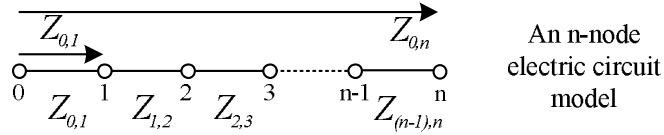


Figure 3.3 : A n -node electrical circuit model.

$$Z_{TOT} = \sum_{i=1}^n Z_{(i-1),i}, \quad (3.6)$$

Z_{TOT} in (3.6) is the total system impedance and n denotes the number of nodes (buses). The distance measure can be given as

$$d = \frac{-V_S + V_R + Z_{TOT} \cdot I_R}{Z_{TOT} \cdot (I_S + I_R)}, \quad (3.7)$$

where subscript S corresponds to node-0 and subscript R corresponds to node- n . In addition, d denotes the distance to the harmonic source and d and n are discrete numbers.

The set of values for the distance measure can be defined as:

$$d = \left\{ 0, \frac{Z_{0,1}}{Z_{TOT}}, \frac{Z_{0,2}}{Z_{TOT}}, \frac{Z_{0,3}}{Z_{TOT}}, \dots, \frac{Z_{0,(n-1)}}{Z_{TOT}}, \frac{Z_{0,n}}{Z_{TOT}} \right\}. \quad (3.8)$$

Note that $Z_{0,n} = Z_{TOT}$.

According to (3.7) and (3.8) the following relation can be formed:

$$\frac{Z_{0,k}}{Z_{TOT}} = d = \frac{-V_S + V_R + Z_{TOT} \cdot I_R}{Z_{TOT} \cdot (I_S + I_R)}, \quad (3.9)$$

and

$$Z_{0,k} = d \cdot Z_{TOT}, \quad (3.10)$$

where k denotes the bus number and it is a discrete number with the property: $k \in [0, n]$. Harmonic order h can be included into (3.9) and (3.10).

These results imply that if the harmonic impedances are known accurately, location of the harmonic source can be determined straightforwardly according to (3.9).

For a network topology given in Figure 3.3 the distance measure set is a $(n+1)$ -size vector. For this topology, in order to locate a single harmonic source, four measurements are required. These are obtained as a set of one voltage and one current measurements at both ends of the network. However, if the system impedance and node voltages are known, current measurement will be redundant. Therefore, by eliminating current parameter, (3.4) and (3.7) can be represented in terms of impedance and voltage values:

$$l = f(z, V), \quad d = f(z, V), \quad (3.11)$$

where l has continuous values and d has discrete values.

3.2.1 Analysis on a 3-branch n -node electric circuit model

It is seen in the previous analysis that to accurately determine the location of the harmonic source, measurement (node voltage) at both ends of the system is required.

To determine the meter positions for a 3-branch n -node circuit model, a 7-node teed feeder electrical circuit given in Figure 3.4 is analyzed. In this circuit, node-6 and node-7 are connected to node-2 through a branch. Some analyses based on measurements at two ends that do not contain node-6 and node-7 are performed. It was observed that when the source is connected to node-2, node-6 or node-7, the

location algorithm can not discriminate the location of the source among these 3 nodes, when extra measurement on the additional branch is not available. This is so because the impedance ratio given by (3.9) is the same for all 3 nodes. It is thus necessary to obtain an extra measurement from the end of the additional branch which includes node-6 and node-7.

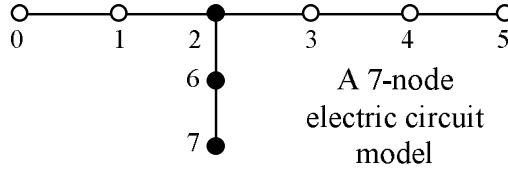


Figure 3.4 : A 7-node 3-branch electrical circuit model.

To conclude, in order to locate the harmonic source accurately, measurements should be obtained at each end-node of each branch. For the network given in Figure 3.3, measurements should be obtained at node-0 and node-n. For the network given in Figure 3.4, measurements should be obtained at node-0 , node-5 and node-7 .

3.3 The Nodal Analysis Approach

When the number of branches increase, the degree of complexity of the distance index increases. This is so because, the relation of distance index with each system equation becomes complicated for networks with 3-branches or more (where each system equation corresponds to the response for the relevant position of the harmonic source in the network). These results affect the applicability of the distance measure index for the complex n -branch networks.

A more practical location approach based on the nodal analysis will be introduced now.

Consider the network given in Figure 3.5. The circuit contains $(n+m+p)$ -nodes.

The system equations under non-sinusoidal conditions can be represented by the following linear equation in compact form as:

$$\mathbf{I}_h = \mathbf{Y}_{bus_h} \cdot \mathbf{V}_h \cdot \tag{3.12}$$

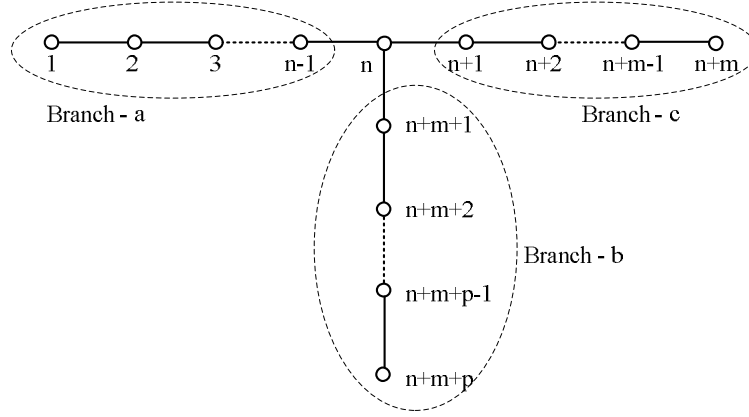


Figure 3.5 : A $(n+m+p)$ -node 3-branch electrical circuit model.

Equation 3.12 can also be stated as:

$$\begin{bmatrix} I_1 \\ I_2 \\ \vdots \\ I_{n+m+p} \end{bmatrix}_h = \begin{bmatrix} Y_{11} & Y_{12} & \cdots & Y_{1,n+m+p} \\ Y_{21} & Y_{22} & \cdots & Y_{2,n+m+p} \\ \vdots & \vdots & \ddots & \vdots \\ Y_{n+m+p,1} & Y_{n+m+p,2} & \cdots & Y_{n+m+p,n+m+p} \end{bmatrix}_h \begin{bmatrix} V_1 \\ V_2 \\ \vdots \\ V_{n+m+p} \end{bmatrix}_h, \quad (3.13)$$

where \mathbf{I}_h is the n -dimensional harmonic current injection vector, \mathbf{Y}_h is the $n \times n$ dimensional system harmonic admittance matrix and \mathbf{V}_h is n -dimensional harmonic bus voltage vector which corresponds to the measurements. The solution of (3.13) yields

$$\mathbf{I}_h = [I_1 \ I_2 \ \cdots \ I_n \ I_{n+1} \ \cdots \ I_{n+m} \ I_{n+m+1} \ \cdots \ I_{n+m+p}]_h^T. \quad (3.14)$$

In (3.14), superscript T refers to transpose operation. (3.14) can be used to locate harmonic sources. If all of the node voltages and system admittance matrix is known in (3.13), the location of harmonic sources can be obtained from (3.14) which will have non zero elements for the positions where the sources are located.

Remark:

- In order to solve (3.13), all of the node voltages in addition to system bus admittance matrix should be known.
- It is seen that the vector \mathbf{I}_h can be used as an indicator to locate the node to where the source is injected.

3.4 Results

- The distance measure index can be applied for each harmonic order circuit according to the superposition theory. If a source with h different harmonic orders is injected to a bus, all of the results will point to the same bus. However, measurement errors in the system can result in changes in distance measure index values.
- As it is seen from (3.4), when the distance measure index is used, there is no need to obtain harmonic source impedance and harmonic source current values for calculating the distance.
- If the system impedance matrix and node voltages are known, current measurement will not be required.
- To correctly locate the harmonic source for a 3-branch system, three measurements (one measurement at each branch end-node) are sufficient.
- To correctly locate the harmonic source for an n -node m -branch system, m -measurements (each measurement at each branch end-node) are sufficient.
- When the number of branches increase, complexity of the distance measure increases since the relation of distance index with each system equation becomes complicated for systems with 3-branches or more. In this condition, it becomes difficult to correctly define the distance measure index from any measurement point to the source location. Due to the difficulty in modelling the distance measure when the branch number in a network increases, the research on this approach is not proceeded and also the effect of measurement errors on the approach is not analysed for the same reason.
- The approach given in Section 3.3 eliminates the difficulty (modelling the distance measure when number of branches increase) of forming such a formulation. There is not a necessity to search such a distance measure from the measurement point to the source.
- As it is stated in Section 3.3 Remark, measurements from all of the nodes in an n -node network must be obtained to solve (3.13) and to locate the harmonic source. On the other hand, this is not a practical solution in power

systems. Therefore, a location approach based on limited metering is required. This issue is solved by the approach proposed in the next chapter.

4. LOCATION OF SINGLE HARMONIC SOURCE USING IMPEDANCE NETWORK APPROACH

4.1 Introduction

Determination of network harmonic impedances is required for designing an effective harmonic source location task. Harmonic impedances of a system characterize the frequency response of the system at specific buses. A typical use of the harmonic impedance is for the designing of harmonic filters, for the verification of harmonic limit compliance, and for the prediction of system resonance [4,58,59].

It is very desirable in many applications to directly measure the network harmonic impedances. Several methods have been proposed in literature for this purpose. These methods can be classified into two types, namely the transients-based methods and the steady-state-based methods [60].

The transients-based methods inject transient disturbances into the system [58,60-63]. The frequency-dependent network impedances are extracted from voltage and current transients using suitable signal processing techniques based on Fourier analysis [58,60]. In [58,59,61] high frequency voltage and current transients are created through capacitor bank switching and then spectral analysis of the transients provides the frequency domain impedance characteristics. The main problems associated with transient-based methods are the need for a high-speed data acquisition system and for the source of disturbances.

The steady-state based methods use pre-disturbance and post-disturbance steady-state waveforms [60,64]. Typical disturbances are harmonic current injections produced by an external source or switching of a network component. Since there are no transients involved, the methods can only determine network impedances at harmonic frequencies. On the other hand, since there is no need for a high-speed data acquisition system, the steady-state method can be implemented with many common, low-cost power quality monitors.

In this thesis, a method is proposed to locate harmonic sources connected to electric power systems. The method is based on the impedance network approach. Prior to analysis, bus impedance matrix for each harmonic should be constructed. Impedance network approach uses the impedance ratios of two rows in bus impedance matrix and compares them to the voltage ratio measured at the corresponding nodes. The meter positions are determined by a new optimization method developed in this thesis.

Let's assume that there is a circuit with n nodes, bus admittance matrix can be easily constructed for each harmonic order. Most of the elements of the matrix may have zero values because usually a full connection does not exist in power systems. The bus admittance matrix for each harmonic order can be written as

$$\mathbf{Y}^{(h)}_{bus} = \begin{bmatrix} Y_{1,1}^{(h)} & Y_{1,2}^{(h)} & \cdots & Y_{1,n}^{(h)} \\ Y_{2,1}^{(h)} & Y_{2,2}^{(h)} & \cdots & Y_{2,n}^{(h)} \\ \vdots & \vdots & \ddots & \vdots \\ Y_{n,1}^{(h)} & Y_{n,2}^{(h)} & \cdots & Y_{n,n}^{(h)} \end{bmatrix}. \quad (4.1)$$

The system harmonic admittance matrix is formed according to the system topology using admittances of each individual power system component which are obtained from the models for harmonic analysis, i.e. models given in Section 2.5. Inverse of the harmonic admittance matrix $\mathbf{Y}^{(h)}_{bus}$ gives harmonic impedance matrix $\mathbf{Z}^{(h)}_{bus}$ such that

$$\mathbf{Z}^{(h)}_{bus} = (\mathbf{Y}^{(h)}_{bus})^{-1}, \quad (4.2)$$

It is conceptually simple to invert $\mathbf{Y}^{(h)}_{bus}$ to find the bus impedance matrix of $\mathbf{Z}^{(h)}_{bus}$, but such direct inversion is not convenient when the systems to be analyzed are large scale; since inverting $\mathbf{Y}^{(h)}_{bus}$ in that case is computationally inefficient. On the other hand, the bus admittance matrix may not need to be determined in order to obtain $\mathbf{Z}^{(h)}_{bus}$. Formulation of $\mathbf{Z}^{(h)}_{bus}$ using a direct building algorithm is a straightforward process on a computer. The direct building algorithm starts by choosing a branch tied to the reference from a node and adding a second branch connected from a new node to this node. The starting node and the new node then have one row and one column each in the (2×2) bus impedance matrix which

represents them. Next, a third branch connected to one or both of the first two chosen nodes is added to expand the evolving network and expand its $\mathbf{Z}^{(h)}_{bus}$ representation. In this manner, the bus impedance matrix is built up one row and one column at a time and the evolving $\mathbf{Z}^{(h)}_{bus}$ matrix is modified until all branches of the physical network have been incorporated into $\mathbf{Z}^{(h)}_{bus}$. Whenever possible at any stage, it is computationally more efficient to select the next branch to be added between two nodes with rows and columns already included in the evolving $\mathbf{Z}^{(h)}_{bus}$. The combination of these steps constitutes the $\mathbf{Z}^{(h)}_{bus}$ building algorithm [65].

It is assumed in this thesis that prior to the harmonic location procedure, the network harmonic impedance matrix is obtained using one of the methods mentioned above.

Bus impedance matrix consisting mostly of non-zero elements is given by

$$\mathbf{Z}^{(h)}_{bus} = \begin{bmatrix} Z_{1,1}^{(h)} & Z_{1,2}^{(h)} & \cdots & Z_{1,i}^{(h)} & \cdots & Z_{1,j}^{(h)} & \cdots & Z_{1,n}^{(h)} \\ Z_{2,1}^{(h)} & Z_{2,2}^{(h)} & \cdots & Z_{2,i}^{(h)} & \cdots & Z_{2,j}^{(h)} & \cdots & Z_{2,n}^{(h)} \\ \vdots & \vdots & \vdots & \vdots & \vdots & \vdots & \vdots & \vdots \\ Z_{k,1}^{(h)} & Z_{k,2}^{(h)} & \cdots & Z_{k,i}^{(h)} & \cdots & Z_{k,j}^{(h)} & \cdots & Z_{k,n}^{(h)} \\ \vdots & \vdots & \vdots & \vdots & \vdots & \vdots & \vdots & \vdots \\ Z_{l,1}^{(h)} & Z_{l,2}^{(h)} & \cdots & Z_{l,i}^{(h)} & \cdots & Z_{l,j}^{(h)} & \cdots & Z_{l,n}^{(h)} \\ \vdots & \vdots & \vdots & \vdots & \vdots & \vdots & \ddots & \vdots \\ Z_{n,1}^{(h)} & Z_{n,2}^{(h)} & \cdots & Z_{n,i}^{(h)} & \cdots & Z_{n,j}^{(h)} & \cdots & Z_{n,n}^{(h)} \end{bmatrix}. \quad (4.3)$$

The superscript h denotes the harmonic order ($h = 2, 3, 4, \dots, k$) representing the integer multiples of the fundamental frequency. $\mathbf{Z}^{(h)}_{bus}$ is the $n \times n$ system harmonic impedance matrix. Since $\mathbf{Y}^{(h)}_{bus}$ is symmetrical around the principal diagonal, $\mathbf{Z}^{(h)}_{bus}$ must also be symmetrical. The impedances on the principal diagonal of the bus impedance matrix are called driving-point impedances. $Z_{i,i}$ is determined by open-circuiting the current sources at all nodes except i^{th} and injecting the current I_i at node i as,

$$Z_{i,i}^{(h)} = \left. \frac{V_i^{(h)}}{I_i^{(h)}} \right|_{I_j^{(h)}=0 \text{ for all } j \neq i}. \quad (4.4)$$

The impedances on the off-diagonal of the bus impedance matrix are called transfer impedances and can be calculated as

$$Z_{i,j}^{(h)} = \frac{V_i^{(h)}}{I_j^{(h)}} \bigg|_{I_k^{(h)}=0 \text{ for all } k \neq j}, \quad (4.5)$$

where $(k, \ell, i, j) \in \{1, 2, \dots, n\}$ and h is the harmonic order indice.

The bus admittance matrix and the bus impedance matrix described by (4.1) and (4.3), respectively, can be developed for each harmonic order. Nevertheless, for the rest of the analyses h will be omitted from the impedances for the sake of simplicity.

According to the nodal analysis, the set of equations defining a circuit with n nodes for a specific harmonic frequency is

$$\begin{bmatrix} V_1 \\ V_2 \\ \vdots \\ V_n \end{bmatrix} = \mathbf{Z}_{bus} \begin{bmatrix} I_1 \\ I_2 \\ \vdots \\ I_n \end{bmatrix}, \quad (4.6)$$

where V_i is the voltage phasor at bus i , $i \in [1, n]$, at a harmonic order h ; I_i is the net current injection phasor at bus i at a harmonic order h . A phasor is a complex number defined by its phase and amplitude. The calculation of the phasor parameters can be accomplished using Fourier analysis.

We will consider two nodes, namely k and ℓ in the system from where voltage measurements are taken. The pair (k, ℓ) will be defined as a “measurement pair”.

Therefore, the voltage measured at k^{th} node is given in a general way as

$$V_k = \sum_{j=1}^n Z_{k,j} I_j. \quad (4.7)$$

The current I_j in (4.7) is the harmonic current source injected to the j^{th} node such that $j \in (1, 2, \dots, n)$. The ratio of voltage phasors at k^{th} node to the voltage at ℓ^{th} node can be denoted as

$$\frac{V_k}{V_\ell} = \frac{\sum_{j=1}^n Z_{k,j} I_j}{\sum_{j=1}^n Z_{\ell,j} I_j}. \quad (4.8)$$

In (4.8), the left side is a known quantity because of measurements taken from node k and node ℓ . The impedances for the specific harmonic order are also known. What is left is the currents of n harmonic sources. In case of a single harmonic current source in the circuit, all currents will be zero except one which is i^{th} current. With a single harmonic current source located at i^{th} node, (4.8) can be written as

$$\frac{V_k}{V_\ell} = \frac{Z_{k,i}}{Z_{\ell,i}}. \quad (4.9)$$

Finding the location of the single harmonic source is based on searching the impedance ratio which is equal to the measured voltage ratio at that specific harmonic frequency. When the equivalence in (4.9) is obtained, the location of harmonic current source, injected to node- i may be detected.

An accurate harmonic location algorithm requires obtaining accurate measurements from the network. Time synchronized phasor measurements, which are achieved by global positioning system (*GPS*) can be used to obtain accurate harmonic measurements [66]. Using this method, several measurements with time synchronization from a large network can be obtained. Phasor measurement units (*PMUs*) are used to provide synchronized measurements of real time phasors of bus voltage and line currents. Synchronicity is achieved by same-time sampling of voltage and current waveforms using timing signals from the global positioning system (*GPS*). The current and potential applications of phasor measurement units have been well-documented [67].

For the task of selecting the measurement pairs, it is obvious that there will be many possibilities among the nodes of the system. To select the nodes from where the measurements will be taken, an optimal meter placement algorithm is proposed. In the developed algorithm, it is aimed to overcome misallocation of the harmonic source because of deviations in network harmonic impedance values.

Let's consider the measured nodes as k and ℓ . An impedance ratio for i^{th} node can be defined as

$$\alpha_i^{k,\ell} = \frac{Z_{k,i}}{Z_{\ell,i}}, \quad (4.10)$$

for $i = 1, \dots, n$. The *impedance ratio set* for nodes k and ℓ can be defined as

$$\alpha^{k,\ell} = \{\alpha_1^{k,\ell}, \alpha_2^{k,\ell}, \dots, \alpha_n^{k,\ell}\}. \quad (4.11)$$

The elements of the impedance ratio set in (4.11) can be either *unique* or *non-unique*. If the elements of the set are unique, then all of the elements in the set will be different and for this reason the harmonic source, at any one of the nodes can be located. Otherwise, locating the harmonic source in certain nodes may not be possible because the value of the voltage ratio could exist more than ones in the impedance ratio set. Extra measurement is needed to overcome this problem. For example, in that case, two or more sets of impedance ratios according to each extra measurement could be used to identify the harmonic source uniquely.

The next section is about harmonic source location procedure. First, the definition of unique and non-unique sets are given. Then an approach developed for selecting the measurement pairs is described. Flow chart of the location procedure is given and the approach is applied to several model systems. Finally the results are discussed.

4.2 Harmonic Source Location Procedure

Single harmonic source location procedure can be described in two cases as unique sets or non-unique sets.

4.2.1 Unique sets

Consider the impedance ratio set $\alpha^{k,\ell}$ for nodes k and ℓ for which the elements of the set obey; $\alpha_i^{k,\ell} \neq \alpha_j^{k,\ell}$ when $(k \neq \ell), (i \neq j)$. This set is then called a *unique set*. In a unique set, set members are not repeated. In fact, a set member which is equal to the measured voltage ratio V_k/V_ℓ is searched in a set. The i^{th} member of $\alpha^{k,\ell}$ which

provides $\alpha_i^{k,\ell} = V_k/V_\ell$ is the node to which the single harmonic current source is injected.

The unique sets can be searched based on

$$\alpha_i^{k,\ell} \neq \alpha_j^{k,\ell} \quad \forall (i, j, k, \ell) \in \{1, 2, \dots, n\} \wedge (k \neq \ell), (i \neq j). \quad (4.12)$$

In (4.12), k and ℓ are corresponding to the two row numbers in (4.3) where measurements are taken and i and j in (4.12) are corresponding to the column numbers in (4.3) to which the current source is injected. If (4.12) is satisfied, the set is called a unique set.

The number of unique sets in a network depends on the network topology as well as the impedance values of the related harmonic. In certain situations, where the impedance ratios in impedance ratio sets for the corresponding measurement pairs are the same due to system topology, unique sets may not exist and more than one set which results from extra measurements may be needed to locate the harmonic source.

4.2.2 Non-unique sets

Consider the impedance ratio set $\alpha^{k,\ell}$ for nodes k and ℓ for which at least one member is repeated more than ones. This implies that $\alpha_i^{k,\ell} = \alpha_j^{k,\ell}$ for some i and j .

This can be also expressed for any two nodes k and ℓ as

$$\alpha_i^{k,\ell} = \alpha_j^{k,\ell} \quad \forall (i, j, k, \ell) \in \{1, 2, \dots, n\} \wedge (k \neq \ell), (i \neq j). \quad (4.13)$$

In (4.13), k and l are corresponding to the two row numbers in (4.3) where measurements are taken, and i and j in (4.13) are corresponding to the column numbers in (4.3) to which the current source is injected.

If the condition in (4.13) is obtained, the set is called a non-unique set. When there are at least two columns that give the value in (4.13); in other words when at least two members of the set in (4.11) are equal to each other, the value of ratio (V_k/V_ℓ) will be repeated in the set in (4.11). In that case, it is not possible to detect the node to which the harmonic current source is connected. Therefore one or more extra measurements are required.

4.3 Selection of Measurement Pairs

In order to locate the harmonic current source, it is first required to determine the nodes from where measurements will be taken. The nodes (k, ℓ) where the measurements are taken for calculating (V_k/V_ℓ) ratio will be defined as a *measurement pair*. Note that for a measurement pair the condition $k \neq \ell$ should exist. There may be many unique sets relating to measurement pairs. A procedure to select the best measurement pairs is required for a good estimation of harmonic source location. The procedure that will be described here is based on a methodology to select a set with *maximum distance between its closest members*. This selection procedure may allow overcoming misallocation of the harmonic source because of voltage measurement errors and deviations in network impedance values.

All measurement pairs (k, ℓ) that satisfy (4.12) may be used to locate the harmonic current source. However, in case of errors, for instance the members of $\alpha^{k,\ell}$ set may deviate from correct values slightly. This will definitely lead mislocation of harmonic source. If a selection algorithm based on finding a set with maximum distance between its closest members is used, slight deviations of the members of the set may be tolerated.

The number of measurement pairs depends on the size of bus impedance matrix. If the matrix size is given by $n \times n$, the number of all measurement pairs (k, ℓ) can be found by permutations $P(n, r)$ such that

$$P(n, r) = \frac{n!}{(n-r)!}. \quad (4.14)$$

The number m will be used to represent the number of permutations, that is, $m = P(n, r)$. There will be m number of impedance ratio sets of $\alpha^{k,\ell}$. The value of r is corresponding to 2 measurements (for (k, ℓ) pair).

As an example, consider a power system with 22 nodes, the number of all measurement pairs will be $22!/(22-2)! = 462$. Note that the measurement pair (k, ℓ) and the measurement pair (ℓ, k) are counted separately because corresponding voltage ratios that will be used in the harmonic location algorithm are different.

The matrix \mathbf{M} will be used to represent the list of all possible measurement pairs for $k \neq \ell$, and the size of this matrix will be $(m \times 2)$.

The members of $\alpha^{k,\ell}$ sets may have repetition as defined by (4.13) in Section 4.2.2. Let's define a function $Num()$ which gives the number of repetitions for a set and also returns an integer number such that $Num(): \mathbb{C} \rightarrow \mathbb{Z}$. The number of similar values (repetitions) in $\alpha^{k,\ell}$ can be represented by

$$Num(\alpha^{k,\ell}): \text{number of repeated } \alpha_i^{k,\ell} \text{ in a set } \alpha^{k,\ell}, \quad (4.15)$$

such that $(i, k, \ell) \in \{1, 2, \dots, n\} \mathcal{A} (k \neq \ell)$ and for all $\alpha_i^{k,\ell}$ the equality $\alpha_i^{k,\ell} = \alpha_j^{k,\ell}$ is valid. For $Num(\alpha^{k,\ell}) = 1$, all elements of $\alpha^{k,\ell}$ set are unique and the harmonic source in any node in the network can be located. Otherwise, there will be similar values in the set where harmonic sources can not be located. For example, if $Num(\alpha^{k,\ell}) = 3$, there are three nodes in the network with the same impedance ratios and if a harmonic source is connected to one of these nodes, it can not be located by the voltage measurements at nodes k and ℓ alone.

The location of harmonic current source may be determined if the impedance ratios in a set $\alpha^{k,\ell}$ are unique. For certain symmetrical topologies and/or impedance values, the value of $Num(\alpha^{k,\ell})$ may not be equal to 1. Nevertheless, there may be many separate $\alpha^{k,\ell}$ sets with the same repetition numbers. For these reasons, a method should be developed to select the suitable measurement pair for the process of harmonic source location.

4.4 Optimal Meter Placement Algorithm (OMPA)

For a proper harmonic source location algorithm, the question of -decision of which (V_k, V_ℓ) measurement pair/pairs should be selected among all measurement pairs- should be answered. And this is defined as an optimization problem that needs to be solved.

An indice is defined for the solution of the problem. This indice is defined by

$$\beta = \max_{k,\ell} \left(\min_{i,j} \left| \alpha_i^{k,\ell} - \alpha_j^{k,\ell} \right| \right), \quad (4.16)$$

which ensures detection of optimum (V_k, V_ℓ) measurement pairs among different (k, ℓ) pairs.

Selection algorithm will be as following:

4.4.1 Step 1

$Num(\alpha^{k,\ell})$ will be calculated according to (4.15) for all possible (k, ℓ) pairs. The number of all possible (k, ℓ) pairs is given by permutation $(m = P(n, 2))$. When all $Num(\alpha^{k,\ell})$ are calculated, a vector which includes the number of repetitions for all possible (k, ℓ) pairs is formed as follows:

$$\mathbf{N} = \begin{bmatrix} Num(\alpha^{1,2}) \\ Num(\alpha^{1,3}) \\ \vdots \\ Num(\alpha^{2,1}) \\ Num(\alpha^{2,2}) \\ \vdots \\ Num(\alpha^{n,n-1}) \end{bmatrix}_{m \times 1}. \quad (4.17)$$

The best (k, ℓ) pairs are the ones with the minimum repetition number in (4.17). Since the repetition number is minimum the chance of correctly locating the harmonic source increases because the location is the node where the voltage ratio is equal to the impedance ratio in $\alpha^{k,\ell}$. That's why the (k, ℓ) pairs with minimum repetitions in $\alpha^{k,\ell}$ allow locating the harmonic source best: For example, when the (k, ℓ) pair with minimum repetition has a repetition value of two for a n node network, this means the harmonic source can be located for all $(n-2)$ nodes and if the source is at one of the nodes which are corresponding to the repeating value in the impedance ratio set, its location can not be discriminated from the other node with the same impedance ratio value in the set in (4.11). In such a condition, extra measurement is required.

For the vector \mathbf{N} , the value of minimum repetition number is

$$s = \min(\mathbf{N}). \quad (4.18)$$

The set that includes all (k, ℓ) pairs obeying (4.18) is defined as

$$S : \text{set of all } (k, \ell) \text{ with } \min(\mathbf{N}). \quad (4.19)$$

If there exists only one measurement pair in (4.19), that is; if the number of members in S is one, the location of harmonic current source can be detected by taking measurements at the nodes given by this measurement pair for the corresponding $\alpha^{k,\ell}$. If the source is not at one of the nodes that are repeating in this $\alpha^{k,\ell}$ set, the location can be determined; however, if the source is at one of the nodes which are repeating in the $\alpha^{k,\ell}$ set, extra measurement will be required. In addition, if there are more than one measurement pairs in S , selecting the best measurement pairs will require an optimization procedure. This procedure is described in step 2 and its procedure is given by the flow chart in Figure 4.1.

4.4.2 Step 2

When there are more than one members in S in (4.19), best measurement pairs will be selected according to the following criteria:

- i. For the (k, ℓ) pairs that result in the *same* minimum repetition number (s) found in step 1, calculate the distance between the members of $\alpha^{k,\ell}$. Then, the minimum value of the distance between the members of $\alpha^{k,\ell}$ will be calculated as

$$D^{k,\ell} = \min_{i,j} (|\alpha_i^{k,\ell} - \alpha_j^{k,\ell}|), \quad (4.20)$$

for all i and j where $i \neq j$.

- ii. Since there may be many (k, ℓ) pairs with the minimum repetition number (s), the best measurement pair will be obtained based on finding the pair with maximum distance value over the pairs with minimum distance value. This is defined by a *maximum value operator* such that

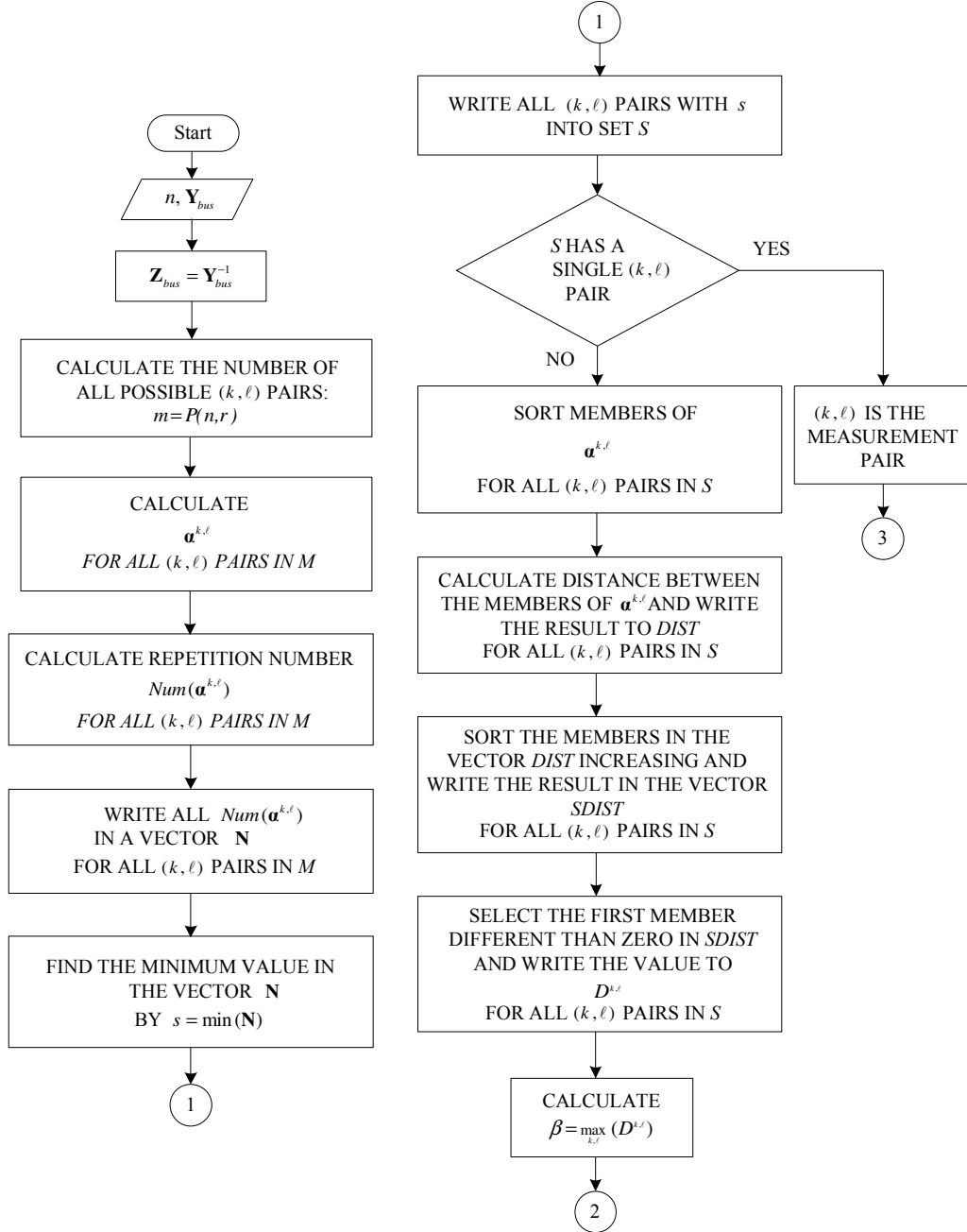


Figure 4.1 : Part *a* of the flow chart for the location algorithm.

$$\beta = \max_{k,\ell} (D^{k,\ell}). \quad (4.21)$$

The pair that satisfies (4.21) is selected as the *best* measurement pair. However, if there are more than one pairs that satisfy (4.21), the *second* minimum distance for each (k, ℓ) pair according to (4.20) will be selected and the maximum over all second minimums will be calculated. This procedure is

illustrated in the flow chart in Figure 4.1 and Figure 4.2. The pair which gives the maximum distance in (4.21) will be selected as the *best* measurement pair. This procedure continues similarly if more than one best measurement pairs (which give the maximum distance in (4.21)) exist. Finally, if multiple best measurement (k, ℓ) pairs are present for all other minimum distances, extra measurement will be required.

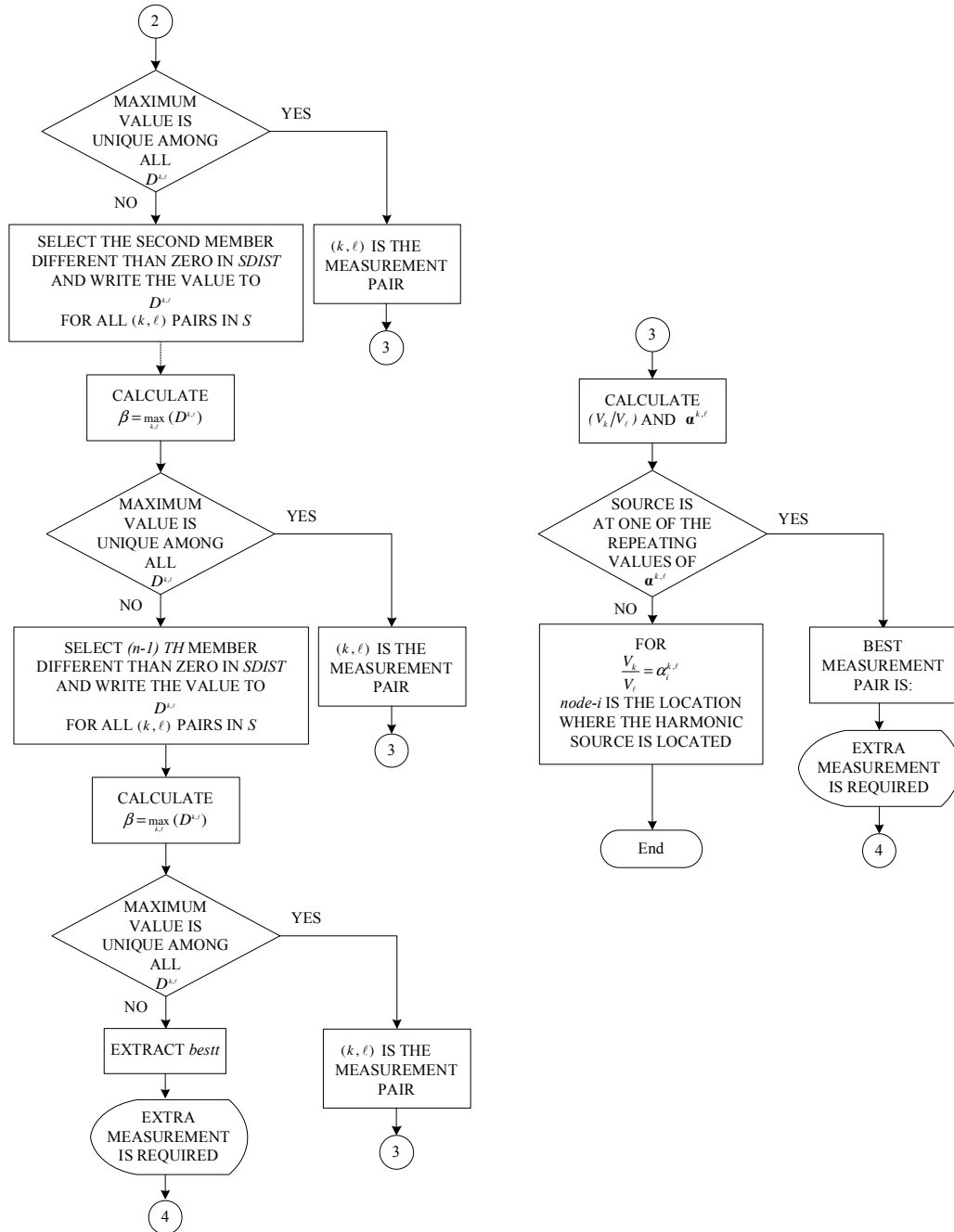


Figure 4.2 : Part *b* of the flow chart for the location algorithm.

- iii. If multiple best measurement (k, ℓ) pairs are present for all minimum distances, *extra measurement* will be required. The procedure can be followed by the flow chart in Figure 4.3. First, any one of the (k, ℓ) pairs from the multiple best measurement pairs will be selected as the *first* measurement pair (since all of the pairs have the same value of minimum repetition number s), and the set $\alpha^{k,\ell}$ for this selected pair will be referred to as *alfa1*. The positions of the elements repeating in *alfa1* will be determined and written to a list t . The list that contains the elements at these repetition positions will be extracted from *alfa1* and written to a vector *alfa1reduced*. (Note that the matrix which is formed by the list of $\alpha^{k,\ell}$ at each row ($k \neq \ell$) will be referred to as *alfa* (its size is defined by $m = P(n, 2)$)). A matrix is formed by extracting the elements with positions t in *alfa* and written to a matrix *alfareduced*. The rows which have the elements different from each other will be searched in *alfareduced* and the positions of rows are written to a set of difference referred to as *differ*. If this set of difference is not null, the (k, ℓ) pairs that correspond to *differ* will be found and written to a list *klextract*. If *klextract* has single element, then this element will be selected as the extra measurement pair. If *klextract* has more than one pair, the k and ℓ elements of *klextract* will be compared with the *first measurement pair* in order to detect the *overlapping elements* of each *extra measurement pair* with the *first measurement pair*. This will provide the condition of using minimum number of voltage meters. Finally, if there are more than one pair that have elements overlapping with the *first measurement pair*, the first one of these pairs will be selected as the *extra measurement pair* (since the value of the minimum repetition number is the same among these pairs). Impedance ratio set for the *extra measurement* and impedance ratio set for the *first measurement* will be evaluated together to locate the harmonic current source.
- iv. If the difference set *differ* found in step-iii is null, then the following procedure should be followed (The procedure can be seen in Figure 4.3.):
- The elements in *alfa1reduced* will be grouped (each of the same elements repeating in the set will form a group). A number of g groups will be obtained and this grouped list will be referred to as *subalfa1reduced*. The positions of

the repeating elements will be written to a list *ssub*. Afterwards, *alfareduced* will be grouped according to *ssub* and the new list will be written to *subalfareduced*.

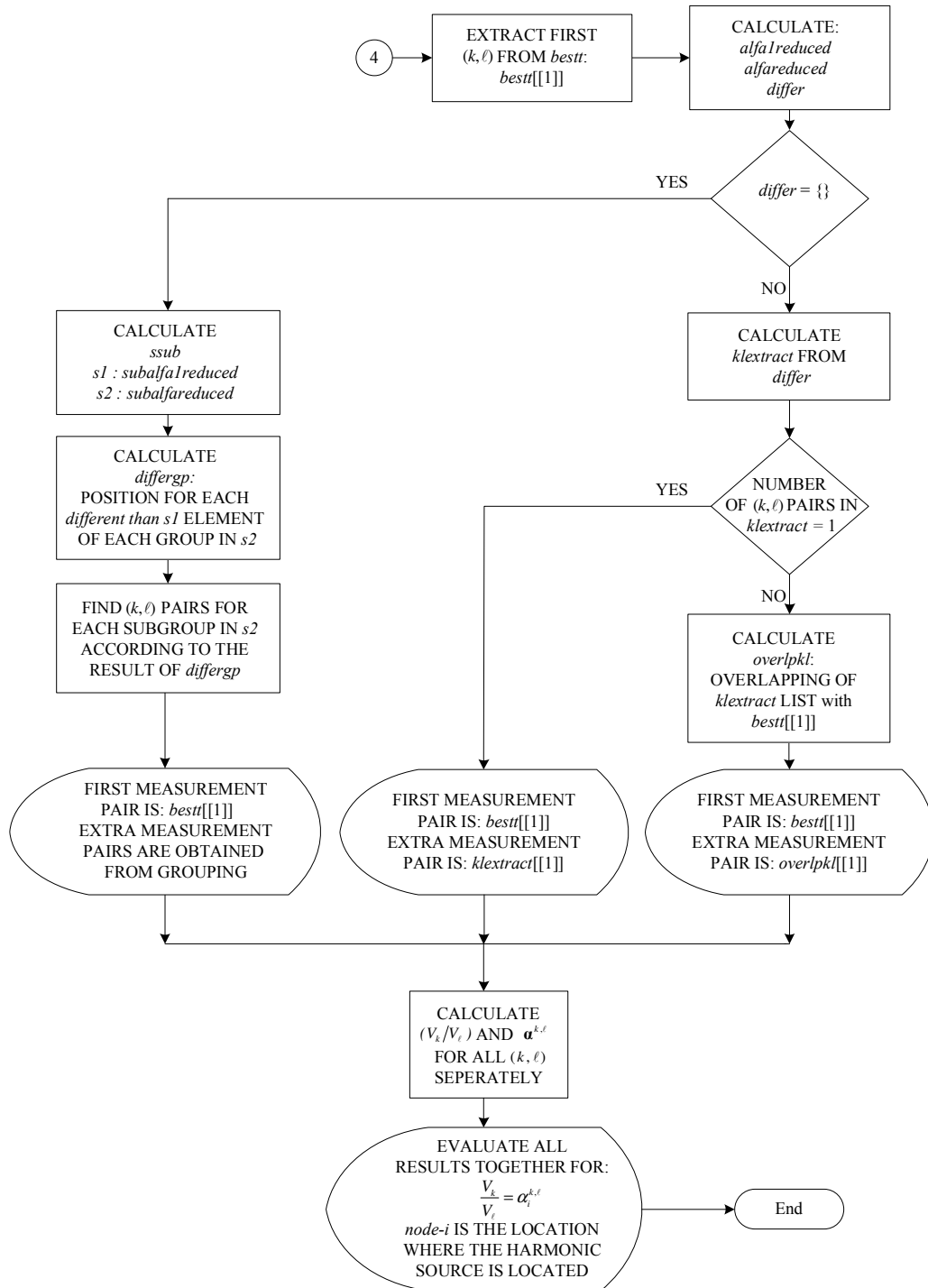


Figure 4.3 : Part c of the flow chart for the location algorithm.

- For the rows (the $\alpha^{k,\ell}$ sets) of *subalfareduced*, the rows with elements different from each other for each group will be searched and the position of rows are written to a difference set referred to as *differgp*”.
 - If there is not any element in *differgp* for the corresponding group, a (k, ℓ) pair for this group will be selected and the positions of the repeating elements in it will be determined. Afterwards, a row element which has the elements different at the positions found will be searched. If there is not a single row, then combination of more than one row will be selected. The (k, ℓ) pairs corresponding to the found rows will be extracted.
 - As a result, at least one (k, ℓ) pair will be obtained for each group.
 - Evaluation of the obtained (k, ℓ) pairs together will result in finding the location of the harmonic current source.
 - Using the criteria based on finding maximum amount of overlapping pairs (described in step-*iii*) provides obtaining minimum number of measurement sensors.
 - However at the end of the algorithm, if there exists repeating elements in the $\alpha^{k,\ell}$, this means it is not possible to locate the source when the source is located on the nodes corresponding to the repeating elements of $\alpha^{k,\ell}$.
- v. Finally at the end of the algorithm, $\alpha^{k,\ell}$ and (V_k/V_ℓ) will be calculated (illustrated in the flow chart in Figure 4.3). If the harmonic current source is located at one of the nodes with repeating elements in $\alpha^{k,\ell}$, extra measurement will be required. Extra measurement can be obtained based on the procedures described in step-*iii* and step-*iv*. The flow chart for this case is given in Figure 4.3.

When the flow charts given by Figure 4.1, Figure 4.2 and Figure 4.3 are combined, the algorithm that summarizes the structure of the approach for locating single harmonic current source can be obtained. It should be noted that in the flow charts *h-indice* is omitted for the sake of simplicity from all elements; however it is obvious that by including the *h-indice*, the algorithm can be run for each individual harmonic order.

Remark:

The *maximum value operator* used in (4.21) increases the efficiency of the location algorithm. For example, when there are impedance deviations present in the system, selection based on the maximum value among the members of the set S in (4.19) ensures selecting the measurement pairs with $\alpha^{k,\ell}$ members which are mostly distant to each other. However, for instance, if *OMPA* were to use the pairs with the minimum distance among the members of the set S , the selected pairs may be equal to each other and the location algorithm would not discriminate them to find the point of injected current source.

If the system topology includes symmetrical structure, the repetition in $\alpha^{k,\ell}$ can occur. When there is repetition in $\alpha^{k,\ell}$ for the selected (k,ℓ) pair, extra measurement is required.

4.5 Application of the Method to Model Systems

The proposed harmonic source location algorithm is applied to practical and impractical test cases. The impractical circuits are included in the analysis on purpose, in order to test the capability of the developed method. All of the analyses are repeated for various random impedance values in order to verify the results obtained. In addition, the algorithm is tested on the *IEEE 30-Bus* test system. The results are explained in Section 4.6.

A circuit with symmetric ring network topology is given in Figure 4.4. The circuit has 8-nodes. The impedance between each node and node to ground is selected arbitrarily as $Z = 0.01 + j0.1$ pu.

When the *OMPA* is used, the best measurement pairs are found as $\{\{1,4\},\{1,6\},\{2,5\},\{2,7\},\{3,6\},\{3,8\},\{4,1\},\{4,7\},\{5,2\},\{5,8\},\{6,1\},\{6,3\},\{7,2\},\{7,4\},\{8,3\},\{8,5\}\}$. All of the pairs satisfy the property in (4.12); therefore $\alpha^{k,\ell}$ set for each pair is unique. That is, for the pairs found above, there is not any repetition for their corresponding $\alpha^{k,\ell}$ sets. The measurement sensors can be replaced at any one of the pairs given above. When a harmonic current source with a value of $I = 1.0 + j0.1$ pu is injected at for example to node-8, the ratio (V_k/V_ℓ) will be equal to $(Z_{k,8}/Z_{\ell,8})$. This shows that the source is injected to node-8. As a result, for a

circuit in the form of the symmetric ring network topology, one measurement pair (two measurements) will be sufficient to find the location of the harmonic current source. The analysis is also repeated for various impedance values and it is seen that network response is the same that one measurement pair is sufficient to locate the harmonic source.

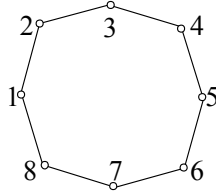


Figure 4.4 : An 8-node network topology.

A hybrid circuit including both radial and ring network topology is given in Figure 4.5. Actually, this circuit is not practical but it is used to test the performance of the method developed. The test circuit has 22-nodes. The impedance between each node and node to ground is selected arbitrarily as $Z = 0.01 + j0.1$ pu.

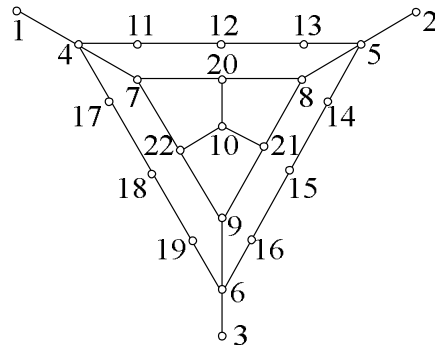


Figure 4.5 : A 22-node network topology.

When the *OMPA* is used, the best measurement pairs are obtained as $\{\{20,1\},\{20,2\},\{21,2\},\{21,3\},\{22,1\},\{22,3\}\}$. All of these pairs satisfy the property in (4.13); therefore $\alpha^{k,\ell}$ set for each pair is not unique. The value of repetition number is 6 for these pairs. Therefore, if the harmonic current source is injected to the nodes corresponding to the nodes of the repeating values in $\alpha^{k,\ell}$ sets, the location can not be determined and extra measurement is required. According to the flow chart in Figure 4.3, one of the pairs from the best measurement pairs will be selected as the first measurement pair. For example, the pair (20,1) is selected. For its

corresponding $\alpha^{20,1}$ set, the positions of repeating values are determined. Then by using this information, *alfareduced* is extracted from *alfa*. The rows with elements not equal to each other are determined and written to a list *differ*. The (k, ℓ) pairs corresponding to *differ* are extracted and found as $\{\{2,3\},\{3,2\}\}$. The overlapping set of these pairs with the first measurement pair $(20,1)$ is null. Therefore the first pair of $\{\{2,3\},\{3,2\}\}$ is selected as the extra measurement pair. Therefore, the measurement sensors will be replaced at the nodes $\{1,2,3,20\}$. When a harmonic current source with a value of $I = 1.0 + j0.1$ pu is injected into node-*i*, the evaluation of the voltage ratio V_2/V_3 and the voltage ratio V_{20}/V_1 together will provide the node-*i* from where the source is injected (for node-*i*, V_k/V_ℓ will be equal to $Z_{k,i}/Z_{\ell,i}$).

The analysis is also repeated when the impedances in the circuit are different from each other and the location of measurement sensors is found as $\{1,2,3\}$. As a result, for such an impractical network topology in Figure 4.5; if the circuit is symmetrical, one measurement inside the ring circuit and measurements at each end-node of the circuit will be sufficient to find the location of the harmonic current source. If the circuit is not symmetrical, measurements at only the end-nodes of the circuit will be sufficient. This result shows that the method can locate the source even for such a symmetrical circuit.

Another analysis is performed for the 18-node circuit given by Figure 4.6. The impedance between each node and node to ground is selected arbitrarily as $Z = 0.01 + j0.1$ pu.

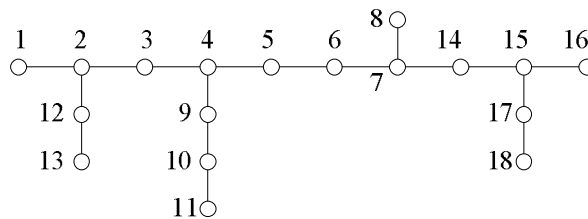


Figure 4.6 : An 18-node radial network topology.

When the *OMPA* is used, the best measurement pairs are obtained as $\{\{18,11\}\}$. This measurement pair satisfy (4.13) and the corresponding $\alpha^{k,\ell}$ sets are not unique sets. The value of repetition number is 10 for the pairs. Therefore, if the harmonic current

source is injected to the nodes corresponding to the repeating values in $\alpha^{k,\ell}$ sets, its location can not be determined and extra measurement is necessary. According to the procedure as described in step-iii in Section 4.4.2, this pair is selected as the first measurement pair and its corresponding $\alpha^{18,11}$ is referred to as *alfa1*. In *alfa1* the positions of repeating values are determined and using this information, *alfareduced* is extracted from *alfa*. The rows with elements not equal to each other are determined and written to a list *differ*. It is seen that *differ* is a null list. Therefore according to the procedure described in step-iv in Section 4.4.2, *alfa1* is grouped and it is seen that there are three groups. *alfareduced* and *alfa1reduced* are grouped to form *subalfareduced* and *subalfa1reduced*. When *subalfareduced* and *subalfa1reduced* are compared it is seen that second group and the third group has some rows with no repeating elements. However *group-1* does not have a unique $\alpha^{k,\ell}$ set, therefore one row from this group is taken and the complementary $\alpha^{k,\ell}$ that has the elements different from this row is found. As a result, all of the (k, ℓ) pairs are obtained for the groups in *alfa*.

The measurement pairs are found as $\{\{18,11\},\{8,11\},\{11,16\},\{8,13\},\{1,8\}\}$. The nodes from where the measurements should be taken are found as $\{1,8,11,13,16,18\}$. It is seen that 6 voltage sensors are sufficient to locate the harmonic current source. As a result, for a circuit given by such a network topology in Figure 4.6, one measurement at each terminal of the circuit will be sufficient to find the location of the harmonic current source. The analysis is also repeated for various impedance values and it is seen that network response is the same that one measurement at each terminal of the circuit is sufficient to locate the harmonic source.

In order to verify the results obtained for the circuit in Figure 4.5, a circuit with network topology given in Figure 4.7 is analyzed. The impedance between each node and node to ground is selected arbitrarily as $Z = 0.01 + j0.1$ pu.

When the *OMPA* is used, the following results are obtained:

- Minimum repetition number is 4.
- The set of measurement pairs is $\{\{8,13\},\{1,16\}\}$.
- The nodes where the sensors will be replaced are $\{1,8,13,16\}$.
- The number of sensors required is 4.

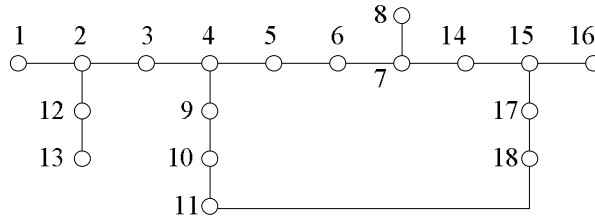


Figure 4.7 : An 18-node radial & ring network topology.

This result verifies the result obtained for the circuit in Figure 4.5. That is, if the circuit is not symmetrical, one measurement at each terminal of the circuit will be sufficient to find the location of the harmonic current source.

In addition, a circuit with network topology seen in Figure 4.8 is also analyzed to verify the results obtained for the circuit in Figure 4.4. The impedance between each node and node to ground is selected arbitrarily as $Z = 0.01 + j0.1$ pu.

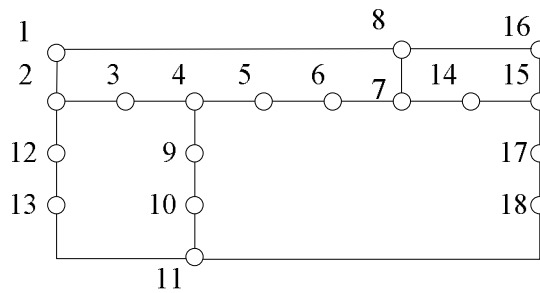


Figure 4.8 : An 18-node ring network topology.

When the *OMPA* is applied, the following results are obtained:

- No repeated values.
- One (k, ℓ) pair from the set of measurement pairs is $\{2, 14\}$.
- The nodes where the sensors will be replaced are $\{2, 14\}$.
- The number of sensors is 2.

After repeating the analysis for various random impedance values it is seen that one measurement pair (two measurements) is sufficient to find the location of the harmonic current source for circuits with ring network topology such as the circuits in Figure 4.4 and Figure 4.8.

4.5.1 IEEE 30-bus test system analysis

The performance of the algorithm is also tested on the *IEEE* 30-bus test system shown in Figure 4.9. The system is assumed to be balanced. The system parameters obtained from fundamental frequency power flow analysis are given in the Appendix A.1. A single harmonic load is assumed to be connected to the system. The load is modeled as a constant harmonic current injection source. In addition to the harmonic load, a transformer is modelled via a short-circuit impedance model. Transmission line is modeled using lumped parameter π circuit model as defined in Section 2.5. All of the simulations are performed using *MATHEMATICA 7.0* program.

The harmonic source can be injected into any one of the thirty nodes in the network. To test the capability of the proposed method, the computer simulations were carried out for the first 50 harmonic orders. However, in practise there may be a less number of harmonic order in the analysis. For example, a six-pulse rectifier which is used in most dc drives, produces harmonics, order of $h = 6k \pm 1$ where $k = (1,2,3,\dots,8)$. For such a load, seventeen simulations would be sufficient (due to harmonic order resolution of seventeen). According to the superposition theory, the system can be divided to harmonic networks, and the result of each simulation (for the corresponding harmonic network) will point to the same location where the harmonic source is located.

The skin effect is not considered in the analyses. On the other hand, since the proposed algorithm is based on system topology and impedance matrix, the addition of skin effect to impedance matrix will only result in changes of impedance values but it will not reduce the performance of the algorithm: i.e. number of meters will not change.

The *OMPA* is evaluated for harmonic frequencies up to harmonic order of 50. The positions of measurement sensors are obtained for each harmonic order. According to the result of the analysis, it is seen that for each harmonic order, five measurement sensors are sufficient to locate the harmonic current source (when it is injected into any node of the system). The results of the meter placement algorithm are listed in Table 4.1.

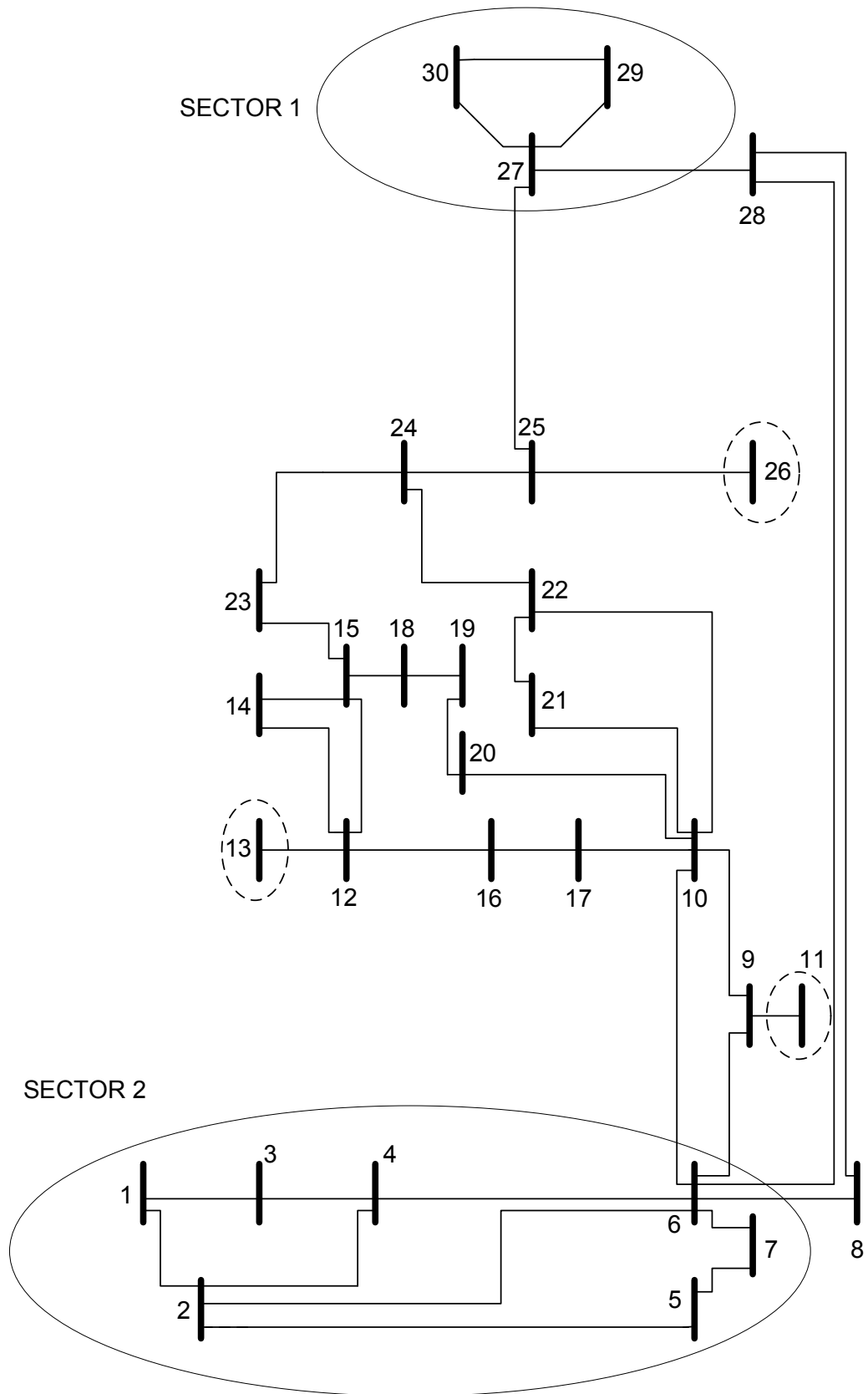


Figure 4.9 : IEEE 30-bus test system.

Table 4.1: Meter placement in *IEEE* 30-bus test system.

Harmonic Order		Meter					Harmonic Order		Meter				
(h.o.)		1	2	3	4	5	(h.o.)		1	2	3	4	5
1.		2	11	13	26	29	26.		3	11	13	26	30
2.		3	11	13	26	29	27.		2	11	13	26	30
3.		1	11	13	26	29	28.		1	11	13	26	30
4.		7	11	13	26	29	29.		7	11	13	26	29
5.		7	11	13	26	29	30.		7	11	13	26	30
6.		2	11	13	26	29	31.		2	11	13	26	30
7.		2	11	13	26	29	32.		7	11	13	26	29
8.		4	11	13	26	29	33.		1	11	13	26	29
9.		5	11	13	26	30	34.		5	11	13	26	30
10.		7	11	13	26	30	35.		1	11	13	26	29
11.		1	11	13	26	29	36.		1	11	13	26	29
12.		1	11	13	26	30	37.		5	11	13	26	29
13.		7	11	13	26	30	38.		7	11	13	26	29
14.		7	11	13	26	30	39.		2	11	13	26	29
15.		7	11	13	26	30	40.		2	11	13	26	29
16.		7	11	13	26	30	41.		4	11	13	26	29
17.		5	11	13	26	30	42.		1	11	13	26	30
18.		7	11	13	26	30	43.		7	11	13	26	30
19.		2	11	13	26	30	44.		7	11	13	26	30
20.		3	11	13	26	30	45.		1	11	13	26	29
21.		2	11	13	26	30	46.		2	11	13	26	29
22.		1	11	13	26	30	47.		2	11	13	26	29
23.		1	11	13	26	30	48.		4	11	13	26	29
24.		5	11	13	26	29	49.		1	11	13	26	30
25.		3	11	13	26	30	50.		1	11	13	26	30

According to the results shown in Table 4.1, it is seen that for meter 2, meter 3 and meter 4, the measurement sensors are located at the end-nodes (terminal nodes) of the system. This result is actually coinciding with the result obtained in Section 3.4 such that one measurement at each branch end-node is required for a m -branch network. The nodes of 11, 13 and 26 are called the terminal or end nodes of the network. Each of the other two sensor positions belong to the sectors marked on the Figure 4.9. It is seen that for each harmonic order five meters are required to locate the harmonic source. On the other hand, to design a system that can locate the harmonic source for harmonic order from one to fifty, it is seen that eleven meters are required; that is three meters for the terminal nodes: {11,13,26}, two meters for the two nodes in *sector-1*: {29,30}, and six meters for the six nodes in *sector-2*: {1,2,3,4,5,7}.

Since the harmonic impedance matrix values changes for different harmonic orders, the positions of the sensors in *sector-1* and *sector-2* will vary. This condition increases the number of sensors in the measurement procedure. However, since certain design condition in the electric power system can decrease the degree of harmonic order in the system, this may help to reduce the number of meters:

- For instance, transformer winding connections have a significant impact on the flow of triplen harmonic currents from the single-phase nonlinear loads. A delta-connected winding will act as an open circuit and a star-connected winding, with neutral point grounded, act as a short circuit to the zero sequence harmonic currents. The delta winding provides triplen harmonics to be trapped in the delta winding. Since triplen harmonics are the odd multiples of the third harmonic, they can be eliminated from the system. Therefore, the meters required for the triplen harmonics can be eliminated.
- Since the common harmonic sources are working in a periodic nature (i.e. power electronic converters), there will be no even components and thus the even harmonic orders can be eliminated. Therefore, the meters required for the even harmonics can be eliminated. However due to harmonic sources such as arcing devices, there may be even harmonics in the system. The behavior of harmonic sources was discussed in Section 2.3.
- Finding the meter locations for only the dominant harmonic orders may also decrease the meter number. For instance the individual harmonic distortion for each harmonic order (as defined in Section 2.2) obtained from the Fourier transform of the voltage waveform can be used to find the degree of each harmonic order in the system. According to the results, the dominant harmonic components can be determined and the meter locations for the corresponding harmonic orders can be obtained which in turn may decrease the number of meters.

Actually, it is obvious to have varying metering positions for *sector-1* and *sector-2*. This is so, since the meter placement algorithm is dependent on the harmonic impedance matrix, the varying values of the elements in this matrix result in finding different meter positions. However as mentioned previously this condition do not

change the response of the network, *i.e.* the number of meters for each harmonic order is 5.

Note that, the meter locations found by the meter placement algorithm are the optimum places. The meter locations found for a harmonic order can also be used for another harmonic order providing the $\alpha^{k,\ell}$ is unique. For example the meter locations (k, ℓ) found for harmonic order 5 can also be used for harmonic order 7 if the $\alpha^{k,\ell}$ obtained by $\mathbf{Z}^{(7)}_{bus}$ is unique. In such a condition, the location of the meters may not be optimum but the location of harmonic source may be still found. Otherwise extra measurement is required.

When the meter positions are determined, the location algorithm can be performed by searching the impedance ratio which is equivalent to the measured voltage ratio at that specific harmonic frequency to find the node where the harmonic source is injected.

4.6 Results

The implementation of the impedance network approach with the proposed meter placement algorithm is investigated to find the location of a single harmonic current source at a harmonic order in electric power networks. The following results are obtained:

- (i) The methodology is dependent on network topology.
- (ii) Harmonic bus-impedance matrix is required for the algorithm.
- (iii) The methodology is independent of the value of the harmonic current source injected to the network: only the voltage measurements are needed.
- (iv) An optimal meter placement algorithm is proposed to select the nodes from where the measurements will be taken. The meter placement algorithm is chiefly designed to cope with deviations in the network harmonic impedance values since obtaining correct network harmonic impedance values may be difficult.
- (v) The meter placement algorithm also aims to perform the location process with a limited number of measurements. This is actually practical in electric power systems where full measurement of the system voltage waveforms at

all of the nodes is not realizable for a large system. Only partial measurement (not necessarily made at the harmonic sources) is practical and these measurements must be complemented by the location algorithm.

- (vi) The location algorithm searches the impedance ratio which is equivalent to the measured voltage ratio at that specific harmonic frequency to locate the single harmonic source.
- (vii) The proposed algorithm can also be used to locate multiple harmonic sources which have different harmonic orders than each other. On the other hand, the method is insufficient to locate multiple harmonic sources which have the same harmonic orders. When each of the multiple harmonic sources in the system inject at least one harmonic component, which are not at the same order with other harmonic sources harmonic components, the proposed algorithm can be used to locate the harmonic sources. For each harmonic component, harmonic impedance matrix is calculated and the location of the source is obtained. For example, let's consider a system with two harmonic sources. If the first is injecting 5^{th} harmonic component and the other one is injecting the 11^{th} harmonic component, the sources can be located by the proposed algorithm.

Analyses with several practical and impractical network test cases are performed to verify the validity of the proposed methodology. The following key aspects are obtained from the performed analyses:

- (i) For circuits with ring network topology as in Figure 4.4 and Figure 4.8, one measurement pair will be sufficient to locate the harmonic current source.
- (ii) For circuits with radial network topology as in Figure 4.6, one measurement at each terminal of the circuit will be sufficient to locate the harmonic current source.
- (iii) For circuits which consists of both radial and ring network topology, if the circuit is symmetrical as in Figure 4.5 (all impedances are equal to each other), one measurement inside the ring circuit and one measurement at each terminal of the circuit will be sufficient to locate the harmonic current source. If the circuit is not symmetrical as in Figure 4.7 and Figure 4.5 (all

impedances are different than each other), one measurement at each terminal of the circuit will be sufficient to locate the harmonic current source.

- (iv) For a network shown in Figure 4.9 which consists of both radial and ring topology, measurements at each end-nodes and each sectors is required for a successful location task. The results obtained for the network in Figure 4.9 for *IEEE* 30-bus test system is coinciding with the results obtained from the study in Section 3.4 such that one measurement at each branch end-node is required for a m -branch network.

The advantage of impedance network approach for locating harmonic sources is that the harmonic current value is not required. However, this situation may be a disadvantage when bus harmonic voltage amplitudes are weak or subject to disturbances.

5. MONTE CARLO VALIDATION OF THE OPTIMAL METER PLACEMENT ALGORITHM

5.1 Introduction

Finding the location of a harmonic source is based on searching the impedance ratio set $\alpha^{k,\ell}$ as given in (4.11). This set is required in order to find the value which is equal to the measured voltage ratio value at a specific harmonic frequency. When the equivalence in (4.9) is obtained, the location of harmonic current source may be found.

In order to locate the harmonic source, first the places of voltage meters must be determined. The locations of the meters are selected according to the optimal meter placement algorithm (*OMPA*). The aim of *OMPA* mainly is to overcome misallocation of the harmonic source because of deviations in network harmonic impedance values. As it was described in Section 4.3, in principle all possible measurement pairs that obey (4.12) can be used to locate the harmonic source. However, in case of deviations in network harmonic impedance values, the members of $\alpha^{k,\ell}$ (the impedance ratio set) may deviate slightly from the correct values and lead to a wrong placement of harmonic source. To avoid this condition, a methodology to select the measurement pair (k, ℓ) of a $\alpha^{k,\ell}$ which has maximum distance between its closest members is employed as the core of the optimal meter placement algorithm. The main goal of this methodology is to be able to tolerate slight deviations of the members of the $\alpha^{k,\ell}$ set given by (4.11). Actually, the *maximum value operator* defined by (4.21) and used in the *OMPA* ensures selecting a (k, ℓ) pair with the most *distant* impedance ratios among its $\alpha^{k,\ell}$ set. When there is deviation in network harmonic impedance matrix, the impedance ratios (for the measurement pair found according to the so called maximum value operator) will not become close to each other and the location algorithm will be able to discriminate them to locate the point of injected current source. Therefore, the *maximum value*

operator will increase the locating efficiency of the algorithm when harmonic impedance errors exist in the system.

5.2 Purpose

It is shown in the previous chapter that the harmonic locating approach with *OMPA* is capable of locating the source with best measurement pairs in case there are no deviations in impedance values. However, the important question is what would be the performance of the *OMPA* when the harmonic network impedance is subject to deviations.

Monte Carlo simulation (*MCS*) will be used to measure the accuracy of *OMPA* in case of network impedance deviations. *MCS* is a method for iteratively evaluating a deterministic model using sets of random numbers as inputs. It is applied to many engineering problems in the literature [68]. The goal of *MCS* is to determine how random variation, lack of knowledge, or error in harmonic impedance matrix affects the performance or reliability of the system. The inputs are randomly generated from probability distributions so that a distribution for the inputs that most closely matches or represents the system is chosen. Random inputs turn the deterministic model into a stochastic model. (In a deterministic model, the same results will be obtained in each time the model is evaluated. On the other hand, a stochastic model is one that involves probability or randomness). The data generated from the *MCS* can be further analyzed to obtain the performance of the model [69].

When a single harmonic current source is injected into a node of an n node network, the set of equations describing the circuit is defined in (4.6) and in a matrix of

$$\mathbf{V} = \mathbf{Z}_{bus} \cdot \mathbf{I}. \quad (5.1)$$

Harmonic indice is omitted from the equations for the sake of simplicity. \mathbf{V} in (5.1) is referred to as *assumed voltage vector* and it consists of the assumed (calculated) voltage phasor values. On the other hand if there is deviation in network harmonic impedance matrix, the equation (5.1) will be defined as

$$\mathbf{V}' = \mathbf{Z}'_{bus} \cdot \mathbf{I}. \quad (5.2)$$

\mathbf{V}' in (5.2) is referred to as *exact voltage vector* and it consists of the exact (measured) voltage phasor values.

\mathbf{Z}_{bus} in (5.1) is the *assumed impedance* matrix. Due to deviations in network harmonic impedance values the exact value of the impedance matrix may be different than \mathbf{Z}_{bus} . The matrix which is different than \mathbf{Z}_{bus} will be referred to as the *exact impedance matrix* and shown as \mathbf{Z}'_{bus} . If the assumed impedance matrix is equal to exact impedance matrix (also assumed voltage vector is equal to exact voltage vector), this means there is no deviation in network harmonic impedance values.

\mathbf{Z}_{bus} is deviated by addition of a random variable δ to each element in \mathbf{Z}_{bus} . This random variable is defined as

$$\delta = N(\mu, \sigma). \quad (5.3)$$

In (5.3), δ defines a pseudo-random real number from a normal distribution function with mean μ and standard deviation σ .

For the analyses, the normal distribution is selected a zero mean function with a variance of σ which is varied in a bounded region.

The admittance for a capacitive element is Y_C and defined as

$$Y_C = j\omega C \quad (5.4)$$

and the admittance for a resistive-inductive element is Y_{RL} and defined as

$$Y_{RL} = \frac{1}{R + j\omega L} \quad (5.5)$$

for $\omega = 2\pi f$ rad/sec. When δ is included to Y_C and Y_{RL} , the following is obtained;

$$Y'_C = j(\omega C + \delta), \quad (5.6)$$

$$Y'_{RL} = \frac{1}{R + \delta + j(\omega L + \delta)}. \quad (5.7)$$

The admittance matrix \mathbf{Y}'_{bus} is formed with the addition of δ according to (5.6) and (5.7). Then, the impedance matrix \mathbf{Z}'_{bus} is calculated according to (4.2). Therefore, the exact impedance matrix is calculated. by the addition of δ .

During Monte Carlo simulation, approximately 68% of the produced random numbers will fall between $\mu - \sigma$ and $\mu + \sigma$ range. For example, if the mean value of R is equal to 0.0192 pu, 68% of deviations in R will be between 0.0182 pu and 0.0202 pu for an h of 1 and for the value of 10^{-3} of σ . Similarly, deviations in X will be between 0.0565 pu and 0.0585 pu for the mean value of 0.0575 pu. The R , ωL , and ωC values between bus-1 and bus-2 in the *IEEE* 30-bus system in Figure 4.9 are given in Appendix A.1 Table A.1.3.

In order to verify the performance of *OMPA*, its performance is compared with the performance of non-optimal meter placement approach (*NOMP*). The *NOMP* developed for this purpose is as follows.

- i. For the (k, ℓ) pairs that result in the *same* minimum repetition number s (found in step 1 in Section 4.4.2), calculate the distance between the members of $\alpha^{k, \ell}$. Then, the minimum value of the distance between the members of $\alpha^{k, \ell}$ will be calculated by (4.20).
- ii. The non-optimal meter locations will be selected by finding the pair with minimum value of the pairs found in the previous step. This is defined by

$$\gamma = \min_{k, \ell} \left(\min_{i, j} \left| \alpha_i^{k, \ell} - \alpha_j^{k, \ell} \right| \right) \quad (5.8)$$

The pair that obeys (5.8) is selected as the non-optimal measurement pair. Actually, the measurement pair according to *NOMP* is the worst case such that it gives the measurement pairs with the closest $\alpha^{k, \ell}$ set members. Therefore, when the harmonic network impedance is subject to a deviation, the worst location performance will be obtained for meters selected according to *NOMP*. It is also expected that the performance of the location algorithm with all other (arbitrarily selected) meter positions will be between the performances of *OMPA* and *NOMP*.

5.3 Procedure

The Monte Carlo validation algorithm is given in Figure 5.1. The variable n in the flow chart corresponds to the number of nodes in the network. The algorithm stages are as follows:

- i. The bus impedance matrix \mathbf{Z}_{bus} is calculated.
- ii. The *OMPA* is used to find the optimal meter (*OM*) pair/s for \mathbf{Z}_{bus} . For the obtained k and ℓ nodes, the impedance ratio set is calculated as $\alpha_O^{k,\ell}$. The sub-index O in $\alpha_O^{k,\ell}$ corresponds to *OMPA*. The set is defined as

$$\alpha_O^{k,\ell} = \frac{Z_{bus_k}}{Z_{bus_\ell}}, \quad (5.9)$$

for all k and ℓ where $k \neq \ell$.

- iii. The *NOMP* is used to find the non-optimal (*NOM*) meter pair/s for \mathbf{Z}_{bus} . For the obtained k and ℓ nodes, the impedance ratio set is calculated as $\alpha_{NO}^{k,\ell}$. The sub-index NO in $\alpha_{NO}^{k,\ell}$ corresponds to *NOMP*. The set is defined as

$$\alpha_{NO}^{k,\ell} = \frac{Z_{bus_k}}{Z_{bus_\ell}}, \quad (5.10)$$

for all k and ℓ where $k \neq \ell$.

- iv. A zero mean normal distribution function with deviation σ is applied to \mathbf{Z}_{bus} for the σ change of 10^{-10} to 10^{-1} with steps 10^{-1} . σ is selected in this range to perform the deviation on \mathbf{Z}_{bus} in limit values. The value of 10^{-10} adds a minimum deviation and the value of 10^{-1} adds a maximum deviation to \mathbf{Z}_{bus} . Thus, \mathbf{Z}'_{bus} is formed with the addition of random changes to individual elements.
- v. \mathbf{Z}'_{bus} is calculated for N iterations for each σ .
- vi. For location index L , a loop for L from 1 to n is performed (n is the number of all nodes in the circuit) to extract the performance of the location algorithm

with *OMPA*. Then \mathbf{V}' is calculated for each L by injecting I^L (the current vector when the source is at node L) to \mathbf{Z}'_{bus} as

$$\mathbf{V}' = \mathbf{Z}'_{bus} \cdot \mathbf{I}^L. \quad (5.11)$$

After \mathbf{V}' is calculated, the voltage ratio is obtained by

$$\frac{\mathbf{V}'_k}{\mathbf{V}'_\ell} = \alpha'_o. \quad (5.12)$$

The constant α'_o in (5.12) is compared with the list in (5.9) to find the closest value to obtain the node where the source is injected. As the node is obtained, it is compared with the location index L . If L and the calculated node are equal, the performance counter is increased.

Note that, the addition of δ to \mathbf{Z}'_{bus} turns the deterministic model given by (5.1) into a stochastic model given by (5.11).

- vii. The performance of *NOMP* is also extracted similar to *OMPA*. The voltage ratio is obtained by

$$\frac{\mathbf{V}'_k}{\mathbf{V}'_\ell} = \alpha'_{NO}. \quad (5.13)$$

The constant α'_{NO} in (5.13) is compared with the list in (5.10) to find the closest value to obtain the node where the source is injected. As the node is obtained, it is compared with the location index L . If L and the calculated node are equal, the performance counter is increased.

- viii. The performance analysis is evaluated for each value of σ for N iterations according to Monte Carlo simulation. Finally, the performance of each approach is compared to see how optimal the result of the *OMPA* is when the harmonic network impedance is subject to deviations.

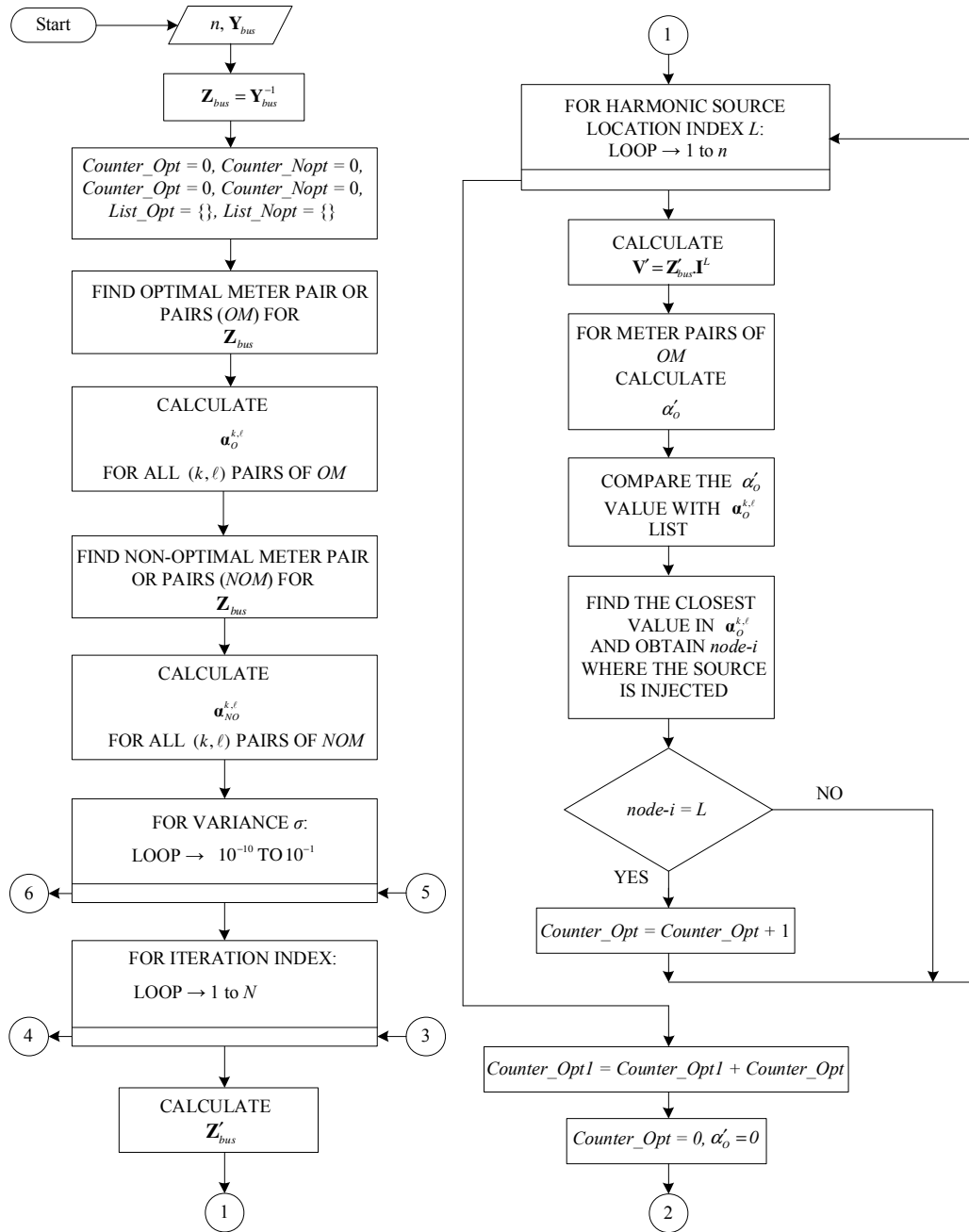


Figure 5.1 : The flow chart of the algorithm that compares the performance of location approach using OMPA and NOMP.

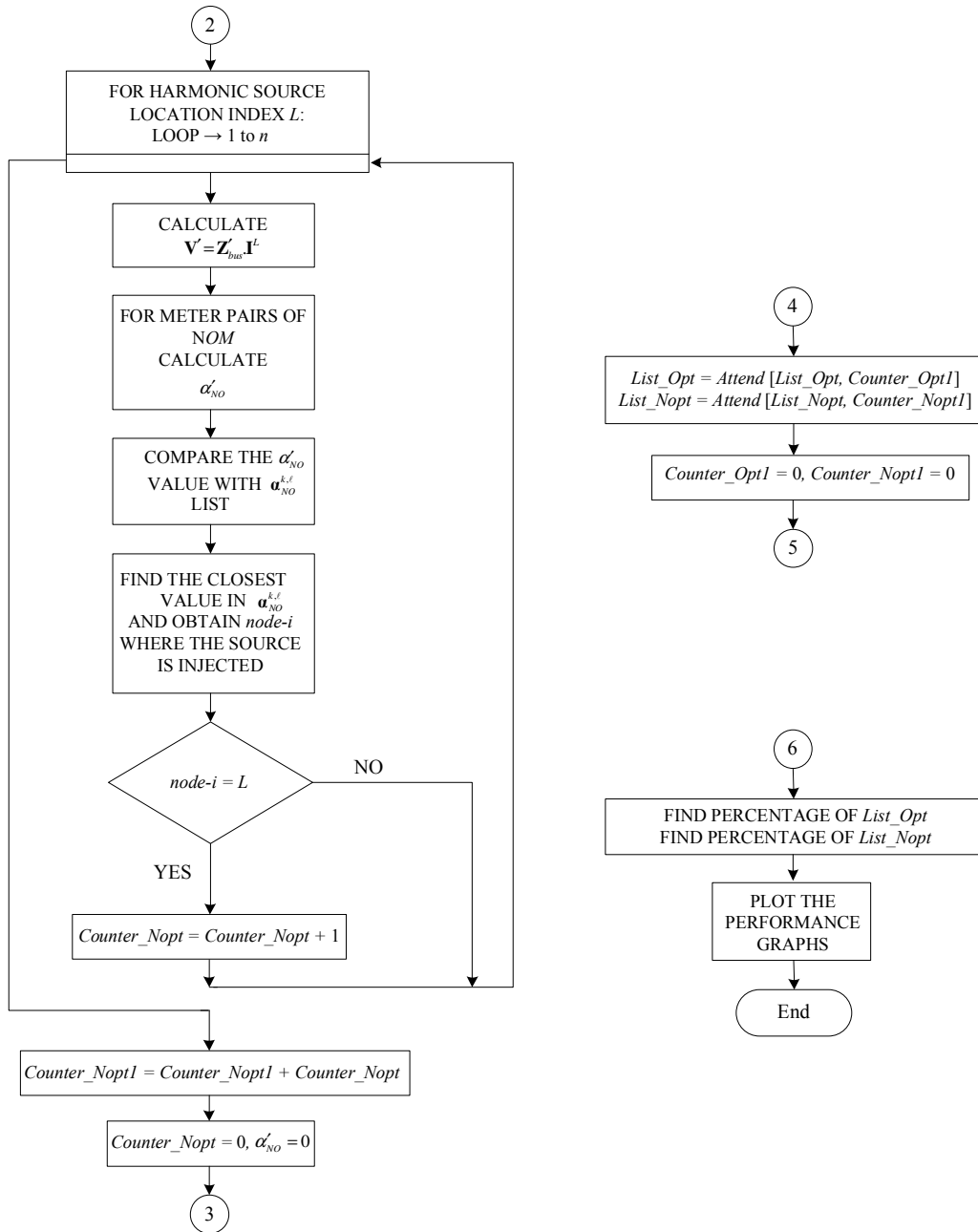


Figure 5.1 : (contd.) The flow chart of the algorithm that compares the performance of location approach using *OMPA* and *NOMP*.

5.4 Results of the Analysis

The flow chart in Figure 5.1 shows the algorithm that compares the performance of location approach with *OMPA* and *NOMP*. Although the harmonic order index is omitted from the flow chart for the sake of simplicity, it is to be understood that the algorithm will be evaluated for each harmonic order. As it was stated in the previous chapter; due to superposition theory, the system can be divided into networks at each

harmonic frequency and the location found for each harmonic frequency should point to the same location (for a harmonic source with multiple harmonic orders). The location algorithm can be evaluated for each harmonic order to locate the harmonic source in this sense.

The analyses were performed on the *IEEE* 30-bus test system shown in Figure 4.9. The test system was defined in Section 4.5.1, in detail.

The analyses were performed for a harmonic source with harmonic order $h = 6k \pm 1$ where $k = (1, 2, 3, \dots, 8)$. The simulations also include the fundamental frequency.

The simulations were performed on 10 computers with 3.00 GHZ *INTEL Pentium 4* processor, 512 MB RAM with *MATHEMATICA 7.0* program. Each simulation was carried out with 400 iterations. One iteration last about 500 minutes. All of the simulations took 6 days.

Figure 5.2 shows performance difference of location with *OMPA* and *NOMP* approaches when $\sigma = 0$ and there is no deviation in harmonic network impedance value ($\mathbf{Z}'_{bus} = \mathbf{Z}_{bus}$).

The y-axis in Figure 5.2 is normalized to unity with respect to performance maximum counter value which is 30 for a 30-node network. The x-axis corresponds to *harmonic order index*. For $x = 1$, the harmonic order corresponds to fundamental frequency; for $x = 2$, the harmonic order is $(6 \times 1 - 1) = 5$; for $x = 3$, the harmonic order is $(6 \times 1 + 1) = 7$; and finally for $x = 17$, the harmonic order is $(6 \times 8 + 1) = 49$. The y-axis value indicates the number of correctly located harmonic sources among 30 nodes. For example, if the value is unity, any harmonic source that is injecting current in one of the 30 nodes can be located for that specific harmonic order.

Two lines are seen in Figure 5.2; the one with *thick* line is for *OMPA* and the one with *dashed* line is for *NOMP*. Both of the lines consist of seventeen points. Note that there is no deviation in impedance matrix. Therefore, *OMPA* algorithm is very successful for locating all the sources for all harmonic orders whereas *NOMP* algorithm fails to locate some of the harmonic sources as seen in Figure 5.2.

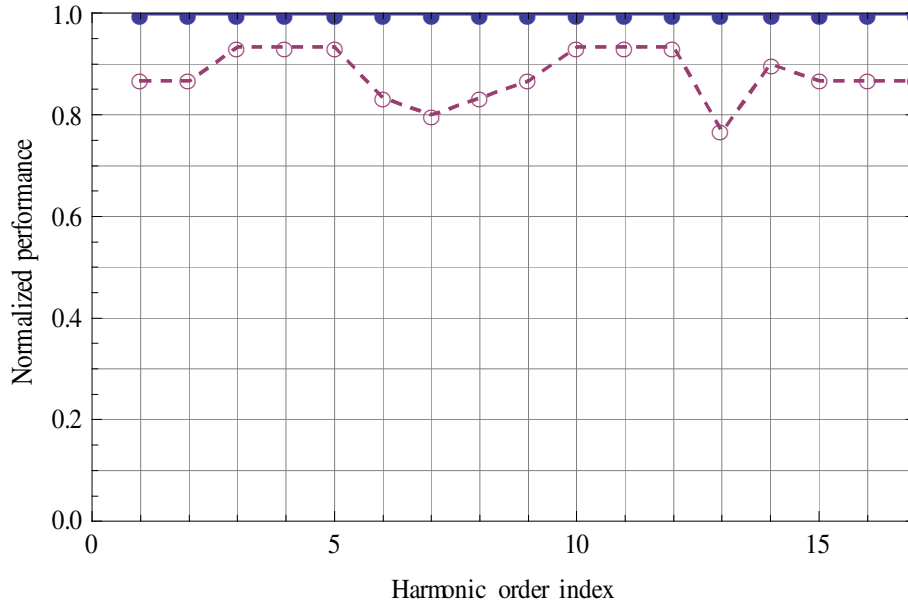


Figure 5.2 : The performance plot for the location algorithm with *OMPA* (thick line) and *NOMP* (dashed line) for the deviation 0 .

In Figure 5.2, the average of the *NOMP* performance is 12.15% lower than the average of *OMPA* performance. This means for this value of σ , the performance of *OMPA* is better than *NOMP*. (Averaging is performed by taking the average of the values at the points for each line on Figure 5.2).

In practice, obtaining correct network impedances may be difficult. Therefore, harmonic source location algorithms may need to tolerate small deviations in network impedances. Now let us observe how the performance of *OMPA* changes when the impedance values are subject to deviation. For 10 different values of σ , simulations of 10 different cases were carried out to analyze how increased deviation of harmonic impedance values change the performance of *OMPA*. The comparative performance analysis of *OMPA* and *NOMP* is calculated over all 30 nodes and results are illustrated by the following figures.

Figure 5.3 shows the performance plot with *OMPA* and *NOMP* approaches when the variance σ is 10^{-10} . The y-axis is normalized to unity with respect to performance maximum counter value. The performance maximum counter value is equal to 12000. Harmonic current source is located to one of 30 nodes and 400 slightly different bus impedance matrixes are produced by using the random generator. With this slight change in impedance matrixes, the number of correct locations of harmonic source is determined. For example, if the harmonic source is located in

node-1 and the *OMPA* algorithm found the correct location in all 400 impedance matrix deviations, then the algorithm performance is 100 % for node-1.

As it is seen from Figure 5.3 the performance of *OMPA* at each harmonic order is better than *NOMP*. On the other hand, the performances are equal when harmonic order is 5. Choosing a larger iteration number in the simulations might make the performance of *OMPA* better than *NOMP* at this point as well.

In Figure 5.3, the average of the *NOMP* performance is 30.58% lower than the average of *OMPA* performance. This means for this value of σ , the performance of *OMPA* is better than *NOMP*.

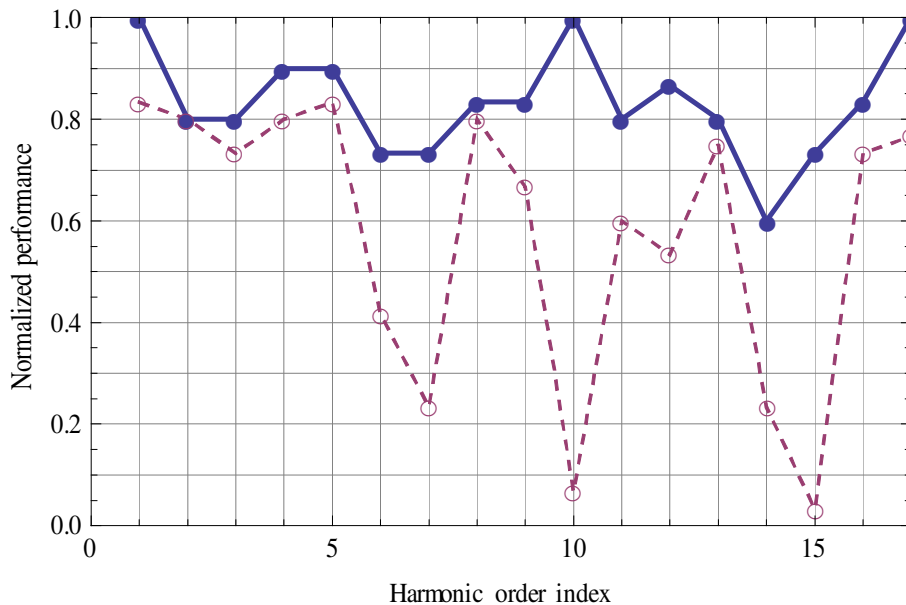


Figure 5.3 : The performance plot for the location algorithm with *OMPA* (thick line) and *NOMP* (dashed line) for the deviation 10^{-10} .

Figure 5.4 shows the performance plot when the deviation σ is 10^{-9} . The average of the *NOMP* performance is 39.82% lower than the average of *OMPA* performance.

Figure 5.5 shows the performance plot when the deviation σ is 10^{-8} . The average of the *NOMP* performance is 53.60% lower than the average of *OMPA* performance.

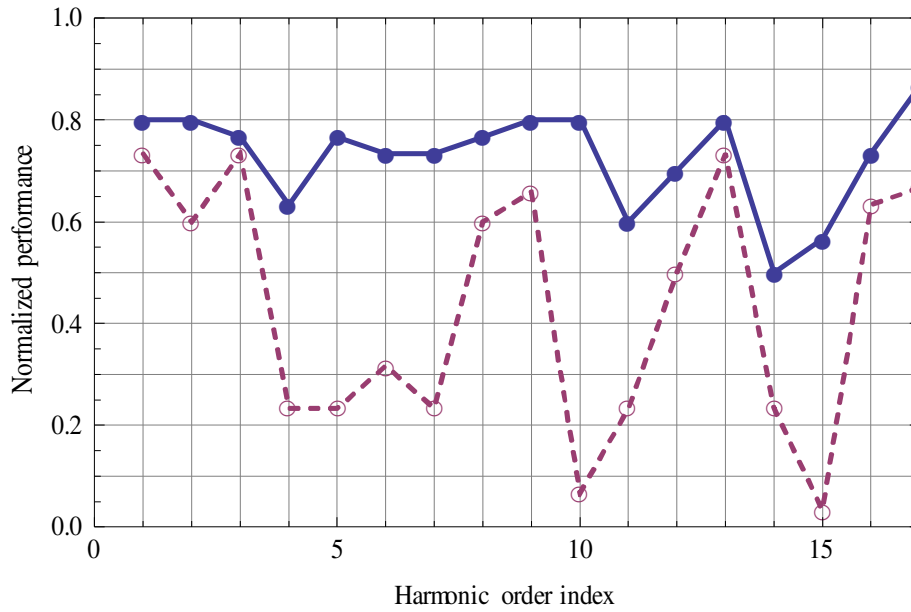


Figure 5.4 : The performance plot for the location algorithm with *OMPA* (thick line) and *NOMP* (dashed line) for the deviation 10^{-9} .

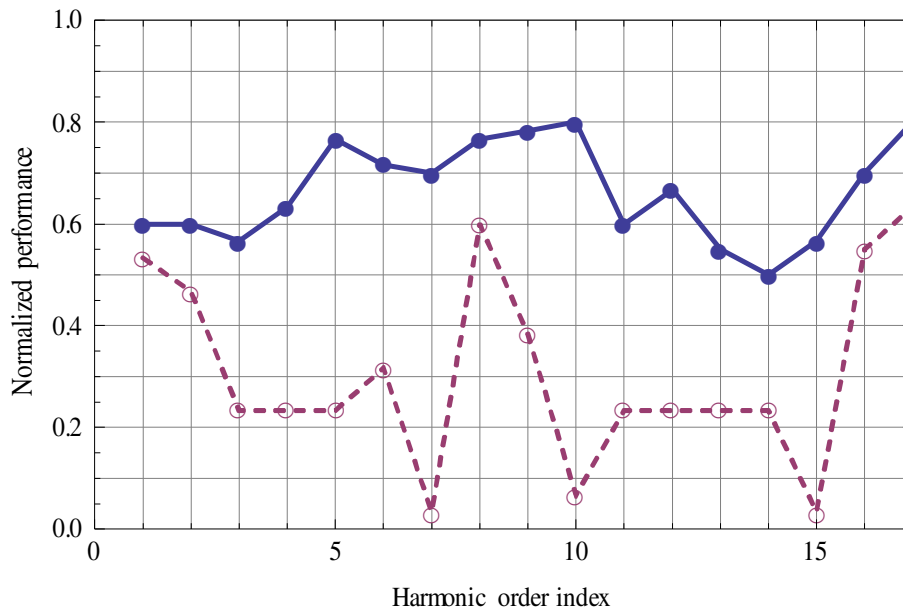


Figure 5.5 : The performance plot for the location algorithm with *OMPA* (thick line) and *NOMP* (dashed line) for the deviation 10^{-8} .

Figure 5.6 shows the performance plot when the deviation σ is 10^{-7} . The average of the *NOMP* performance is 66.09% lower than the average of *OMPA* performance.

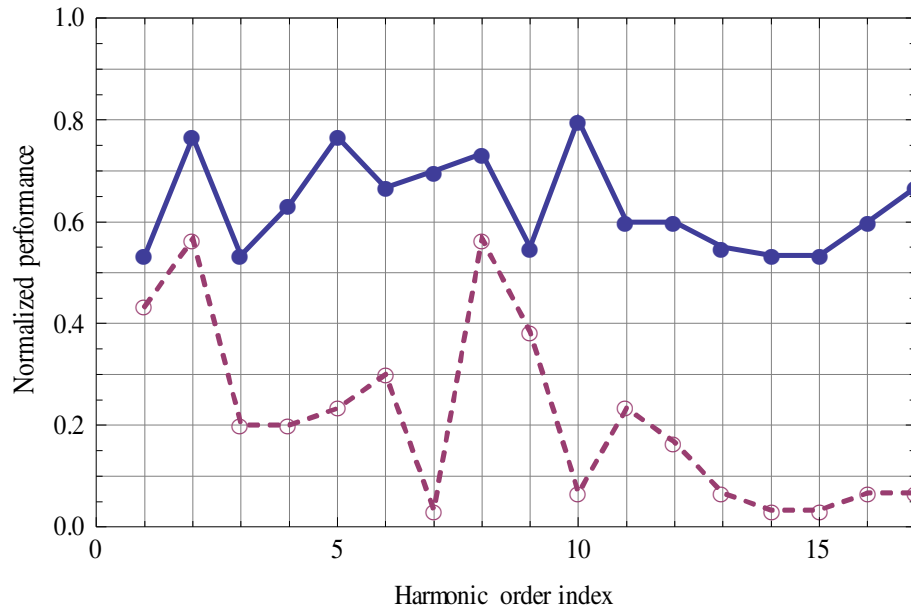


Figure 5.6 : The performance plot for the location algorithm with *OMPA* (thick line) and *NOMP* (dashed line) for the deviation 10^{-7} .

Figure 5.7 shows the performance plot when the deviation σ is 10^{-6} . The average of the *NOMP* performance is 64.89% lower than the average of *OMPA* performance.

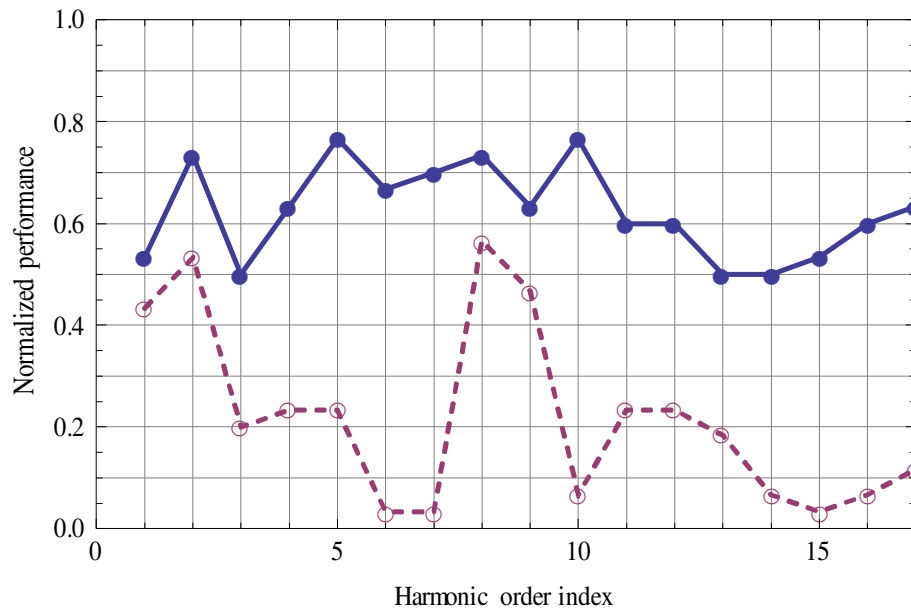


Figure 5.7: The performance plot for the location algorithm with *OMPA* (thick line) and *NOMP* (dashed line) for the deviation 10^{-6} .

Figure 5.8 shows the performance plot when the deviation σ is 10^{-5} . The average of the *NOMP* performance is 66.98% lower than the average of *OMPA* performance.

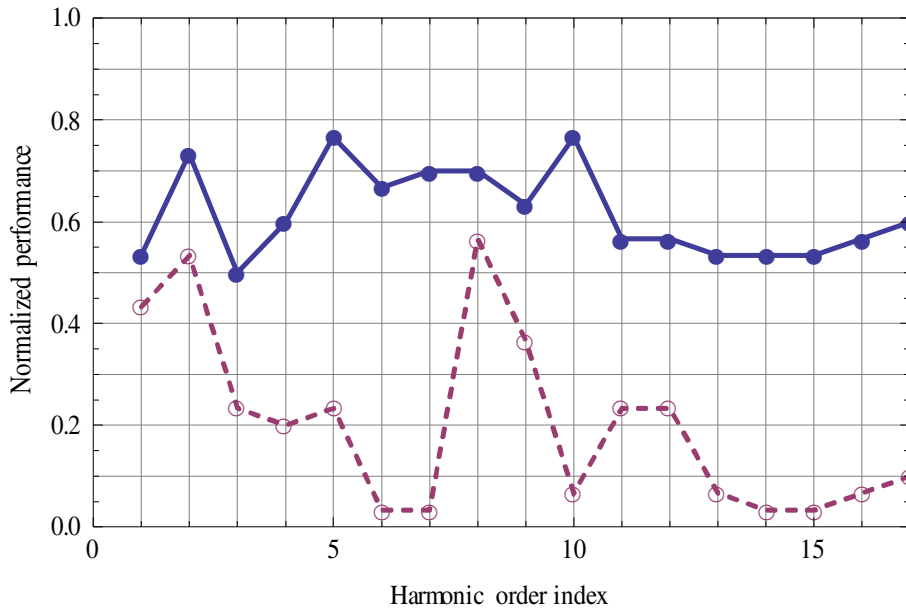


Figure 5.8 : The performance plot for the location algorithm with *OMPA* (thick line) and *NOMP* (dashed line) for the deviation 10^{-5} .

Figure 5.9 shows the performance plot when the deviation σ is 10^{-4} . The average of the *NOMP* performance is 65.63% lower than the average of *OMPA* performance.

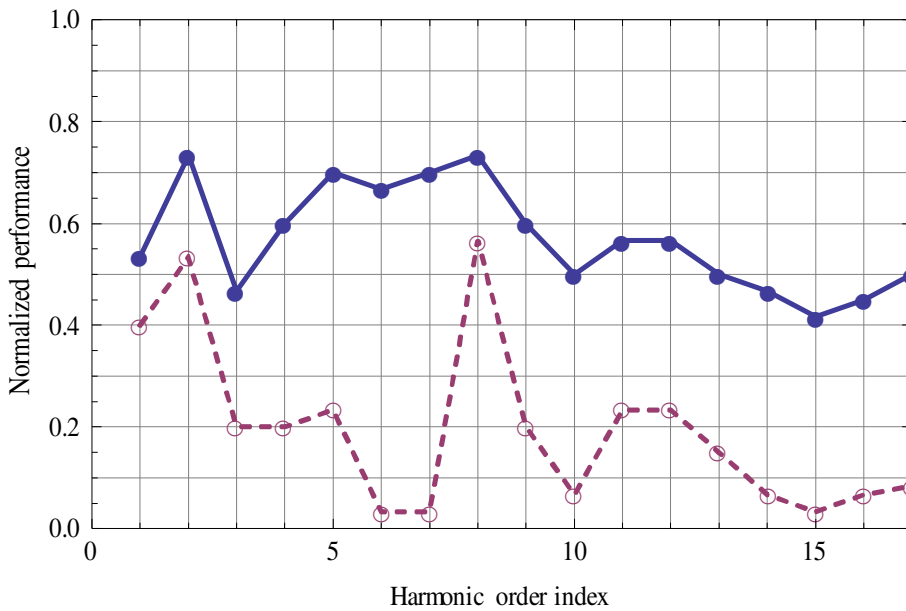


Figure 5.9 : The performance plot for the location algorithm with *OMPA* (thick line) and *NOMP* (dashed line) for the deviation 10^{-4} .

Figure 5.10 shows the performance plot when the deviation σ is 10^{-3} . The average of the *NOMP* performance is 59.55% lower than the average of *OMPA* performance.

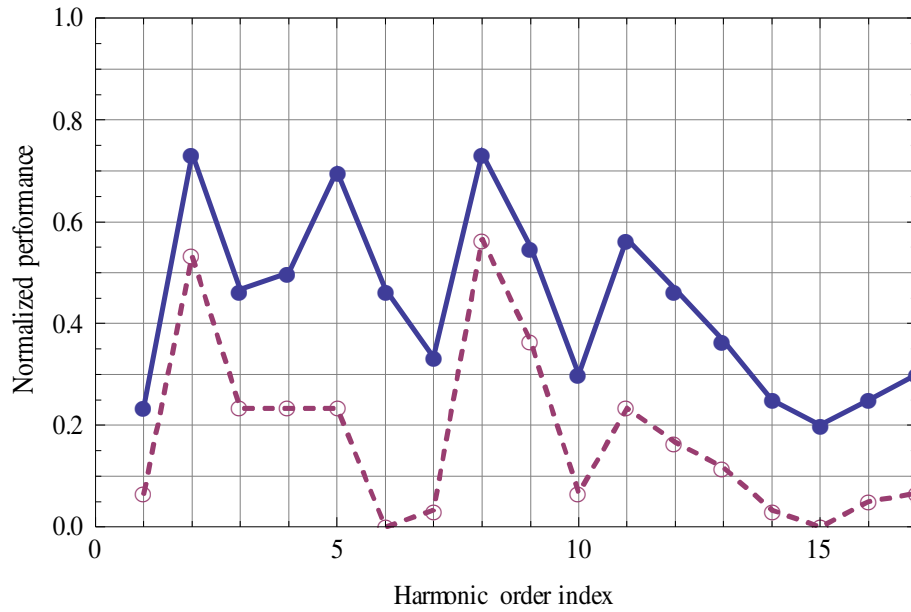


Figure 5.10 : The performance plot for the location algorithm with *OMPA* (thick line) and *NOMP* (dashed line) for the deviation 10^{-3} .

Figure 5.11 shows the performance plot when the deviation σ is 10^{-2} . The average of the *NOMP* performance is 57.34% lower than the average of *OMPA* performance.

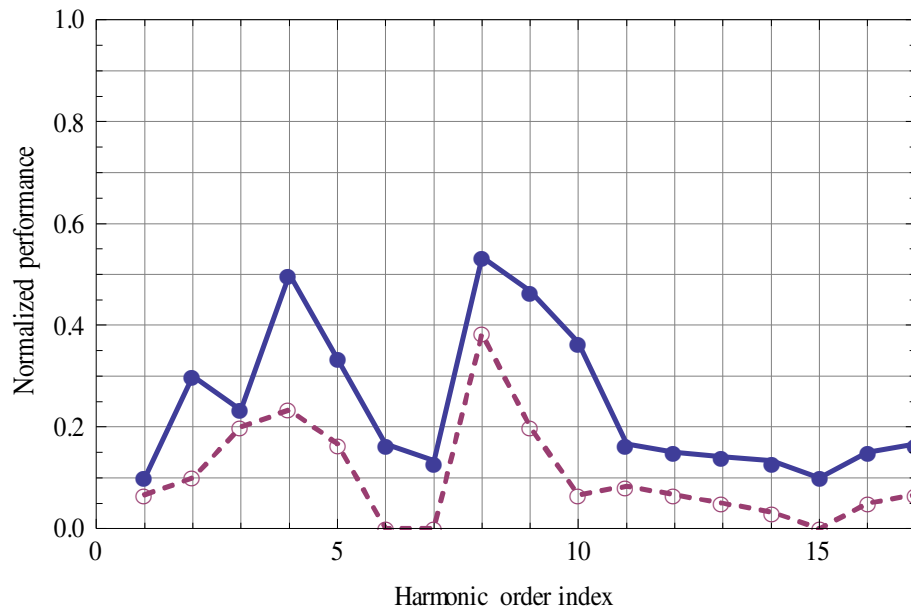


Figure 5.11 : The performance plot for the location algorithm with *OMPA* (thick line) and *NOMP* (dashed line) for the deviation 10^{-2} .

Figure 5.12 shows the performance plot when the deviation σ is 10^{-1} . The average of the *NOMP* performance is 86.61% lower than the average of *OMPA* performance.

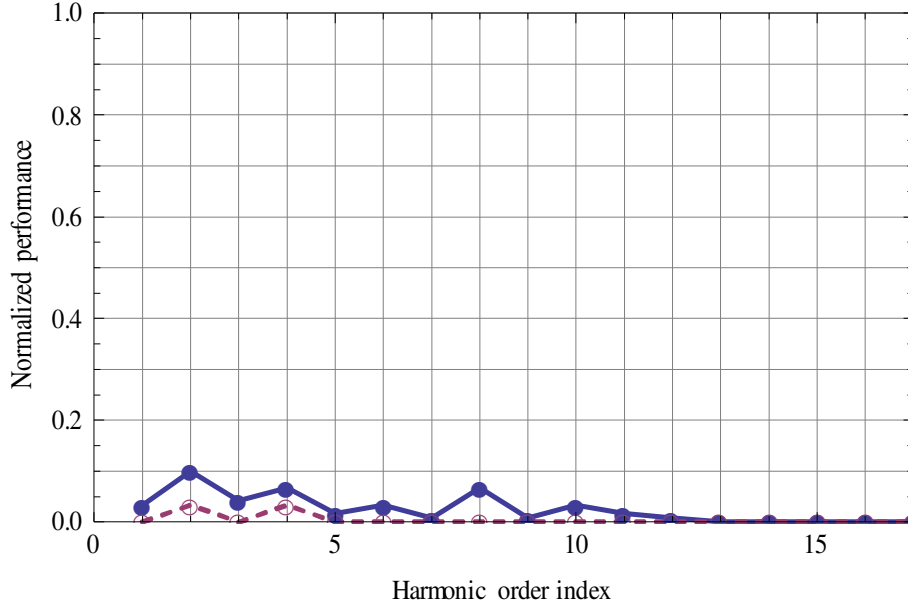


Figure 5.12 : The performance plot for the location algorithm with *OMPA* (thick line) and *NOMP* (dashed line) for the deviation 10^{-1} .

The average of the *NOMP* performance is lower than the average of *OMPA* performance in all figures from Figure 5.2 to Figure 5.12. This means, the performance of *OMPA* is better than *NOMP*.

Remark:

For the simulation studies for the 10 different values of σ , the following results are obtained:

- When the bus impedance matrix is deviated by a factor of σ , the voltage ratios α'_O and α'_{NO} in (5.12) and (5.13) vary from their *assumed* values and thus they are not equal to the exact values in their corresponding impedance ratio sets $\alpha_O^{k,\ell}$ and $\alpha_{NO}^{k,\ell}$ in (5.9) and (5.10). As a result, the harmonic source can not be located in all circumstances.
- On the other hand, it is seen that the performance of the harmonic source location with *OMPA* is better than location with *NOMP* in all cases. Therefore the meter locations found by *OMPA* is optimal.
- There is a dramatic change in some performance values of *NOMP* in the figures. For example, for Figure 5.3 to Figure 5.12, the performance of *NOMP* is close to *OMPA* for $x=8$ (the harmonic order is 23). This is

because the distance between the impedance ratio elements of $\mathbf{a}^{k,\ell}$ for the corresponding (k, ℓ) is more distant to each other in comparison to the performance of *NOMP* at other points. For this reason, the performance of *NOMP* is high at $x = 8$ for all figures. For the other points, the distance between the elements in $\mathbf{a}^{k,\ell}$ are more close to each other, thus the performance of *NOMP* is worse than *OMPA*. This response is due to the harmonic impedance matrix for the corresponding σ values. To validate this statement, the simulations for the case at Figure 5.9 are evaluated for a iteration number of 300. The reason of this analysis is to test whether decreasing the iteration number instead of increasing will produce similar response as the iteration number of 400. If the response obtained for less iteration number will be similar, this will show that the iteration number is sufficient and higher number of iteration is not required. Figure 5.13 shows the performance plot when the deviation σ is 10^{-4} and iteration number is 300.

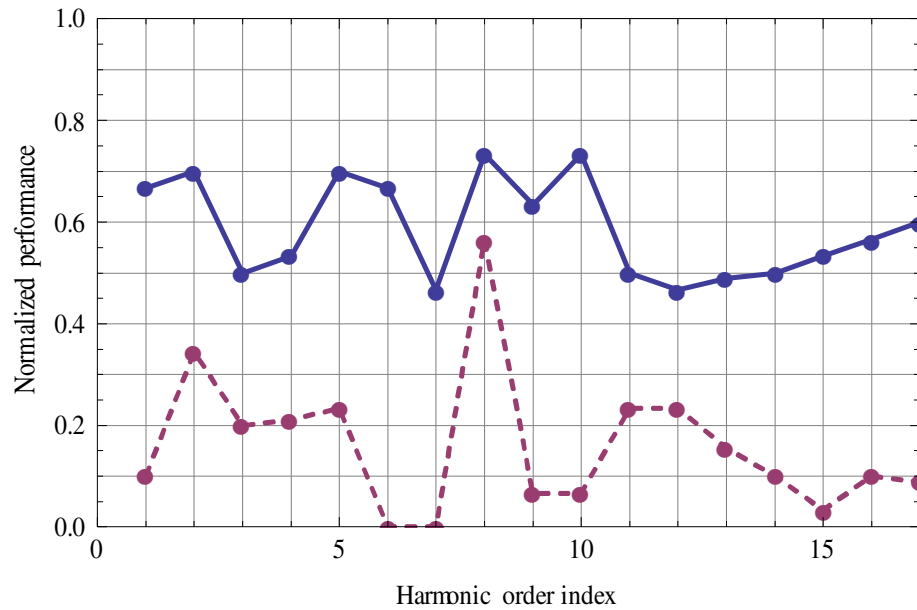


Figure 5.13 : The performance plot for the location algorithm with *OMPA* (thick line) and *NOMP* (dashed line) for 300 iterations.

For Figure 5.13, it is seen that the performance of *NOMP* and *OMPA* for the simulations of all harmonic orders are similar to the performances for Figure 5.9. The same analysis is also performed for 200 iterations: It is seen

that, the characteristic is similar although some slight variations in values is observed. According to these response, it is seen that iteration number higher than 400 will not effect the performance of the proposed algorithm considerably. This result also validates the statement that the response of *NOMP* at $x=8$ is not due to the iteration number but it is due to the harmonic impedance matrix for the corresponding σ values.

5.4.1 Summary of the analyses

Figure 5.14 illustrates the performance difference between *NOMP* and *OMPA* in percentage. The y-axis corresponds to the percentage difference. Each point in the plot shows the percentage of difference between the average values of *OMPA* and *NOMP* performances. Averaging is calculated by taking the average of the values at the points for each line on Figure 5.2 to Figure 5.12.

The x-axis corresponds to the degree of deviation in harmonic impedance matrix. The standard deviation of σ takes values from 0 to 10^{-1} for the values of x from 1 to 11. For $x=1$, the standard deviation is 0; for $x=2$, the standard deviation is 10^{-10} ; and finally for $x=11$, the standard deviation is 10^{-1} . For $\sigma=0$ there is no deviation in harmonic impedance values and for $\sigma=10^{-1}$, the deviation amount is maximum.

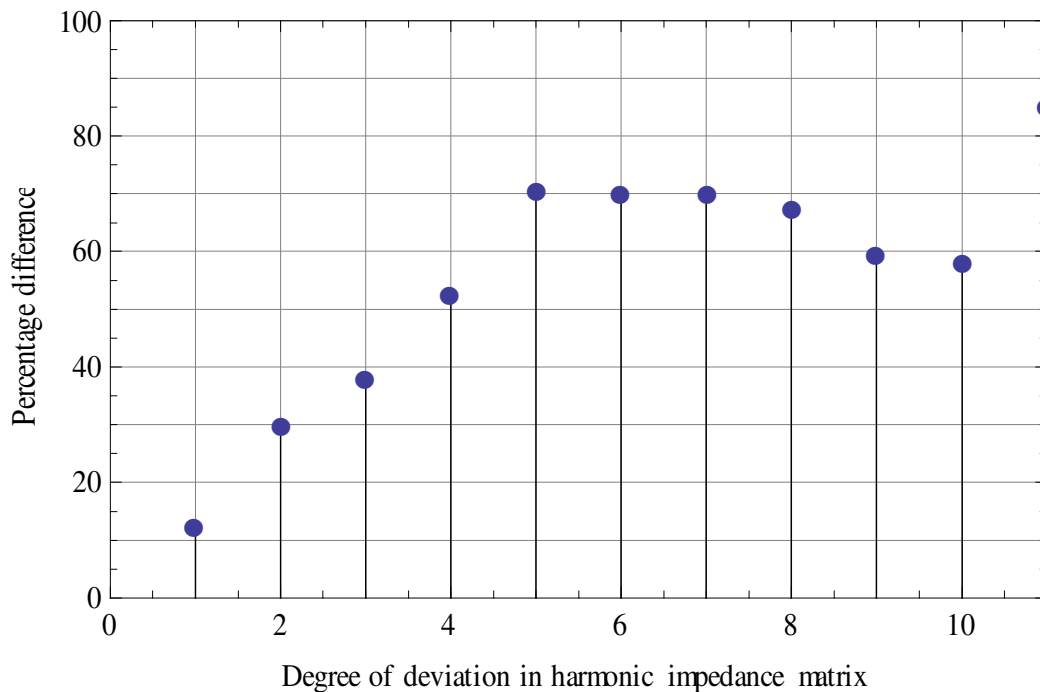


Figure 5.14 : Percentage performance difference between *OMPA* and *NOMP*.

It is seen from Figure 5.14 that the performance difference is 12.15% for $\sigma = 0$ and 86.61% for $\sigma = 10^{-1}$. This shows that performance of the *OMPA* is better than performance of the *NOMP*.

Figure 5.15 shows the overall comparative performances of *OMPA* and *NOMP*. Similar to Figure 5.14, the x -axis corresponds to degree of deviation in harmonic impedance matrix. The standard deviation σ changes from 0 to 10^{-1} for values of x from 1 to 11.

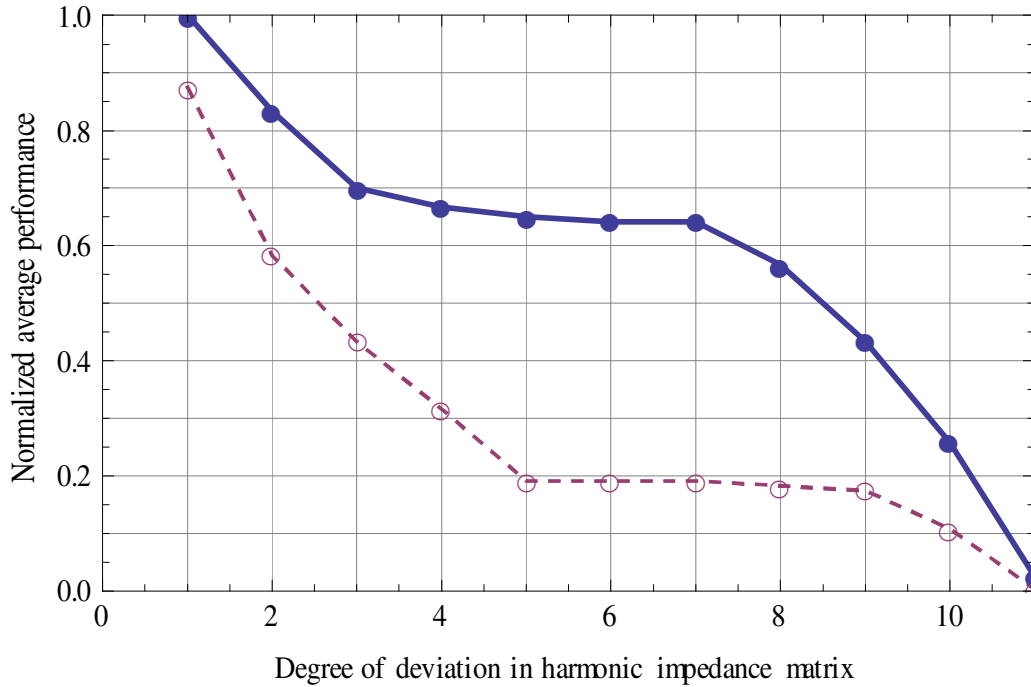


Figure 5.15 : Comparative performances of *OMPA* and *NOMP*.

The y -axis in Figure 5.15 corresponds to normalized average performance values for *OMPA* and *NOMP*. The plot with *thick* line corresponds to average values obtained for location algorithm with *OMPA*, and the plot with *dashed* line corresponds to average values obtained for location algorithm with *NOMP*. The figure illustrates the advantage of selecting meter positions according to *OMPA*. It is seen that when there is no deviation in bus impedance matrix (for $x = 1$), the performance of *OMPA* is 12.15% better than *NOMP*. It can be inferred that, all of the simulations with other measurements (the arbitrarily selected measurements from all possible (k, ℓ) pairs) will be between the two curves in Figure 5.15. It is also clearly seen that the maximum value operator in *OMPA* increases the locating efficiency of the algorithm

when there are impedance errors in the system. This selection procedure allows overcoming misallocations of the harmonic source because of deviations in network impedance values.

5.5 Results

The harmonic source location approach with the proposed optimal meter placement algorithm is capable of locating a harmonic source when harmonic network impedance is subject to deviations or errors. The performance of metering approach for such a condition is investigated by Monte Carlo simulation using the *IEEE* 30-bus test system. The performance of the proposed *OMPA* is compared with that of *NOMP* which picks the worst metering positions. For the simulations of 10 different cases (10 different σ values) of network harmonic impedances and for 17 harmonics, it is seen that when there is no deviation on harmonic impedance matrix, the performance of location with *OMPA* is 12.15% better than *NOMP*. On the other hand, when the variance of δ is increased, the error in impedance matrix increases (the estimation error of impedance matrix increases) and the performance of the *OMPA* algorithm decreases. However, its performance is always better than location with arbitrarily selected measurements. For the last analysis when standard deviation σ is 10^{-1} , the performance of both algorithm is minimum as it is seen from Figure 5.12. Almost non of the harmonic injection can be located for both algorithm; because the deviation in \mathbf{Z}_{bus} is maximum. The results of the analyses show that the optimal meter placement algorithm is capable of dealing with the affects of deviations in network impedance values.

6. CONCLUSION AND RECOMMENDATIONS

In this thesis, the problem of locating a harmonic source in electric power networks is investigated. Two approaches are developed. These are:

- (i) Harmonic source location using distance measure approach.
- (ii) Harmonic source location using impedance network approach based on a new optimal meter placement algorithm.

The optimal meter placement algorithm can be considered as the main contribution of this thesis.

The analyses carried out in this thesis are based on the following assumptions that;

- (i) the power system consists of linear devices,
- (ii) the harmonic source is represented by linear models which inject harmonic current to network,
- (iii) the injected harmonic current is independent of the voltage distortion at the device terminals.

According to the last assumption, the equivalent circuits of the system at various harmonic frequencies are independent from each other. Therefore, superposition principle can be used to divide the system into harmonic networks and solve the system at each frequency individually. For a harmonic source with multiple harmonic orders, the harmonic location process can be performed at each harmonic order and the location found by the process should point to the same location.

The following results are obtained from the studies performed in this thesis:

- A single harmonic source location method in analogy to two-terminal impedance-based fault location approach is developed. The distance from the harmonic source to one of the metering points is used as a measure to locate the single harmonic source. The distance measure can be applied for each harmonic order circuit according to the superposition theory. If a source with h different harmonic orders is injected to a bus, all of the results will point to

the same harmonics location. Harmonic source impedance and harmonic source current values are not needed for the proposed approach. The required data is system impedance and measurements at each end nodes of an m -branch n -node network. It is stated that, to locate the harmonic source correctly for an n -node m -branch system, m -measurements (each measurement at each branch end-node) are sufficient. For networks with 2-branch, this measure can be accurately used to locate the harmonic source. On the other hand when the number of branches increases, the problem of correctly defining the distance from any measurement point to the unknown location of harmonic source limits the approach and it is not practically applicable for the networks with 3-branch or more.

- For the networks with 3-branches or more, the nodal analysis can be used to locate harmonic sources in the network. When the system equations under non-sinusoidal conditions are solved, the result yields the current vector given by (3.14). This vector will have non zero elements for the positions where the source/s are located. For this approach voltage measurements at all of the nodes are required; however this is not a cost effective solution. This problem is solved by a new optimal meter placement algorithm with impedance-ratio based source location approach.
- A new optimal meter placement algorithm with impedance-ratio based source location approach is proposed to obtain a limited number of meter positions for harmonic source location process. This method uses impedance ratios of harmonic impedance matrix. The ratios are selected according to the measurement pairs obtained by the optimal meter placement algorithm. Then, these ratios are matched with voltage ratios at the corresponding meter positions to locate the harmonic source. The meter placement approach selects measurement pairs with impedance ratios that have maximum distance between their closest members to overcome slight deviations in harmonic impedance values. The results obtained from several test conditions show that
 - (i) for circuits with ring network topology, one measurement pair (two measurements);
 - (ii) for circuits with multi-ended radial network topology, one measurement at each terminal (end) node of the circuit;

(iii)for symmetrical circuits which include both radial and ring network topology, one measurement inside the ring circuit and measurements at each end node of the circuit;

(iv)for non-symmetrical circuits which include both radial and ring network topology, measurements at each end node of the circuit are sufficient to locate the harmonic source.

- It is also possible to locate multiple harmonic sources (which have different harmonic orders than each) with the proposed algorithm. However, the method is insufficient to locate multiple harmonic sources which have the same harmonic orders. When each of the multiple harmonic sources in the system inject at least one harmonic component, which are not at the same order with other harmonic sources harmonic components, the proposed algorithm can be used to locate the harmonic sources. For each harmonic component, harmonic impedance matrix is calculated and the location of the source is obtained.

Simulations on *IEEE* 30-bus test system also verify the accuracy of the proposed harmonic source location approach; since with the obtained limited meters, the location of harmonic source can be accurately determined for the network topology in *IEEE* 30-bus test system.

- The impedance-ratio based source location approach is a generalization of the distance measure approach which uses the impedance ratios to find the distance from the harmonic source to a node to which the meter is connected.
- The harmonic source location approach with the optimal meter placement algorithm is capable of accurately locating a harmonic source when there is no deviation in the harmonic network impedance. However, obtaining correct network impedances may be difficult in practice. Therefore, harmonic source location algorithms may need to tolerate small deviations in network impedances. The performance of the proposed metering algorithm for such a condition is investigated by Monte Carlo simulation (*MCS*). The *MCS* is used to analyse how errors and random variations of network impedances affect the performance of the harmonic location algorithm. The performance of the proposed optimal meter placement algorithm (*OMPA*) is compared with the non-optimal meter placement (*NOMP*) algorithm. The *NOMP* is a metering

algorithm which picks the worst metering positions. The worst metering positions are obtained by selecting the measurement pairs with impedance ratios which have minimum distance between their closest members. Thus, the measurement pairs have the *closest* $\alpha^{k,\ell}$ set members. For the simulations on the *IEEE* 30-bus test system, ten different deviation values in the network harmonic impedances and seventeen harmonics were used. It is seen that when there is no deviation in the harmonic impedance matrix, the performance of location with the proposed *OMPA* metering algorithm is 12.15% better than the *NOMP* algorithm which gives the worst metering positions. On the other hand, when the variance in the simulations is increased, the error in impedance matrix also increases and the performance of the proposed metering algorithm decreases. However, its performance is always better than location with arbitrarily selected measurements. These results show that the proposed optimal meter placement algorithm is capable of dealing with the affects of deviations in network impedance values.

- A similar method to locate a harmonic source based on matching voltage ratio to impedance ratio is encountered in the literature [70]. In this approach, the ratio of voltages measured in two *arbitrary* nodes of the circuit is used as a localizing coefficient. For the corresponding arbitrary nodes, this coefficient is compared with the impedance ratio obtained from the impedance matrix. For the impedance ratio which is equal to the localizing coefficient, the location of harmonic source is found. The weakness of this study is that when there are multiple equal impedance ratios, the proposed algorithm can not discriminate the exact location of the harmonic source because it selects only two measurement pairs. Moreover, when there are errors in impedance values, the algorithm can not locate the harmonic source because the measurement pairs are selected arbitrary and the algorithm can not tolerate the deviations in impedance values. These disadvantages are removed by the *OMPA* approach proposed in this thesis. The *OMPA* can both tolerate deviations in harmonic impedance and select the minimum number of measurement pairs.
- When the harmonic source location approach with the optimal meter placement algorithm is compared to the studies in literature, the proposed

approach has several advantages. First, the proposed meter placement algorithm is capable of performing the location process with a limited number of measurements. This is practical in electric power systems where full measurement of the system voltages at all of the nodes is not reasonable for a large system. Only limited number of measurements is reasonable and these measurements must be complemented by the location algorithm. On the other hand, the proposed meter placement algorithm is capable of dealing with the affects of network harmonic impedance errors on the location approach. The performance of the proposed metering approach is always better than location with arbitrarily selected measurement positions. Moreover, the harmonic current value is not required to obtain the location of harmonic source in the electric network.

- The proposed approach in comparison to studies in the literature has some weakness. First, the proposed approach is a topology dependent method. The exact network topology and impedance matrix is required for the location approach. However, the topological data may be obtained from electric power utilities. Also there are studies in literature regarding the measurement of harmonic impedance value of loads, as mentioned in Chapter 4. Moreover, the *OMPA* method can tolerate slight deviations in harmonic impedance values: If the load harmonic impedance values are not exact, this problem can be solved by the meter placement algorithm which finds the optimum meter places. The measurement pairs are selected with $\alpha^{k,\ell}$ set members which are mostly distant to each other, thus the deviation in impedance matrix can be tolerated. The second weakness of the proposed approach is such that when bus harmonic voltages are weak or subject to disturbances, the advantage of metering only harmonic voltage waveforms may become a disadvantage. This problem can be solved by the addition of harmonic current value to the algorithm. The harmonic current can be calculated from the known quantities of the proposed approach in this thesis. These quantities are harmonic voltage from measurements and knowledge of harmonic impedance matrix. On the other hand, if \mathbf{Z}_{bus} is not subject to deviation, the calculated and measured values of harmonic current will be equal. Therefore, measurement regarding harmonic current is redundant. However, if the \mathbf{Z}_{bus} is subject to deviations,

then the calculated and measured values of harmonic current will not be equal. In this condition, addition of harmonic current value to the algorithm can enhance the location performance of the method.

6.1 Future Work

The following research topics that need more investigation are obtained from the studies performed in the thesis:

- The addition of harmonic current measurements can enhance the performance of the harmonic location procedure especially for the case when the harmonic voltage amplitudes are weak or subject to disturbances.
- The proposed approach is developed for balanced three-phase systems. It can be enhanced for unbalanced three-phase networks.
- Since there were not enough real measurement data available, the proposed approach was only tested by computer simulations; however the performance can be tested on real systems as well.
- Locating multiple harmonic sources, which have the same harmonic orders, can be investigated in a future work.

REFERENCES

- [1] **Arrilaga, J., Watson, N. R.**, 2003: *Power System Harmonics*, Second Edition. Wiley&Sons.
- [2] **IEEE Std. 1159-1995**, IEEE Recommended Practice for Monitoring Electric Power Quality, *IEEE*, USA.
- [3] **IEEE Std. 519-1992**, IEEE Recommended Practices and Requirements for Harmonic Control in Electrical Power Systems, *IEEE*, USA.
- [4] **Dugan, R. C., McGranaghan, M. F., Santoso, S., Beaty, H. W.**, 2002. *Electrical Power Systems Quality*, Second Edition, McGraw-Hill.
- [5] **Cristaldi, L., Ferrero, A.**, 1994: A Digital Method for the Identification of the Source of Distortion in Electric Power Systems. *IEEE Transactions on Instrumentation and Measurement*, Vol. **44**, No. 1, February, 14-18.
- [6] **Cristaldi, L., Ferrero, A., Salicone, S.**, 2002: A Distributed System for Electric Power Quality Measurement. *IEEE Transactions on Instrumentation and Measurement*, Vol. **51**, No. 4, August, 776-781.
- [7] **CIGRE 36.05/ CIRED 2 Joint WG CC02**, 1999: Review of methods for measurement and evaluation of harmonic emission level from an individual distorting load, *CIGRE (Voltage Quality)*, January, 791-800.
- [8] **Timothy, A. G., Bones, D.**, 1991: Harmonic Power Flow Determination using the Fast Fourier Transform, *IEEE Transactions on Power Delivery*, Vol. **6**, No. 2, April, 530-535.
- [9] **Aiello, M., Cataliotti, A., Cosentino, V., Nuccio, S.**, 2005: A Self-Synchronizing Instrument for Harmonic Source Detection in Power Systems, *IEEE Trans. Instrum. Meas.*, Vol. **54**, No. 1, February, 15-219.
- [10] **Sasdelli, R., Muscas, C., Perretto, L.**, 1998: A VI-based measurement system for sharing the customer and supply responsibility for harmonic distortion, *IEEE Trans. Instrum. Meas.*, Vol. **47**, No. 5, October, 1335-1340.
- [11] **Pretorius, J. H., Wyk, J. D., Swart, P. H.**, 2000: An evaluation of some alternative methods of power resolution in a large industrial plant, *IEEE Trans. Power Delivery*, Vol. **15**, No. 3, July, 1052-1059.
- [12] **IEEE Std. 1459-2000**, IEEE Trial-Use Standard Definitions for the Measurement of Electric Power Quantities Under Sinusoidal, non Sinusoidal, Balanced or Unbalanced Conditions, *IEEE*, USA.
- [13] **Emmanuel, A. E.**, 1995: On the assessment of harmonic pollution, *IEEE Transactions on Power Delivery*, Vol. **10**, No. 3, January, 1693-1698.

- [14] **Davis, E. J., Emmanuel, A. E., Pileggi, D. J.**, 2000: Evaluation of single-point measurement method for harmonic pollution cost allocation, *IEEE Transactions on Power Delivery*, Vol. **15**, No. 1, January, 14-18.
- [15] **Tanaka T., Akagi, H.**, 1995: A new method of harmonic power detection based on the instantaneous active power in three-phase circuits, *IEEE Transactions on Power Delivery*, Vol. **10**, No. 4, October, 1737-1742.
- [16] **Xu, W., Liu, X., Liu, Y.**, 2003: An investigation on the validity of power-direction method for harmonic source determination, *IEEE Transactions on Power Delivery*, Vol. **18**, No. 1, January, 214-219.
- [17] **Barbaro, P. V., Cataliotti, A., Cosentino, V., Nuccio, S.**, 2007: A Novel Approach Based on Nonactive Power for the Identification of Disturbing Loads in Power Systems, *IEEE Transactions on Power Delivery*, Vol. **22**, No. 3, July, 1782-1789.
- [18] **Cataliotti, A., Cosentino, V., Nuccio, S.**, 2008: Comparison of Nonactive Powers for the Detection of Dominant Harmonic Sources in Power Systems, *IEEE Trans. Instrum. Meas.*, Vol. **57**, No. 8, August, 1554-1561.
- [19] **Heydt, G. T.**, 1989: Identification of Harmonic Sources by a State Estimation Technique, *IEEE Transactions on Power Delivery*, Vol. **4**, No. 1, January, 569-576.
- [20] **Du, Z. P., Arrillaga, J., Watson, N.**, 1996: Continuous harmonic state estimation of power systems. *IEE Proceedings-Generation Transmission and Distribution*, Vol. **143**, Issue 4, July, 329-336.
- [21] **Du, Z. P., Arrillaga, J., Watson, N., Chen, S.**, 1999: Identification of harmonic sources of power systems using state estimation. *IEE Proceedings-Generation Transmission and Distribution*, Vol. **146**, Issue 1, January, 7-12.
- [22] **Meliopoulos, A. P. S., Zhang, F., Zelingher, S.**, 1994: Power-System Harmonic State Estimation, *IEEE Transactions on Power Delivery*, Vol **9**, Issue 3, July, 1701-1709.
- [23] **Xu, W., Liu, Y.**, 2000: A method for determining customer and utility harmonic contributions at the point of common coupling, *IEEE Transactions on Power Delivery*, Vol. **15**, No. 2, April, 804-811.
- [24] **Hamzah, N., Mohamed, A., Hussain, A.**, 2003: Methods for determining utility and customer harmonic contributions at the point of common coupling, *Proceedings of Power Engineering Conference, PECon 2003*, 15-16 December, 167-171.
- [25] **Srinivasan, K.**, 1996: On separating customer and supply side harmonic contributions, *IEEE Transactions on Power Delivery*, Vol. **11**, No. 2, April, 1003-1012.
- [26] **Li, C., Xu, W., Tayjasanant, T.**, 2004: A Critical Impedance Based Method for Identifying Harmonic Sources, *IEEE Transactions on Power Delivery*, Vol. **19**, No. 2, April, 671-678.

- [27] **Najjar, M., Heydt, G. T.**, 1991: A Hybrid Nonlinear-Least Squares Estimation of Harmonic Signal Levels in Power Systems, *IEEE Transactions on Power Delivery*, Vol. **6**, No. 1, January, 282-288.
- [28] **Beides, H. M., Heydt, G. T.**, 1991: Dynamic state estimation of power system harmonics using Kalman filtering methodology, *IEEE Transactions on Power Delivery*, Vol. **6**, No. 4, October, 1663-1669.
- [29] **Farach, J. E., Grady, W.M., Arapostathis, A.**, 1993: An Optimal Procedure for Placing Sensors and Estimating the Locations of Harmonic Sources in Power Systems, *IEEE Transactions on Power Delivery*, Vol. **8**, No. 3, July, 1303-1310.
- [30] **Gursoy, E., Niebur, D.**, 2009: Harmonic Load Identification Using Complex Independent Component Analysis, *IEEE Transactions on Power Delivery*, Vol. **24**, No. 1, January, 285-292.
- [31] **Baghzouz, Y., Burch, R. F., Capasso, A., Cavallini, A.**, 1998: Time-varying harmonics: Part I – Characterizing measured data, *IEEE Transactions on Power Delivery*, Vol. **13**, No. 3, July, 938-944.
- [32] **Baghzouz, Y., Burch, R. F., Capasso, A., Cavallini, A., Emanuel, A. E., Halpin, M., Langella, R., Montanari, G., Olejniczak, K. J., Riberio, P., Rios-Marcuello, S., Ruggiero, F., Thallam, R., Testa, A., and Verde, R.**, 2002: Time-varying harmonics: Part II – Harmonic summation and propagation, *IEEE Transactions on Power Delivery*, Vol. **17**, No. 1, January, 279-285.
- [33] **Hartana, R. K., Richards, G. G.** 1993: Constrained Neural Network-Based Identification of Harmonic Sources, *IEEE Transactions on Industry Applications*, Vol. **29**, No. 1, January/February, 202-208.
- [34] **Kumar, A., Das, B., Sharma, J.**, 2005: Simple technique for placement of meters for estimation of harmonics in electric power system, *IEE Proc.-Gener. Transm. Distrib.*, Vol. **152**, No. 1, January, 67-78.
- [35] **Hong, Y. Y., Chen, Y. C.**, 1999: Application of algorithms and artificial-intelligence approach for locating multiple harmonics in distribution systems, *IEE Proc.-Gener. Transm. Distrib.*, Vol. **146**, No.3, May, 325-329.
- [36] **Cronje, W., Rens, A.**, 2004: Investigating the Validity of Applying Artificial Neural Networks to Localise Harmonic Distortion sources, *IEEE AFRICON 2004*, 645-650.
- [37] **Hartana, R. K., Richards, G. G.** 1990: Harmonic Source Monitoring and Identification Using Neural Networks, *IEEE Transactions on Power Systems*, Vol. **5**, No. 4, November, 1098-1104.
- [38] **Wakileh, G. J.**, 2001: *Power System Harmonics: Fundamentals, Analysis and Filter Design*. Springer.
- [39] **Emanuel, A. E.**, 1999: Apparent Power Definitions for Three-Phase Systems, *IEEE Transactions on Power Delivery*, Vol. **14**, No. 3, July, 767-772.
- [40] **Emanuel, A. E.**, 1990: Powers in Nonsinusoidal Situations a review of definitions and physical meaning, *IEEE Transactions on Power Delivery*, Vol. **5**, No. 3, July, 1377-1389.

- [41] **Filipski, P. S., Baghzouz, T., Cox, M. D.**, 1994: Discussion of Power Definitions Contained in the IEEE Dictionary, *IEEE Transactions on Power Delivery*, Vol. **9**, No. 3, July, 1237-1244.
- [42] **IEEE Working Group on Nonsinusoidal Situations**, 1996: Practical Definitions for Power in Systems with Nonsinusoidal Waveforms and Unbalanced Loads, *IEEE Transactions on Power Delivery*, Vol. **11**, No. 1, January, 79-101.
- [43] **Sharon, D.**, 1996: Power Factor Definitions and Power Transfer Quality in Nonsinusoidal Situations, *IEEE Trans. Instrum. Meas.*, Vol. **45**, No. 3, June, 728-733.
- [44] **Czarnecki, L. S., Swietlicki, T.**, 1990: Powers in Nonsinusoidal Networks: Their Interpretation, Analysis, and Measurement, *IEEE Trans. Instrum. Meas.*, Vol. **39**, No. 2, April, 340-345.
- [45] **Ferrero, A., Furga, G. S.**, 1991: A new approach to the Definition of Power Components in three-Phase Systems under nonsinusoidal conditions, *IEEE Trans. Instrum. Meas.*, Vol. **40**, No. 3, June, 568-577.
- [46] **Salmeron, P., Montano, J. C.**, 1996: Instantaneous power components in polyphase systems under nonsinusoidal conditions, *IEE Proc.-Sci. Meas. Technol.*, Vol. **143**, No. 2, March, 151-155.
- [47] **IEEE Std. C57.110-2008**, IEEE Recommended Practice for Establishing Liquid-Filled and Dry-Type Power and Distribution Transformer Capability When Supplying Nonsinusoidal Load Currents, *IEEE Power Engineering Society*, USA.
- [48] **Ribeiro, P. F.**, 1992: Guidelines On Distribution System And Load Representation For Harmonic Studies, *ICHPS V International Conference on Harmonics in Power Systems*, September 22-25, 272-280.
- [49] **Task Force on Harmonic Modeling and Simulation**, 2003: Impact of Aggregate Linear Load Modeling on Harmonic Analysis: A Comparison of Common Practice and Analytical Models, *IEEE Transactions on Power Delivery*, Vol. **18**, No. 2, April, 625-630.
- [50] **Task Force on Harmonic Modeling and Simulation**, 2001: Characteristics and Modeling of Harmonic Sources-Power Electronic Devices, *IEEE Transactions on Power Delivery*, Vol. **16**, No. 4, October, 791-800.
- [51] **Task Force on Harmonic Modeling and Simulation**, 1996: The modeling and simulation of the propagation of harmonics in electric power networks-Part I: Concepts, models and simulation techniques, *IEEE Transactions on Power Delivery*, Vol. **11**, No. 1, January, 452-465.
- [52] **Meliopoulos, A. P. S., Zhang, F.**, 1996: Multiphase Power Flow and State Estimation for Power Distribution Systems, *IEEE Transactions on Power Systems*, Vol. **11**, No. 2, May, 939-946.
- [53] **Kezunovic, M., Drazenovic, B.**, 1999: *Fault Location*, Wiley Encyclopedia of Electrical and Electronics Engineering, December.

- [54] **Takagi, T., Yamakoshi, Y., Yamaura, M., Kodow, R., Matsushima, T.,** 1982: Development of a new type fault locator using the one-terminal voltage and current data, *IEEE Transactions on Power Apparatus and Systems*, Vol. **PAS-101**, No. 8, August, 2892-2898.
- [55] **IEEE Std. C37.114-2004,** IEEE Guide for Determining Fault Location on AC Transmission and Distribution Lines, *IEEE Power Engineering Society*, USA.
- [56] **Girgis, A. A., Fallon, C. M.,** 1992: FaultLocation Techniques for radial and loop Transmission Systems using digital fault recorded data, *IEEE Transactions on Power Delivery*, Vol. **7**, No. 4, October, 1936-1945.
- [57] **Novosel, D., Hart, D. G., Udren, E., Garitty, J.,** 1996: Unsynchronized Two-Terminal Fault Location Estimation, *IEEE Transactions on Power Delivery*, Vol. **11**, No. 1, January, 130-138.
- [58] **Girgis, A. A., McManis, R. B.,** 1989: Frequency domain techniques for modeling distribution or transmission networks using capacitor switching induced transient, *IEEE Transactions on Power Delivery*, Vol. **4**, No. 3, July, 1882-1890.
- [59] **Morched, A. S., Kundur, P.,** 1987: Identification and modeling of load characteristics at high frequencies, *IEEE Transactions on Power Systems*, Vol. **2**, No. 1, February, 153-159.
- [60] **Robert, A., Deflandre, T.,** 1997: Guide for assessing the network harmonic impedance, *Joint CIGRE/CIREN Working Group CC02*, June.
- [61] **Nagpal, M., Xu, W., Sawada, J.,** 1998: Harmonic impedance measurement using three phase transients, *IEEE Transactions on Power Delivery*, Vol. **13**, No. 1, Jan, 272-277.
- [62] **Sumner, M., Palethorpe, B., Thomas, D., Zanchetta, P., Piazza, M.,** 2002: A technique for power supply harmonic impedance estimation using a controlled voltage disturbance, *IEEE Transactions on Power Electronics*, Vol. **17**, No. 2, March, 207-215.
- [63] **Sumner, M., Palethorpe, B., Thomas,** 2004: Impedance Measurement for Improved Power Quality-Part 1: The Measurement Technique, *IEEE Transactions on Power Delivery*, Vol. **19**, No. 3, July, 1442-1448.
- [64] **Oliveira, A., Oliveira, J. C., Resende, J. W., Miskulin, M. S.,** 1991: Practical approaches for AC system harmonic impedance measurements, *IEEE Transactions on Power Delivery*, Vol. **6**, No. 4, October, 1721-1726.
- [65] **Grainger, J. J., Stevenson, W. D. Jr.,** 1994. *Power System Analysis*, McGraw-Hill.
- [66] **Phadke, A. G.,** 1993: Synchronized Phasor Measurements in Power Systems, *IEEE Computer Applications in Power*, April, 10-15.
- [67] **Novosel, D., Vu, K., Centeno, V., Skok, S., Begovic, M.,** 2007: Benefits of synchronized-Measurement Technology for Power-Grid Applications, *Proceedings of the 40th Hawaii International Conference on System Sciences*, January, 1-9.

- [68] **Dubi, A.**, 2000. *Monte Carlo Applications in Systems Engineering*, John Wiley&Sons, Ltd.
- [69] **Robert, C. P., Casella, G.**, 2004. *Monte Carlo Statistical Methods*, Springer.
- [70] **Korovkin, N., Balagula, Y., Adalev, A., Nitsch, J.**, 2005: A method of a disturbance source localization in a power system, *IEEE Power Tech Russia*, 1-6.

APPENDICES

APPENDIX A.1 : Test system parameters

APPENDIX A.2 : Computer program

APPENDIX A.1

Table A.1.1: Bus load and injection data of *IEEE* 30-bus system.

Bus	Load (MW)	Bus	Load (MW)
1	0.0	16	3.5
2	21.7	17	9.0
3	2.4	18	3.2
4	67.6	19	9.5
5	34.2	20	2.2
6	0.0	21	17.5
7	22.8	22	0.0
8	30.0	23	3.2
9	0.0	24	8.7
10	5.8	25	0.0
11	0.0	26	3.5
12	11.2	27	0.0
13	0.0	28	0.0
14	6.2	29	2.4
15	8.2	30	10.6

Table A.1.2: Reactive power limit of *IEEE* 30-bus system.

Bus	Qmin (p.u.)	Qmax (p.u.)	Bus	Qmin (p.u.)	Qmax (p.u.)
1	-0.2	0.0	16		
2	-0.2	0.2	17	-0.05	0.05
3			18	0.0	0.055
4			19		
5	-0.15	0.15	20		
6			21		
7			22		
8	-0.15	0.15	23	-0.05	0.055
9			24		
10			25		
11	-0.1	0.1	26		
12			27	-0.055	0.055
13	-0.15	0.15	28		
14			29		
15			30		

Table A.1.3: Line parameter of *IEEE* 30-bus system.

Line	From Bus	To Bus	R (p.u.)	X (p.u.)	B (p.u.)
1	1	2	0.0192	0.0575	0.0528
2	1	3	0.0452	0.1852	0.0408
3	2	4	0.0570	0.1737	0.0368
4	3	4	0.0132	0.0379	0.0084
5	2	5	0.0472	0.1983	0.0418
6	2	6	0.0581	0.1763	0.0374
7	4	6	0.0119	0.0414	0.009
8	5	7	0.0460	0.1160	0.0204
9	6	7	0.0267	0.0820	0.017
10	6	8	0.0120	0.0420	0.009
11	6	9	0.0000	0.2080	0
12	6	10	0.0000	0.5560	0
13	9	11	0.0000	0.2080	0
14	9	10	0.0000	0.1100	0
15	4	12	0.0000	0.2560	0
16	12	13	0.0000	0.1400	0
17	12	14	0.1231	0.2559	0
18	12	15	0.0662	0.1304	0
19	12	16	0.0945	0.1987	0
20	14	15	0.2210	0.1997	0
21	16	17	0.0824	0.1932	0
22	15	18	0.1070	0.2185	0
23	18	19	0.0639	0.1292	0
24	19	20	0.0340	0.0680	0
25	10	20	0.0936	0.2090	0
26	10	17	0.0324	0.0845	0
27	10	21	0.0348	0.0749	0
28	10	22	0.0727	0.1499	0
29	21	22	0.0116	0.0236	0
30	15	23	0.100	0.2020	0
31	22	24	0.1150	0.1790	0
32	23	24	0.1320	0.2700	0
33	24	25	0.1885	0.3292	0
34	25	26	0.2544	0.3800	0
35	25	27	0.1093	0.2087	0
36	28	27	0.0000	0.3960	0
37	27	29	0.2198	0.4153	0
38	27	30	0.3202	0.6027	0
39	29	30	0.2399	0.4533	0
40	8	28	0.0636	0.2000	0.0428
41	6	28	0.0169	0.0599	0.013

CURRICULUM VITA



Candidate's full name: Oben Dağ

Place and date of birth: Istanbul – 13.06.1978

Permanent address: 26 Ağustos yerleşimi, Kayışdağı Cad. 34755
Kayışdağı/İstanbul Yeditepe Üniversitesi Mühendislik
ve Mimarlık Fakültesi Elektrik ve Elektronik Müh.
Bölümü

Universities and colleges attended: Yıldız Technical Univ. – B.S. – 1999
Istanbul Technical Univ. – M.S. – 2002

Publications:

- **Dağ O.**, Uçak C., ve Usta Ö., 2008: Empedans Devreleri Yaklaşımıyla Harmonik Kaynağının Yerinin Saptanması. *ELECO 2008*, 2008 Bursa, Türkiye.
- **Dağ O.**, Uçak C., 2004: Fault Classification for power Distribution Systems via a Combined Wavelet-neural Approach. *PowerCON 2004 International Conference on Power System Technology IEEE*, 21-24 November 2004, Singapore.
- **Dağ O.**, Uçak C., 2004: Birleşik Dalgacık-sinir ağı yaklaşımı ile Elektrik Güç Sistemlerinde Arıza Sınıflama. *ELECO 2004*, 2004 Bursa, Türkiye.
- **Dağ O.**, Uçak C., 2003: Combined Wavelet-neural Fault classifier for Power Distribution Systems. *ARI ITU Bulletin*, Vol. **53**, No. 1, 82-97.